Project THEMIS

1. This document has been approved for public release and sale; its distribution is unlimited.

College of Engineering
UNIVERSITY OF UTAH
Salt Lake City, Utah

Annual Report

1 September 1968--31 August 1969

THE CHEMISTRY AND MECHANICS OF COMBUSTION

WITH

APPLICATION TO ROCKET ENGINE SYSTEMS

September 1969 UTEC TH 69-073

A Project THEMIS Program

through the

U. S. Air Force
Office of Scientific Research

M. L. Williams
Program Manager

College of Engineering
UNIVERSITY OF UTAH
Salt Lake City, Utah

This research was supported by the Air Force Office of Scientific Research, Office of Aerospace Research, United States Air Force under Contract F44620-68-0022.

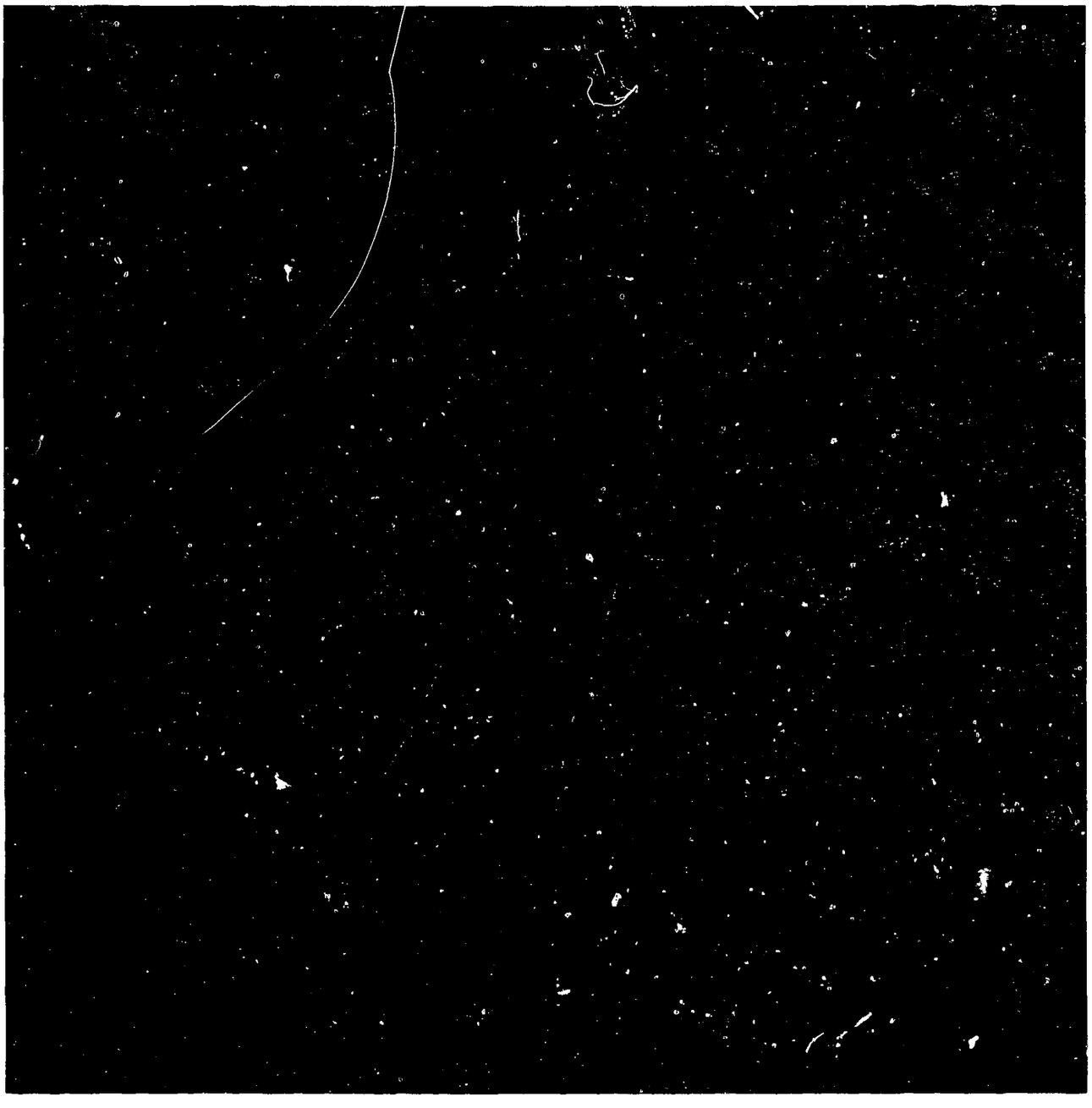

"Computer Graphic Display of the Calculated Structure of a Section of a Polyoxymethylene Chain."

Molecular mechanics is being used to calculate the conformational properties of polymer chains. The calculated conformational properties are then correlated with mechanical properties in hopes that useful predictions of polymeric behavior may be made.

FOREWORD

As part of Project THEMIS, the Department of Defense, acting through the U. S. Air Force Office of Scientific Research with Dr. B. A. Wolfson and Dr. J. F. Masi as Cognizant Scientists, awarded an integrated applied research program concerned with the "Chemistry and Mechanics of Combustion with Application to Rocket Engine Systems" to the University of Utah. This investigation in the College of Engineering is under the general direction of Professor M. L. Williams as Program Manager and was initiated in September 1967.

The purpose of this program, which is integrated with out academic objectives, is to study the interdependence of combustion processes and the physics-mechanical behavior of solid fuel materials within the context of a rocket engine system. It is intended to capitalize upon a quantitative understanding of molecular structure, which affects both the combustion and mechanics behavior, and treat the propellant fuel and associated inert components as a materials system--from processing, to a determination of the constitutive equation as needed to assess structural integrity, and failure under various environmental and loading conditions. Concurrently, the tasks are concerned with propellant as an energy source--from ignition, through burning, gas dynamics, interaction with nozzle and insulation components, and consideration of electron noise and radar attenuation in the plume.

Six task areas are presently envisioned, each of which is under the direction of a Principal Investigator. Coordination of the various tasks is accomplished by regular meetings of the senior investigators and appropriate external consultants from industrial and government organizations. The six areas, not necessarily of equal emphasis, include:

1. Combustion and Transport Mechanisms
2. Flow and Heat Transfer
3. Ablation Mechanisms
4. Radiation Attenuation and Plasma Physics
5. Mechanics of Solids
6. Transition to Detonation Mechanisms

External Comments are solicited and direct contact with the individual investigators is encouraged.

PREFACE

The establishment of a Project THEMIS program at the University of Utah has, in conjunction with other associated research, permitted the College of Engineering to embark upon a consolidated and integrated series of investigations in the general area of combustion and combustion related research. As a particular and immediate result of Project THEMIS several specific studies, which have the molecular morphology as the common thread affecting both the combustion and mechanical behavior, have been initiated. While as individual components they supplement a broader program, they also comprise individual tasks and as such are being reported separately. Their internal coordination and integration with the broader academic and research program of the College is being accomplished through frequent meetings of the senior investigators.

A study of the combustion process is intimately associated with an accurate knowledge of chemical kinetics, as analytically established and experimentally verified. Many of the present observations of polymer decomposition have been made at unrealistically low burning rates. In Task 1, data are reported which were obtained by two new techniques for determining the thermal effects of solid propellant reactions at heating rates in excess of $111^{\circ}K/sec$, approximately two orders of magnitude faster than conventional ones.

A comparison of our data at high heating rates to those from differential scanning calorimeter tests shows general correspondence for the low-temperature, endothermic reactions, but indicates differences in the critical temperatures at which the high-temperature, exothermic reactions are manifested.

The association of mechanical behavior with chemical structure is a companion interest. As an outgrowth of some preliminary studies, we have shown that it is possible to relate certain micro and macroscopic properties. For example, the range of stiffness of a viscoelastic material has been correlated quantitatively with the number of molecular segments of the polymer chain. This type of investigation will eventually lead to tailoring of the molecule to achieve mechanical, and combustion, efficiency. (See Frontispiece.)

As an extension of the foregoing invest gations, wherein the chemical structure may affect both the combustion and the mechanical behavior, Task 5 seeks to pursue in greater detail the appropriate form of the mechanical equation of state governing the deformation of a rate sensitive solid. As a point of departure, the coupled thermo-mechanical state is under investigation, i.e. the effect of internal viscous heating during mechanical, usually cyclic, loading with special emphasis upon the nonlinearities introduced by a high filler content, approaching 80-90 percent.

Viscoelastic materials have a "memory." Their present state depends upon the entire past loading time. Experience indicates, however, that many materials are relatively more sensitive to the immediate past than very long times ago. In other words, they tend to forget somewhat the far distant past. Hence the concept of a "fading memory" has been introduced. The nonlinearity effects being considered, e.g. the Mullin's Effect, are presently too complicated to include the fading memory concept, so that present work is directed toward incorporating them into a non-fading memory constituitive law as a first step. Ultimately, it is hoped to incorporate into these equations any chemical effects sensitive to high rate loading input. Such inclusion would possess the incidental advantage of providing a reference point in the event the ablation studies of Task 3 indicate strong coupling between materials and structural integrity.

The principal objective of Task 3 is to attain methods for controlling the chemical kinetics of the subsurface internal endothermic-exotheric reactions, with particular reference to the possibility of weight reduction in rocket components such as nozzles. The results are expected also to have a certain benefit in the general area of flammability, a subject of considerable interest in fire safety today. During the past year, a number of high temperature polymers were obtained and thermogravimetric and effluent gas analyses have begun. A quasilinearization technique is being applied to the data to determine pyrolysis kinetic parameters. A high temperature, high pressure gas flow facility has finally been delivered and is being installed in a specially designed tunnel for hazardous experiments. Some analytical techniques for characterizing surface ablation involving melt layer flow have also been initiated along with designs for certain experiments for securing

the required basic property data.

Inasmuch as Task 3 is examining the interdependency of pyrolysis of materials and surface chemical attack during combustion along the interface between the ablating material and the flowing gas, some aspects of this task are closely related to the aims of Task 2 which is concerned with temperature and velocity measurements in a turbulent boundary layer subject to mass injection and combustion. The supersonic facility should be completed during the next year. In the meantime, the existent subsonic experiments have revealed a very strong coupling between the velocity profile through the turbulent boundary layer and the external or free-stream favorable axial pressure gradient. This dynamic coupling amplifies the velocity overshoot observed in the turbulent boundary layer with combustion. Results obtained from the cooled constant temperature heat flux probe in the combustion experiments have indicated that turbulent bursts or eddies of hot gases are present in outer regions of the boundary layer much further from the surface than had been previously reported. These experiments lend support to the mixing jet theory of turbulent boundary layer structure which has gained popularity in the last few years.

The last of the current tasks, Task 4, is still not fully integrated into the overall program. The major objective is to use microwave diagnostic techniques to deduce the electron temperature inside a combustion chamber, essentially by measuring the attenuation of microwave radiation and correlating it with the ionization density and collision frequency in the combustion products. So far, a subscale motor has been designed and fabricated for firing one-pound fuel charges while measuring 24 GHz microwave attenuation through the combustion chamber. Measured attenuation is being related to chamber temperature using Saha's equation to determine the amount of ionization of the potassium-seeded fuel. Subsequent to the verification of the temperature with other measurements and computations, an effort will be made to extend the technique to give temperature as a function of both time and position, so that non-uniformities in the combustion process can be observed. Data reduction can include analytical provision for pressure waves, non-uniform combustion and source-sink reactions which are occurring in the chamber. Such deductions and proper interpretation of the electron temperature should be of considerable value in achieving

the objectives of Task 1 wherein the chemical kinetics of combustion are being investigated. Very recently there has been renewed interest in our last year's use of microwave diagnostic techniques to detect internal voids in filled solid fuel materials, especially in conjunction with some exploratory work on the mechanisms involved in burning in cracks. Essentially we are inquiring as to how open a crack needs to be for burning to take place within it. The detection and behavior of flaws in rocket motors are both important and Task 4 and Task 1 may develop an important working relation.

This overall description is intended to reflect a balance between program definition and flexibility, is appropriate to the time the work has been in development. In pursuing our basic objective of relating chemical structure with both combustion and mechanical behavior, with particular reference to engineering problems arising in rocketry, comments are solicited from the technical community and direct communication with the individual senior investigators is encouraged.

In conclusion, it is particularly fitting to acknowledge the collaboration of Dr. George F. P. Trubridge, former Technical Director of the Summerfield Research Center of Imperial Metal Industries, as Distinguished Visiting Professor during the latter part of the past academic year. He has participated in both our research and academic programs under the auspices of Project THEMIS and his contributory efforts are reflected through this report.

THE CHEMISTRY AND MECHANICS OF COMBUSTION

WITH

APPLICATION TO ROCKET ENGINE SYSTEMS

TABLE OF CONTENTS

Table of Contents

UTEC TH 69-073a

THE CHEMISTRY AND MECHANICS OF COMBUSTION

WITH

APPLICATION TO ROCKET ENGINE SYSTEMS

Task 1 Combustion and Transport Mechanisms

A. D. Baer
N. W. Ryan

September 1969

College of Engineering
UNIVERSITY OF UTAH
Salt Lake City, Utah

PREFACE

Data are reported which were obtained by two new techniques for determining the thermal effects of solid propellant reactions at heating rates in excess of $100^{\circ}K/sec$. Increased accuracy and sensitivity is achieved by use of one technique. The second new method is suitable for the study of transparent materials.

The results reported are in essential agreement with previously reported data. A comparison of our data at high heating rates to those from differential scanning calorimeter tests shows general correspondence for the low temperature, endothermic reactions but it indicates significant differences for the critical temperatures at which high temperature, exothermic reactions are manifested.

TABLE OF CONTENTS

TASK 1 Combustion and Transport Mechanisms

1.0 INTRODUCTION

The thermal effects of the PBAA decomposition reaction and the AP-PBAA interaction reaction at high heating rates were previously studied under AFOSR sponsorship using a technique in which 100 micron thick films of sample material were bonded to copper-disc calorimeters and the free sample surface was exposed to the thermal radiation of a tube furnace.[1]

By use of this technique, which is called the thin-film copper-calorimeter method, it is possible to heat the sample at a rate of 50 to 150°K per second. Such a heating rate, which is higher than that possible in most other analytical devices, approaches the high rates which occur in rocket ignition and combustion. Endothermic or exothermic reactions occurring in the sample cause variations in the heating rate when the surface radiation is constant and uniform. A knowledge of these variations makes it possible to characterize the energy effects of the decomposition reaction and gives insight into the mechanism of the propellant reaction. The main deficiencies of this technique are the difficulties of bonding the film to the disc without introducing a large thermal resistance at the film-calorimeter interface and the necessity of estimating the film surface temperature by estimation of the large temperature gradient through the film during a test.

The deficiencies of the thin-film copper-calorimeter method are essentially eliminated by two new techniques developed in the past eight months under Project THEMIS sponsorship. In the first method, a layer of sample material is cast on 25.4 micron thick stainless-steel strips which are heated by an electrical current. The sample layer is 100 to 500 microns thick. The temperature of the strip is monitored by a chromel-alumel thermocouple or by a germanium-gold infrared detector. This technique is referred to in this report as the supported film with conductive heating method. In the second method, sample films 1 cm in diameter and 50 to 300 microns thick are supported by an annular ring around the outer curved edge. One

side of the film is heated by radiation, and the temperature on the other face is measured by focusing the radiation from the surface onto an infrared-sensitive detector. This method is referred to as the unsupported film with radiative heating method. Both of these methods show promise and will be used to characterize the reactions of various solid propellant-like materials. Such measurements will make possible a better evaluation of ignition models and will give insight into the important combustion reactions.

2.0 EXPERIMENTAL APPROACH

2.1 *Supported Film with Conductive Heating Method*

The essential features of this method are shown in Figure 1. The metal strip on which the sample material has been cast and cured is bolted into the terminals. When the strip temperature was measured by use of a thermocouple, it was held in contact with the bottom of the strip by a steel spring. Tests have been conducted in which the heating rate was varied from 50 to 500°K per second by control of the current from an automobile battery through the strip. When the results of tests which measured the strip temperature with the thermocouple were compared with the previous work, the apparent temperatures at which reactions occur were found to be about 100°K low. The reproducibility of these data were, however, very good. It is believed that the low temperatures were caused largely by the heat sink effect of the thermocouple. When the strip temperature was monitored by use of an infrared-sensitive device, the results compared favorably with the previous work.

Since the sample material is cast directly onto the strip, the difficulty with a large thermal resistance at the film-metal interface, as in the previous work, is largely overcome. Since the energy flow was from the strip to the film, the temperature gradient of the film is essentially negligible at low heating rates. The major advantage of this method is that transparent films can be used because the heating is by conduction.

One disadvantage of this method is a loss in sensitivity which results from having to heat the metal strip as well as the sample. The major objection is that the hottest part of the film is in contact with a metal surface and normal surface reactions may be suppressed. The same difficulty occurs for slow heating methods.

2.2 *Unsupported Film with Radiative Heating Method*

Figure 2 illustrates how the apparatus is arranged for the unsupported film method. The films are prepared by casting and curing the sample material between carefully spaced optically flat glass plates. The film is then mounted on the 1 cm diameter rings and placed in the apparatus at the position shown. During a test, thermal radiation impinges on the front surface and heats the film while the radiation from the back of the film is focused on a germanium-gold infrared detector. The detector output is calibrated in terms of temperature by use of metallic discs placed at the sample position. The metal disc temperature is measured by a thermocouple. The sample and disc surface coatings are the same.

The unsupported film method has an important advantage over the supported film method in that there is no metal which must be heated along with the sample. This greatly increases the sensitivity of the experiment. In addition, the unsupported film samples are much easier to prepare because there are no problems of bonding the sample to metal.

This method has the disadvantage of being influenced by the transmissivity of the film which either must be measured and this effect noted in the data analysis, or eliminated by modifying the sample material. In the work to date, elimination of transmission of radiation was achieved by dispersing three percent carbon black in the 100 micron films. Although the films tested so far have remained structurally stable until the important reactions occur, another problem will arise when low melting polymers are used with the AP. It is anticipated that most important fuel-binders will remain stable to high temperatures at high heating rates.

3.0 PRELIMINARY RESULTS

3.1 *Supported Film with Conductive Heating*

It was found that this method was not sensitive enough to give reproducible results when polymer films were tested, but the more energetic reactions which occur when a 50% AP and 50% PBAA sample is heated were easily detectable. A typical temperature history is shown in Figure 3. Table I contains results for 14 of such tests. In general, these results indicate that an endothermic reaction occurs at about 500°K followed by an exothermic reaction at about 545°K. These temperatures are about 25°K lower than results obtained by other methods, and it is believed that this may be due to a systematic error in calibrating the infrared detector.

3.2 *Unsupported Film with Radiative Heating*

A typical result for a PBAA film is shown in Figure 4. This plot indicates endothermic influences at about 655°K and 678°K. The heating rate for this test is about 50°K/sec. Cheng[1] reported this endotherm at 620°K for roughly the same material and conditions. It is interesting to compare this result to data from a Differential Scanning Calorimeter (DSC) for the same material at a heating rate of 40°K/min. as shown in Figure 6; both methods indicate an endothermic influence at about 650°K, and this is likely the same reaction in each case.

A typical temperature history for a sample which is 50% AP and 50% PBAA is shown in Figure 5. An endotherm is indicated at about 525°K followed by an exothermic influence in the neighborhood of 560°K. Cheng[1] reported the exotherm as 590°K at twice the heating rate. The temperature of this endothermic compares favorably with DSC data shown in Figure 7, although the composition of the sample in the DSC test was only 5% AP.

Because of the difference in heating rates, it would be anticipated that the DSC temperature would be the lower. The exothermic reaction temperatures (660°K from the DSC and less than 600°K at the higher heating rates) are the inverse of anticipation. It is likely that

TABLE I

SUPPORTED FILM WITH CONDUCTIVE HEATING METHOD,
HEATING RATES, EXOTHERMIC TEMPERATURES, AND
ENDOTHERMIC TEMPERATURES USING INFRARED DETECTOR

Run No.	Heating Rate ^{o}K/second	Exothermic Temperature ^{o}K	Endothermic Temperature ^{o}K
AP-1	55.0	536.0	493.2
AP-2	92.8	541.0	498.6
AP-3	102.5	540.0	504.2
AP-4	55.0	540.2	503.5
AP-5	70.0	540.2	503.6
AP-6	71.6	535.0	*
AP-7	82.9	535.0	503.7
AP-8	475.0	532.0	*
AP-9	525.0	536.0	*
AP-10	475.0	534.7	*
AP-20	28.8	560.6	503.7
AP-21	28.6	545.0	498.5
AP-22	28.4	557.3	498.6
AP-23	31.3	549.3	495.0

*These temperatures were off the screen of the oscilloscope.

different reactions or different stages of the same reaction are detected in the two devices.

In all cases, the first apparent pure fuel-binder reactions occur at significantly higher temperatures than did either the endothermic or exothermic AP-PBAA interaction reactions. This result negates the still prevalent concept of independent fuel-binder and AP decomposition during ignition or combustion processes.

4.0 PLANS FOR FUTURE WORK

The preliminary results indicate that the supported film with conductive heating and the unsupported film with radiative heating methods have several advantages over the methods used in the previous work. These methods also have advantages over conventional methods, such as DSC analysis, in that much higher heating rates are obtainable. Therefore, it is planned to use these methods to study AP-PBAA materials as well as other polymer-AP materials. Because the DSC is a widely used device for thermal decomposition studies, DSC data will also be obtained so that a comparison can be made. Work will be started on fitting these data and prior results of polymer-hot oxygen tests into a comprehensive model, to give predictions of the thermal effects of the condensed phase and gas-solid phase reactions.

REFERENCES

1. Cheng, J. T., Baer, A. D., Ryan, N. W., "Thermal EFfects of Composite-Propellant Reactions," Technical Report No. ADOAE 68-0243, Department of Chemical Engineering, University of Utah, Technical Report under Air Force Grants AROSR 40-66 and 40-67 (August 1967).

LIST OI FIGURES

DIAGRAM OF SUPPORTED FILM WITH CONDUCTIVE HEATING METHOD

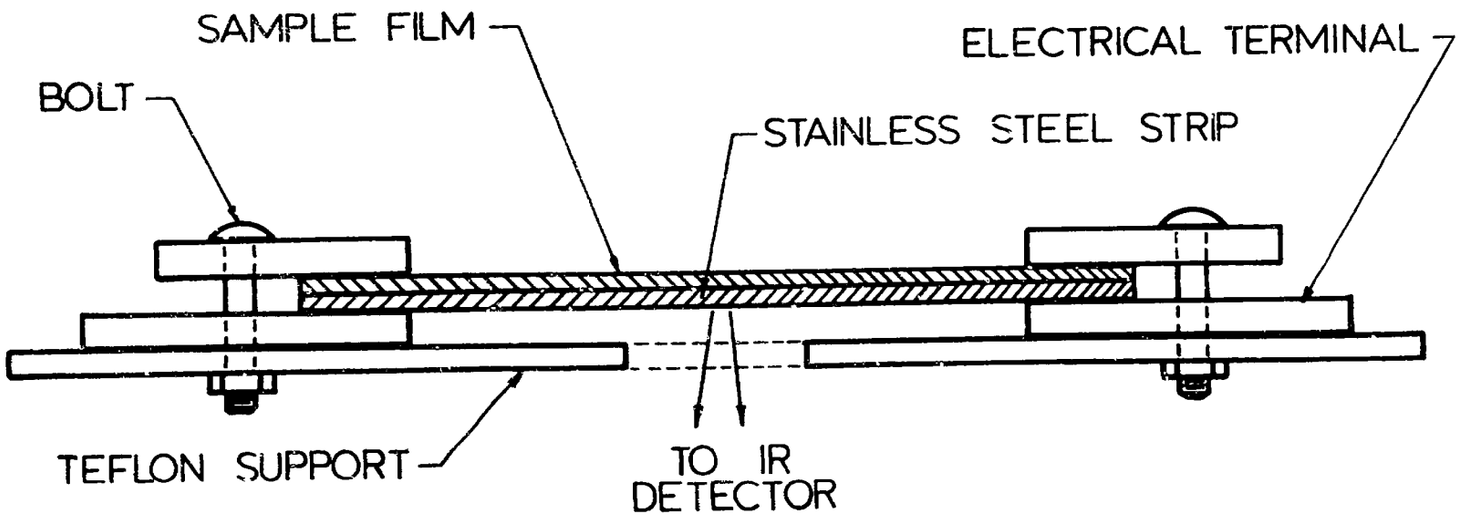

Figure 1. Diagram showing apparatus arrangement in the supported film with conductive heating method.

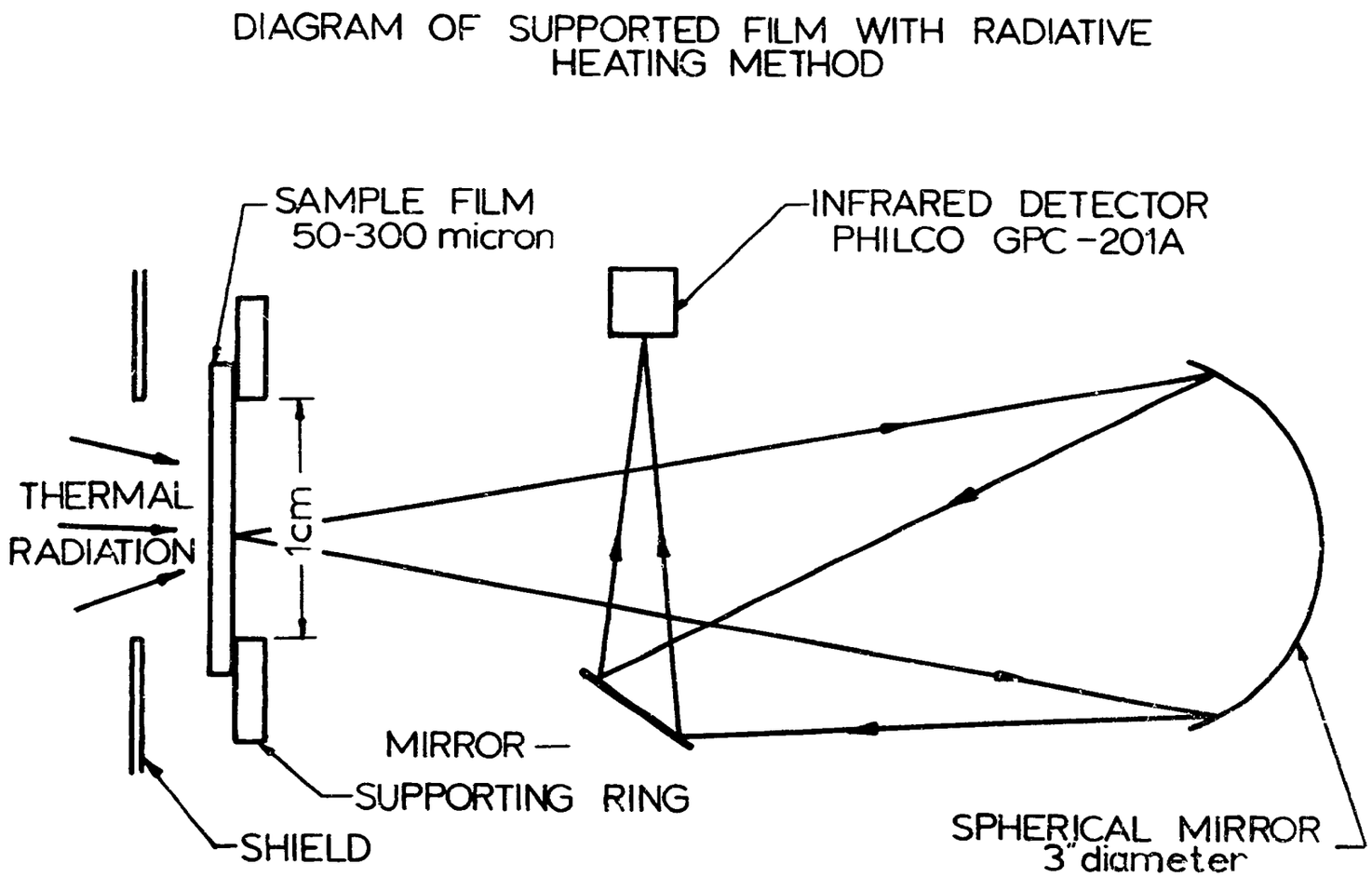

Figure 2. Diagram showing apparatus arrangement in the unsupported film with radiative heating method.

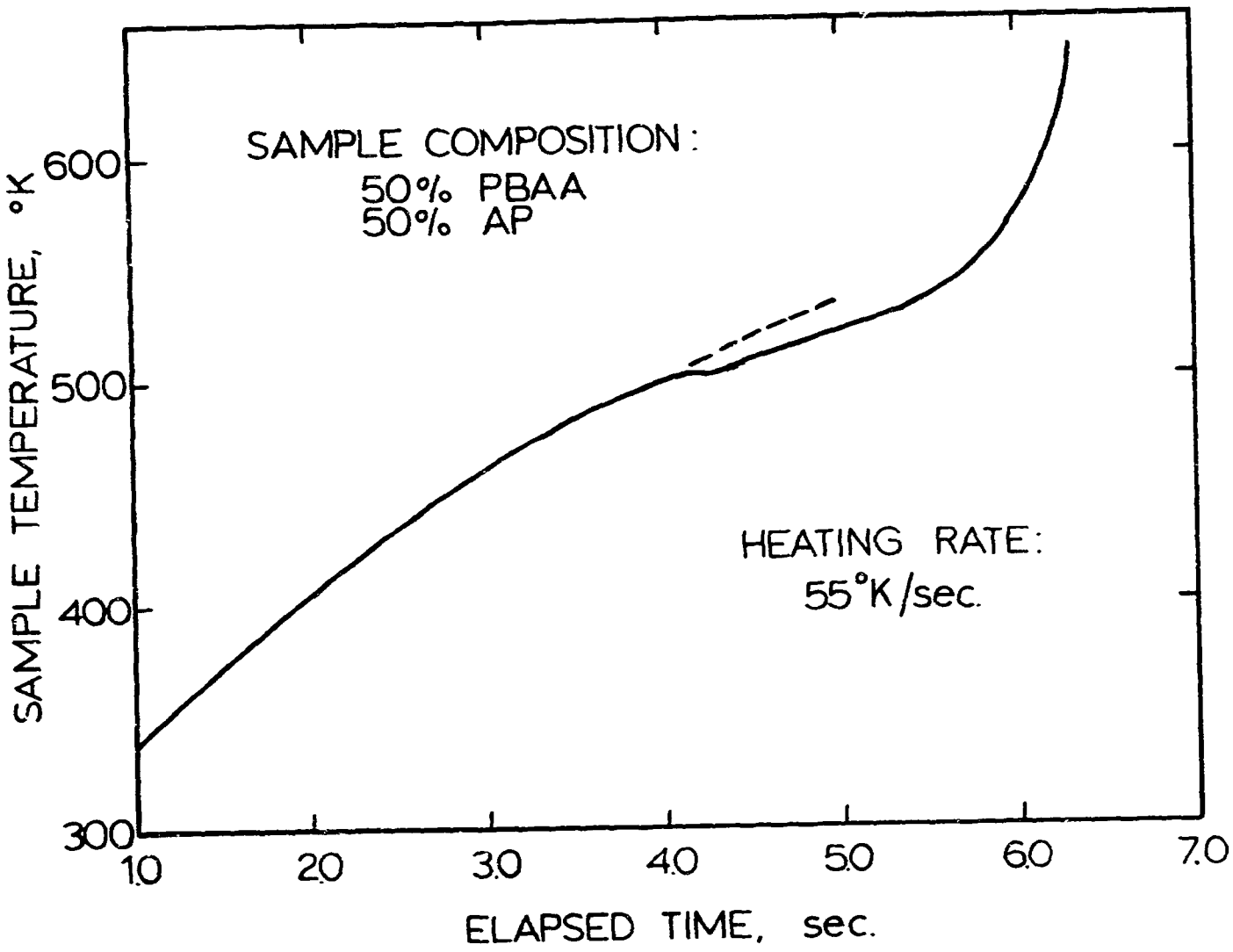

Figure 3. Temperature history of a 50% AP and 50% PBAA sample made using the supported film with conductive heating technique. The temperature is measured by an infrared detector. The dashed line is extrapolation for the anticipated no reaction time-temperature curve.

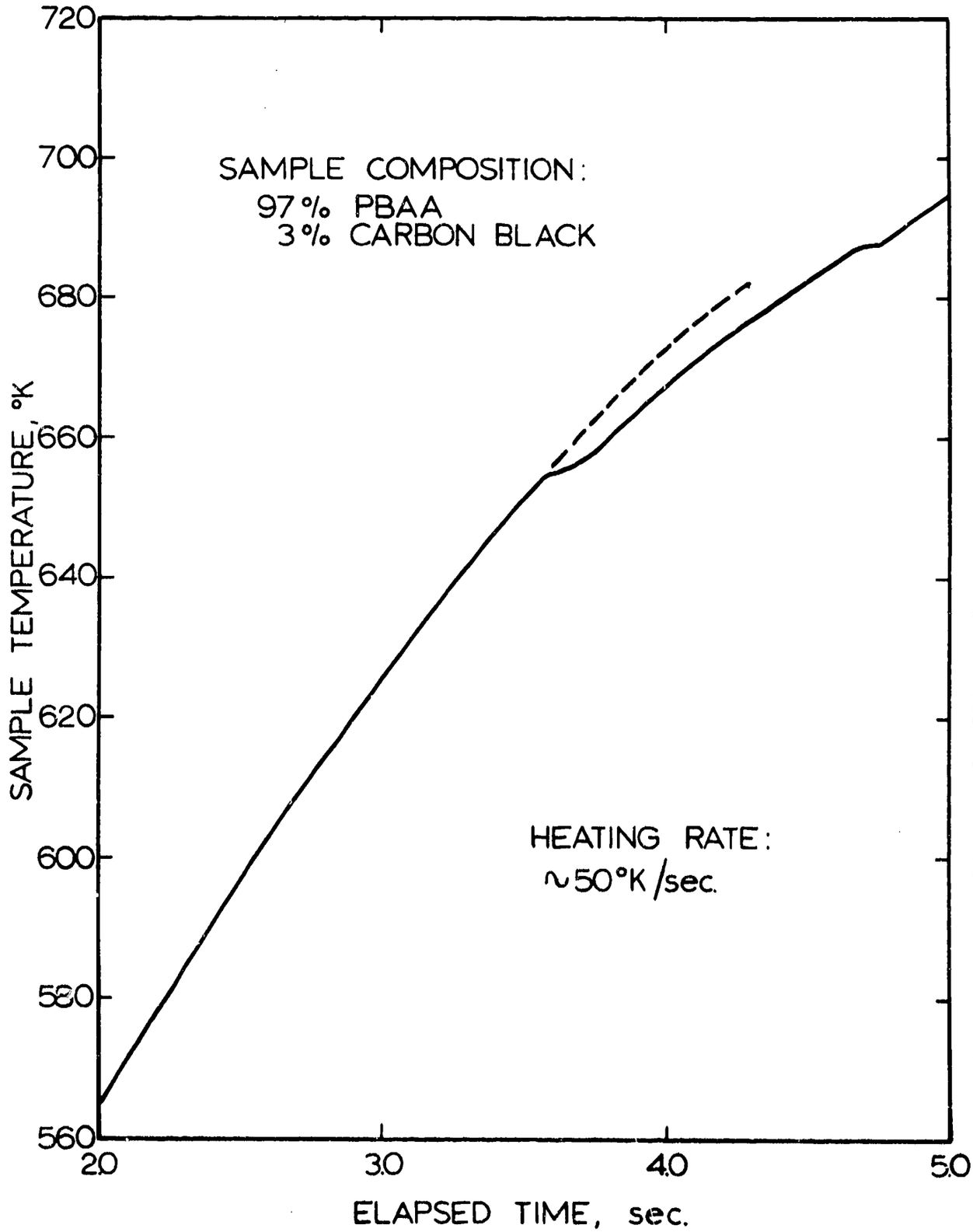

Figure 4. Temperature history of a PBAA sample.

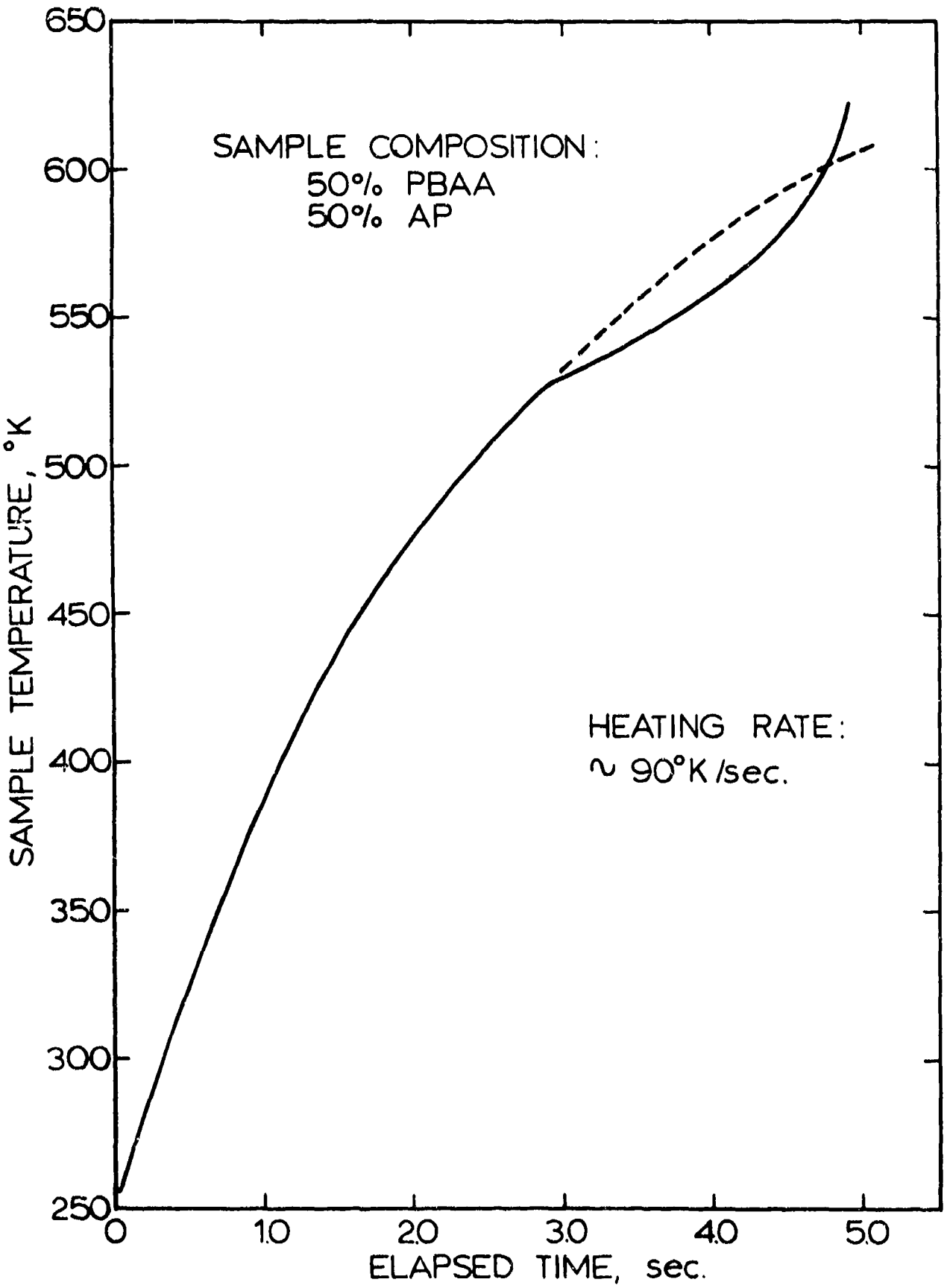

Figure 5. Temperature history of a 50% PBAA and 50% AP sample.

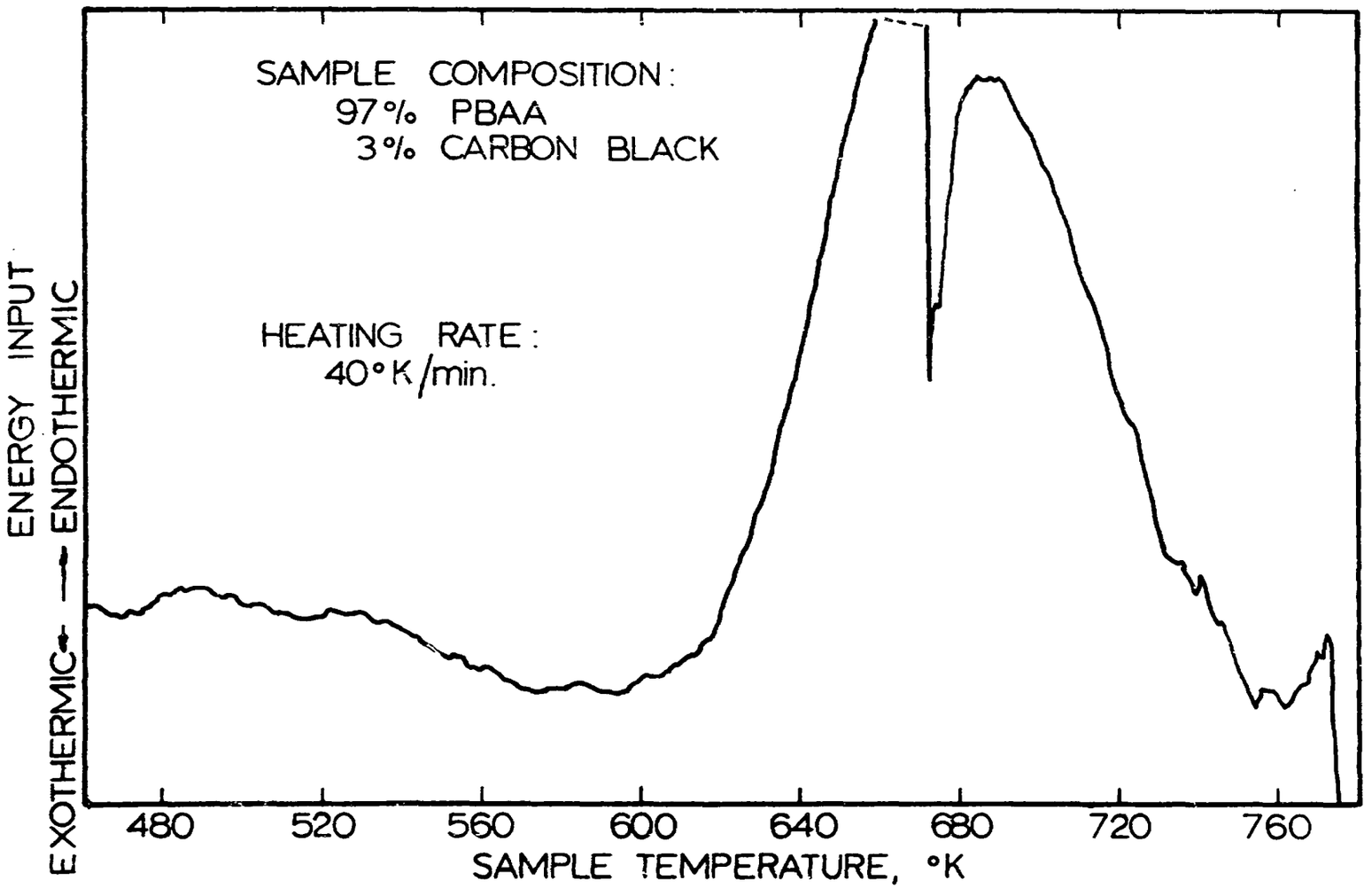

Figure 6. Differential Scanning Calorimeter data for a PBAA sample.

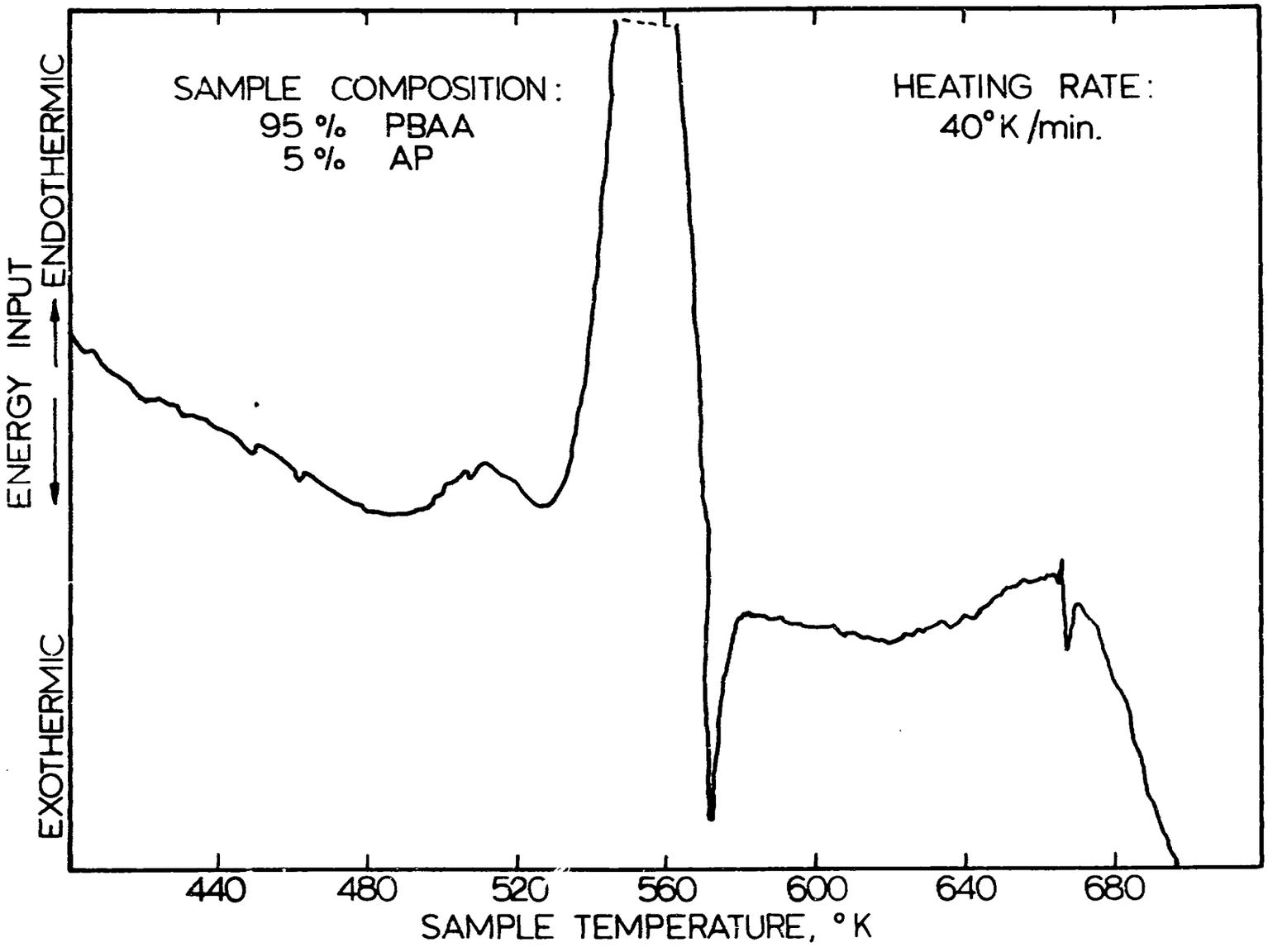

Figure 7. Differential Scanning Calorimeter data for a 95% PBAA and 5% AP sample.

UTEC TH 69-073b

THE CHEMISTRY AND MECHANICS OF COMBUSTION

WITH

APPLICATION TO ROCKET ENGINE SYSTEMS

Task 2 Flow and Heat Transfer

L. K. Isaacson

September 1969

College of Engineering
UNIVERSITY OF UTAH
Salt Lake City, Utah

PREFACE

Task 2, "Flow and Heat Transfer," of Project THEMIS at the University of Utah has been concerned with the study of a subsonic turbulent boundary layer with mass injection and combustion, and with the development of a supersonic combustion boundary layer channel for similar studies at supersonic speeds.

In the course of the subsonic combustion experiments a very strong coupling was found to exist between the velocity profile through the turbulent boundary layer and the external or free-stream favorable axial pressure gradient. This dynamic coupling amplifies the velocity overshoot observed in the turbulent boundary layer with combustion. Study of this interesting phenomenon is continuing.

Results obtained from the cooled constant temperature heat flux probe in the combustion experiments have indicated that turbulent bursts or eddies of hot gases are present in outer regions of the boundary layer much further from the surface than had previously been reported. These results lend support to the mixing jet theory of turbulent boundary layer structure which has gained popularity in the last few years.

The supersonic combustion facility is nearing completion. Detailed drawings of the combustion channel have been completed and fabrication will begin in the near future. The facility, exclusive of the channel, has been calibrated and the results are presented in this report.

TABLE OF CONTENTS

TASK 2 Flow and Heat Transfer

1.0 INTRODUCTION

One of the critical areas of analysis in present-day rocket engine systems design is concerned with accurately evaluating the convective heat transfer to the rocket nozzle surface. Methods still in use employ empirical correlations of data which were obtained in rather different environments. However, new computational techniques are being adapted for evaluating nozzle heat transfer characteristics.[1,2] These new methods are based upon numerical solutions of the governing differential equations and yield information concerning velocity and temperature profiles through the boundary layer in addition to surface skin friction and heat transfer. These techniques are much more powerful than previously used integral methods because the only input required are the boundary conditions and the turbulence transport characteristics since the boundary layers of interest are by and large of a turbulent nature.

Task 2 of Project THEMIS has been concerned with examining the characteristics of a subsonic turbulent boundary layer with mass injection and combustion with a two-fold objective in mind. First, the turbulent characteristics of the boundary layer, i.e. velocity profile, temperature profile, heat flux fluctuations, etc. would be obtained so that basic eddy viscosity or turbulent kinetic energy characteristics could be evaluated for an environment which had surface mass injection and large heat transfer to the surface. Second, the characteristics of a cooled constant temperature heat flux probe would be examined so that more confidence could be placed in its utilization as a diagnostic tool in relatively high temperature environments.

A second major area of interest under Task 2 is the extension of the study of the turbulent boundary layer with mass addition and combustion to the supersonic flow regime. To facilitate this extension, a supersonic combustion boundary layer facility is being developed. The facility, excluding the boundary layer channel, has been calibrated while fabrication of the channel and installation of the gas injection system is proceeding.

2.0 SUBSONIC TURBULENT BOUNDARY LAYER WITH COMBUSTION

During the past year the work on this area of the project has consisted of upgrading the facility to meet current experimental requirements and conducting an experimental program investigating the characteristics of a subsonic turbulent boundary layer with mass injection and combustion. This phase of the program is being carried out by Jerold W. Jones, a graduate research assistant in mechanical engineering.

The facility modification consisted of the redesign and instrumentation of the porous injection plates and the associated flow system. The redesign was needed to provide a system which was both more flexible and more reliable in terms of establishing reproducible test conditions. Early experiments showed that close control of both the injection rate and the composition were necessary to obtain good reproducibility. In addition, the instrumentation used in characterizing the flow field has been augmented to provide more rapid and reliable data acquisition. The facility and instrumentation are shown in Figures 1 and 2.

The experimental effort of this past year has had the dual purpose of considering the characteristics of the turbulent boundary layer with mass injection and combustion from both a phenomonological orientation considering the basic process of turbulent diffusion and a rather direct experimental investigation of the interaction of the combustion process and the dynamic flow field. It has been pointed out [3] that the basic factor in determining flame propagation in a turbulent stream is not combustion kinetics but rather turbulent diffusion. The cooled film probe presently in use in the subsonic combustion wind tunnel is particularly well suited to the study of the turbulent diffusion process in the presence of combustion as it is able to withstand the severe environment and provide sufficiently fast response to record turbulent fluctuations. At present the probe in use is limited by the pre-heating of the cooling fluid prior to its reaching the sensing element. Experimental techniques have been developed to compensate for this difficulty to a large measure. It should also be noted that cooled film probes with externally cooled

shields are available and one has been obtained for use in both the subsonic and supersonic facilities. This probe will provide experimental results which will give an accurate check on the results obtained from the original cooled sensor probe. The end result of this effort will be to provide the turbulent transport properties such as eddy diffusivity and turbulent Prandtl number required for accurate determination of skin friction and wall heat transfer.[4]

Recent developments in the computation of turbulent boundary layers (Reference 5) have indicated the possibility of computing the eddy viscosity distribution from the turbulent kinetic energy equation and the resulting possibility that the boundary layer development may be computed beginning at the initiation of the laminar boundary layer, through transition, and into the fully turbulent region with no requirement that the transition Reynolds number and eddy viscosity be specified. Methods of analysis based upon the turbulent kinetic energy equation depend upon experimental results for the modeling of the production and dissipation of turbulent kinetic energy through the boundary layer. Results of this type are scarce at present. Instrumentation has been obtained over the past year for obtaining turbulent kinetic energy data by both fluctuation intensity measurements and space-time correlation measurements using hot-film sensors. Initial experimental results will be obtained in a subsonic turbulent boundary layer with mass injection and compared with the NASA turbulent boundary layer computer program, which has been obtained by this laboratory from Langley Research

The second portion of the experimental research effort has produced some significant information on the interaction of the combustion process and the dynamic flow field.[6] These experiments have also been conducted in the subsonic combustion wind tunnel following test procedures outlined previously.[7] A schematic of the combustion test section is shown in Figure 3. It has been found that combustion in the boundary layer drastically alters the dynamic flow field. This occurs as a result of a strong density gradient induced by the energy release in the combustion process. Figure 4 shows a typical experimental temperature profile through the combusting turbulent boundary layer. As the maximum absolute temperature is approximately four

times that of the freestream temperature the corresponding density is one fourth that of the density in the freestream. This strong density gradient causes a pronounced change in the velocity profile through the boundary layer as shown in Figure 5. The broken line in this figure is a locus of data points representing the velocity profile in a turbulent boundary layer with mass injection but no combustion. The second curve, with the data represented by the circle symbols, is that for a turbulent boundary layer with mass injection and combustion but no axial pressure gradient. It may be observed that the velocity profile for this case lies to the left of that with no combustion between the wall and the flame zone and to the right in the region between the flame zone and the boundary layer edge. It should also be noted that there is a significant difference between the velocity profiles in the wall region. This change has a pronounced effect on the wall heat transfer and skin friction. Work reported by Wooldridge and Muzzy in 1965[8] for a similar case of injection and combustion with no axial pressure gradient shows a similar trend. However, the deviation of the combustion profile from the non-combustion profile is somewhat larger in the present experiment. Wooldridge and Muzzy attributed the difference between the combustion and non-combustion velocity profiles to a change in the character of the turbulent structure in a combustion zone. However, the current experimental results and preliminary analysis indicate that the strong density gradient may be more significant in producing a distorted velocity profile in the turbulent boundary layer with combustion than the contribution of a hypothesized change in the turbulent eddy structure. The third curve in Figure 5 with the data represented by the square symbols is for the case of mass injection, combustion and a favorable axial pressure gradient. This profile shows an even greater deviation from the non-combustion profile with the velocity within the boundary layer exceeding that of the freestream. The parameters shown in this figure are F, the ratio of the injected mass flux to the freestream mass flux, and β, a pressure gradient parameter. These parameters are defined as

$$F = \rho_w v_w / \rho_e u_e$$

$$\beta = \frac{2x}{u_e} \frac{du_e}{dx}$$

The distortion of the velocity profiles appears to be insensitive to the blowing parameter F, and rather dependent upon the density gradients produced by the combustion process for each injection rate.

It must be noted that the last case, that of injection, combustion, and a favorable axial pressure gradient, is most representative of the environments to be expected in applications.

The velocity overshoot observed here experimentally for the turbulent boundary layer with mass injection, combustion and an axial pressure gradient has been predicted analytically for a laminar boundary layer with mass addition, combustion, and an axial pressure gradient by Chen & Toong.[9] An analysis similar to that of Chen and Toong is presently underway. In this analysis the conservation equation for a subsonic turbulent boundary layer are first transformed by the Lees-Doroduitsyn transformations resulting in the following equations for momentum, energy and species;

Momentum Equation:

$$\left(\frac{\rho\mu}{\rho_e\mu_e}\,[1 + \varepsilon/\nu]f''\right)' + ff'' + \beta(\rho_e/\rho - [f']^2) = 0$$

Energy Equation:

$$\left(\frac{1}{Pr_t}\,\frac{\rho\mu}{\rho_e\mu_e}\,[1 + \frac{\varepsilon}{\nu}\,\frac{Pr}{Pr_t}]\;\theta'\right)' + f\,\theta' = 0$$

Species Equation:

$$\left(\frac{1}{Sc_T}\,\frac{\rho\mu}{\rho_e\mu_e}\,[1 + \frac{\varepsilon}{\nu}\,\frac{Sc}{Sc_T}]\;g'\right)' + fg' = 0$$

where f', θ, and g are normalized velocity, enthalpy and species concentration respactively. The prime (') indicates differentiation with respect to the transformed normal coordinate. Assuming the laminar and turbulent Lewis Numbers are unity, the energy and species relations are of the same form and a system of two non-linear ordinary differential equations describe the variation of the velocity, energy and species profiles in the direction normal to the surface. A slight extension of the work of Smith & Cebeci [10] allows an analytical

description of ε/ν, for the case under consideration, and thus the means of a numerical solution of the equations,

$$\left(\frac{\rho\mu}{\rho_e\mu_e}\,[1 + \varepsilon/\nu]f''\right)' + ff'' + \beta(\rho_e/\rho - [f']^2) = 0$$

and

$$\left(\frac{1}{Pr_t}\,\frac{\rho\mu}{\rho_e\mu_e}\,[1 + \varepsilon/\nu\,\frac{Pr}{Pr_t}]\,\theta'\right)' + f\,\theta' = 0$$

The development of this numerical procedure is now in progress.

3.0 CALIBRATION OF A SUPERSONIC COMBUSTION BOUNDARY-LEVEL FACILITY

The calibration of the supersonic combustion boundary-level facility has been completed. [11] This work has been completed by David Boyd and LaMar Moon. The facility is shown in Figure 7. Each of the components of the supersonic channel has been evaluated and tested to determine its operating characteristics. These components and their operating characteristics are discussed below.

3.1 *Plenum and Mixing Chamber*

The plenum and mixing chamber shown in Figure 8 is a cylindrical section which accepts air from the pebble-bed heater for the purpose of straightening the air and providing a uniform flow into the subsonic portion of the nozzle. Within the plenum and mixing chamber are four items of interest. They are:

1. The hot gas valve
2. The turbulence ring
3. The bypass air injector
4. The turbulence grid

The hot gas valve is a water cooled, flat-plate, flapper-type valve with a seat and flapper that do not affect a positive pressure seal but do prevent the hot gases in the pebble-bed heater from enter-

ing the channel during the heating cycle. The turbulence ring is perpendicular to the flow and is attached to the circumference of the plenum chamber by eight spokes. The ring helps straighten the flow as it emerges from the pebble-bed heater. The turbulence ring could also be used in the future as a fuel injector if the need arises for more heat addition to the flow. The bypass air injector mixes cold (room temperature or lower) air with the heated air from the pebble-bed heater thus allowing temperature regulation of the flow. The turbulence grid further straightens the flow and aids in equalizing the stream temperature after injection of the cold bypass air.

Cooling of the structural components of the plenum and mixing chamber is an important facet in the operation of the supersonic channel. All of these components are water-cooled and experiments have shown that water flow rates of 0.25 lbm/sec for the four components and 1.00 lbm/sec for the plenum and mixing chamber walls provide sufficient cooling for channel operation up to 1000°F. Much larger flow rates are available, thus providing for cooling at higher operating temperatures. At the low water flow rates, approximately 25 percent of the pebble-bed exit temperature is lost due to structural cooling by the time the flow has reached the test section.

The pebble-bed heater has the capacity of heating air to 2600°F. Thus, for high temperature operation, it is necessary not only to cool the channel components, but to cool the air before it is exhausted into the atmosphere. The cooling is accomplished by a heat exchanger downstream of the diffuser. The cooler capacity is 450 Btu/sec at a water flow rate of 60 Gpm. Experimentation has shown that the cooler does have the capacity to cool the exhaust to a safe temperature. At 1000°F channel operation the exhaust temperatures never rose above 120°F for flow rates as low as 5 Gpm of water.

3.2 *Nozzle Flow Characteristics*

Two nozzles are available for use with the supersonic combustion boundary-layer facility. The nozzles were fabricated for operation at Mach number of 2.5 and 3.0, respectively, with the total temperature not to exceed 1500 F. Both nozzles are converging-diverging two-

dimensional types with a continuous contour on the bottom side and a flat plate on the top side. This type of nozzle design was used so that any particles in the flow would be accelerated downward away from the top flat plate where sensitive probes will be in use. The nozzles are water cooled and experimentation has shown that the cooling is sufficient for present channel operation. The supersonic channel is equipped with an air ejector that is capable of pulling a vacuum of over five psi in the present free jet test section.

Experiments using the Mach 2.5 nozzle have shown that separation is occurring at the top side of the nozzle due to a mismatch between the free-jet test and the diffusion section. With the new solid wall test section there will be no mismatch and the problem of separation will be eliminated since it will be possible to establish the flow by over-pressurization of the test section and driving the starting normal shock to a stable position in the diffuser.

At the present time the highest Mach number achieved in the test section is M = 1.82.

3.3 *Mass Injection Test Section*

The supersonic combustion boundary-layer facility was constructed in order that the problems of air-fuel mixing, ignition, and combustion in a supersonic flow could be studied. The simulation mass injection test section has been designed to accommodate these different studies.

The test section will be 1.50 inches high, 2.75 inches wide, and 21.0 inches long. There will be eight viewing ports (four on each side) that allow viewing of ignition and mass injection. The top wall of the test section will consist of a built up injection plate and a solid plate fabricated from stainless steel. The top wall of the test section will be turned up at an angle of 2½° from the parallel nozzle flow. Fernandez and Zukoski [12] have stated that the external flow produced by injection resembles that produced by a wall which turns towards the flow through a small angle. The maximum angle from mass injection in the test section will be of the order of 2 to 3°. Thus by turning the wall away from the flow by this amount the strong oblique shock at the start of the injection can be avoided. At flow

rates causing lesser angles an expansion fan will be present that can be compensated for by a movable bottom wall of the test section. An ignition plate adaptable to various ignition systems will be incorporated ahead of the test section.

A gas manifold will be provided over the porous plate. The manifold will be constructed of three chambers, isolated from each other so that one, two, or three of the chambers can be used for mass injection, thus giving different injection lengths. The mass injection plate will be instrumented with thermocouples and the entire test section will be water cooled providing a control volume for an energy balance. The bottom of the test section will have several probe access ports that will allow probing of the turbulent boundary layer along the full length of the test section. The present traversing mechanism will support the probes and allow an automatic traverse of the flowstream and boundary layer.

Combustion in the test section will increase the static pressure and thicken the boundary layer. The test section, having a variable bottom wall, can be adjusted to account for this increase in boundary layer thickness and thus provide a stable flow.

At the present time the complete design of the mass injection test section has been completed and installation by Edrede Company will be accomplished in August.

REFERENCES

1. Isaacson, L. K. and Erickson, R. D., "Laminar Boundary Layer and Heat Transfer Analysis of Solid Propellant Rocket Motors," Report Ref. 17-10203/6/40-893, Hercules Incorporated, Bacchus, Utah, 7 August 1968.

1. Isaacson, L. K., "Development of the Turbulent Boundary Layer Equations for Submerged Nozzle Rocket Motors," Report Ref. 17-10203/6/40-895, Hercules Incorporated, Bacchus, Utah, 7 November, 1968.

3. Shchentinkov, E. S., "Calculation of Flame Propagation in a Turbulent Flow," Combustion in Turbulent Flow, L. N. Khitrin, ed. NSF Translation from Russian Akademiny Nauk SSSR.

4. Smith, T. H., "Hot-Film Characteristics in a Turbulent Boundary Layer with Foreign-Gas Injection," Ph.D. dissertation, Department of Mechanical Engineering, June 1969.

5. Beckwith, I. E. and Bushnell, D. M., "Detailed Description and Results of a Method for Computing Mean and Fluctuating Quantities in Turbulent Boundary Layers," NASA TN D-4815, October 1968.

6. Jones, J. W. and Isaacson, L. K., "Thermal-Dynamic Coupling in a Turbulent Boundary Layer with Mass Injection and Combustion" Project THEMIS Report, UTEC TH-69-076, College of Engineering, University of Utah, June, 1969.

7. Project THEMIS Annual Report, UTEC-DO-68-065, Task 2, Section 3, University of Utah, College of Engineering, October 1968, Salt Lake City, Utah.

8. Wooldridge, C. E. and Muzzy, R. J., "Measurements in a Turbulent Boundary Layer with Porous Wall Injection," Tenth (International) Combustion Symposium, Cambridge University, Cambridge, England, August 1964.

9. Chen, T. N. and Toong, T. Y., "Laminar Boundary Layer Wedge Flows with Evaporation and Combustion," Progress in Astronautics and Aeronautics. 15. Hetrogeneous Combustion, p. 463.

10. Cebeci, T., Smith, A. M. D. and Mosiniskis, G., "Calculation of Compressible Adiabatic Turbulent Boundary Layers," AIAA Paper No. 69-687, AIAA Fluid and Plasma Dynamics Conference, San Francisco, California, June 16 - 18, 1969.

11. Boyd, D. L., "Theoretical and Experimental Performance of a Supersonic Combustion Boundary Layer Facility", Project THEMIS Report, UTEC TH-69-064, College of Engineering, University of Utah, June 1969.

12. Fernandez, F. L. and Zukoski, E. E., "Experiments in Supersonic Turbulent Flow with Large Distributed Surface Injection," Report No. 68-129, AIAA, January, 1968.

LIST OF FIGURES

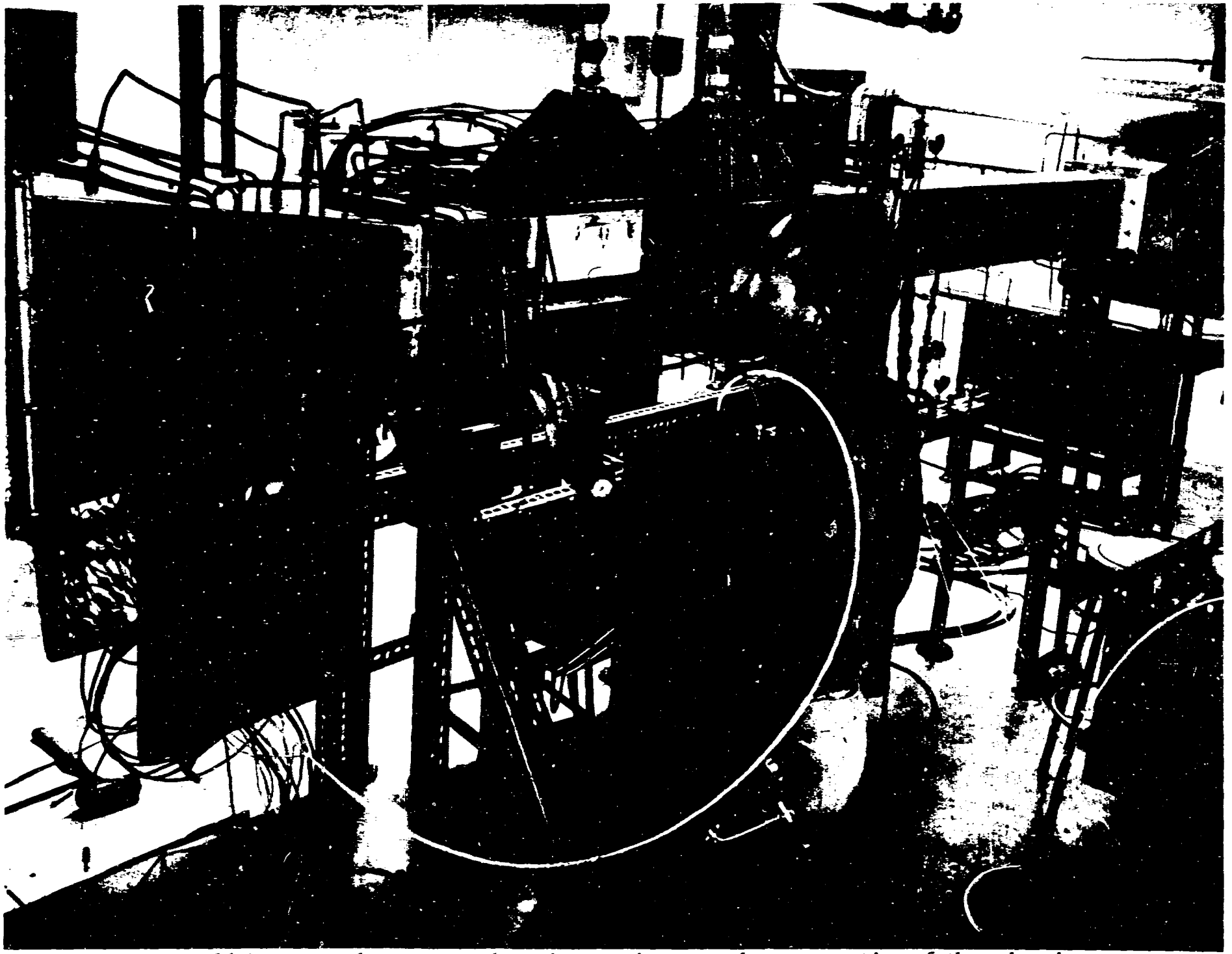

Figure 1. Mr. Jerold Jones, graduate research assistant, inspects the test section of the subsonic combustion wind tunnel.

Figure 2. Instrumentation for the subsonic combustion experiments including the constant temperature anemometer, correlator, FM tape recorder, and dual beam oscilloscope.

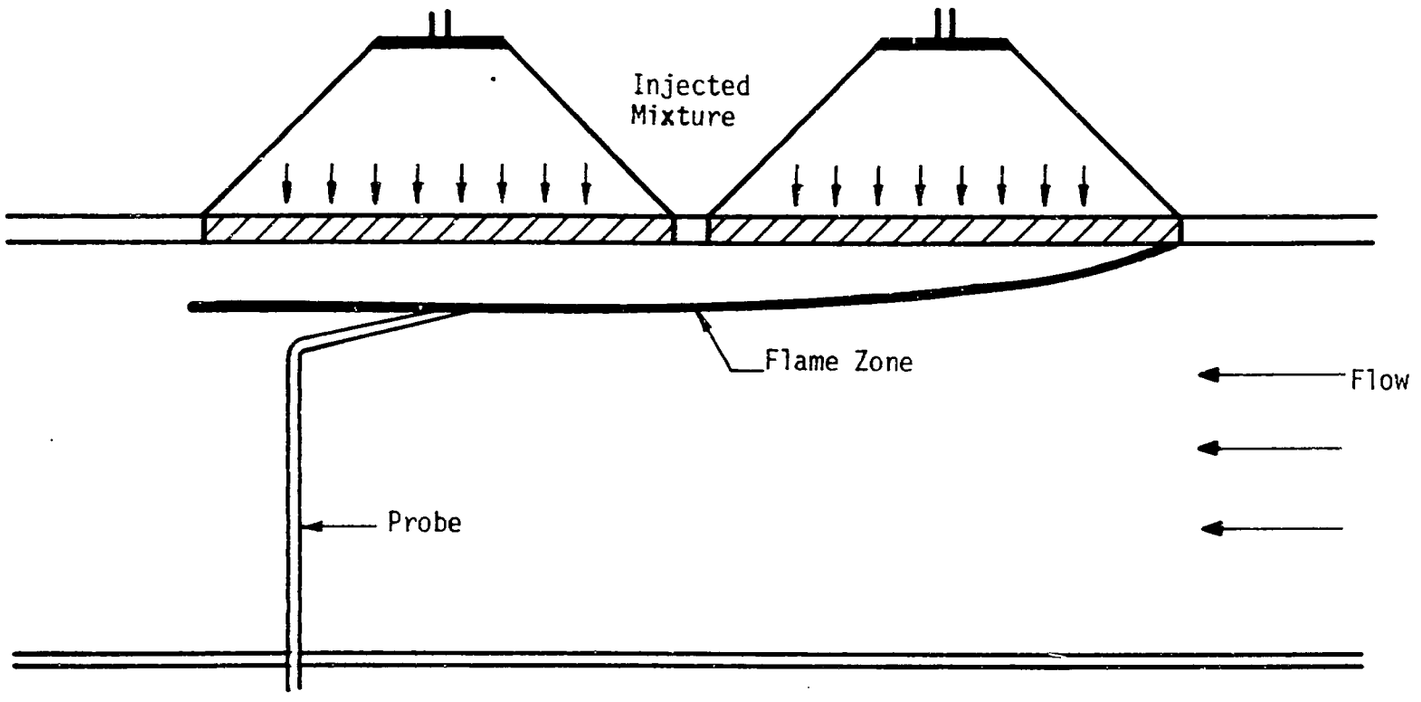

Figure 3. Schematic diagram of the subsonic combustion wind tunnel with combustion occurring in the boundary layer.

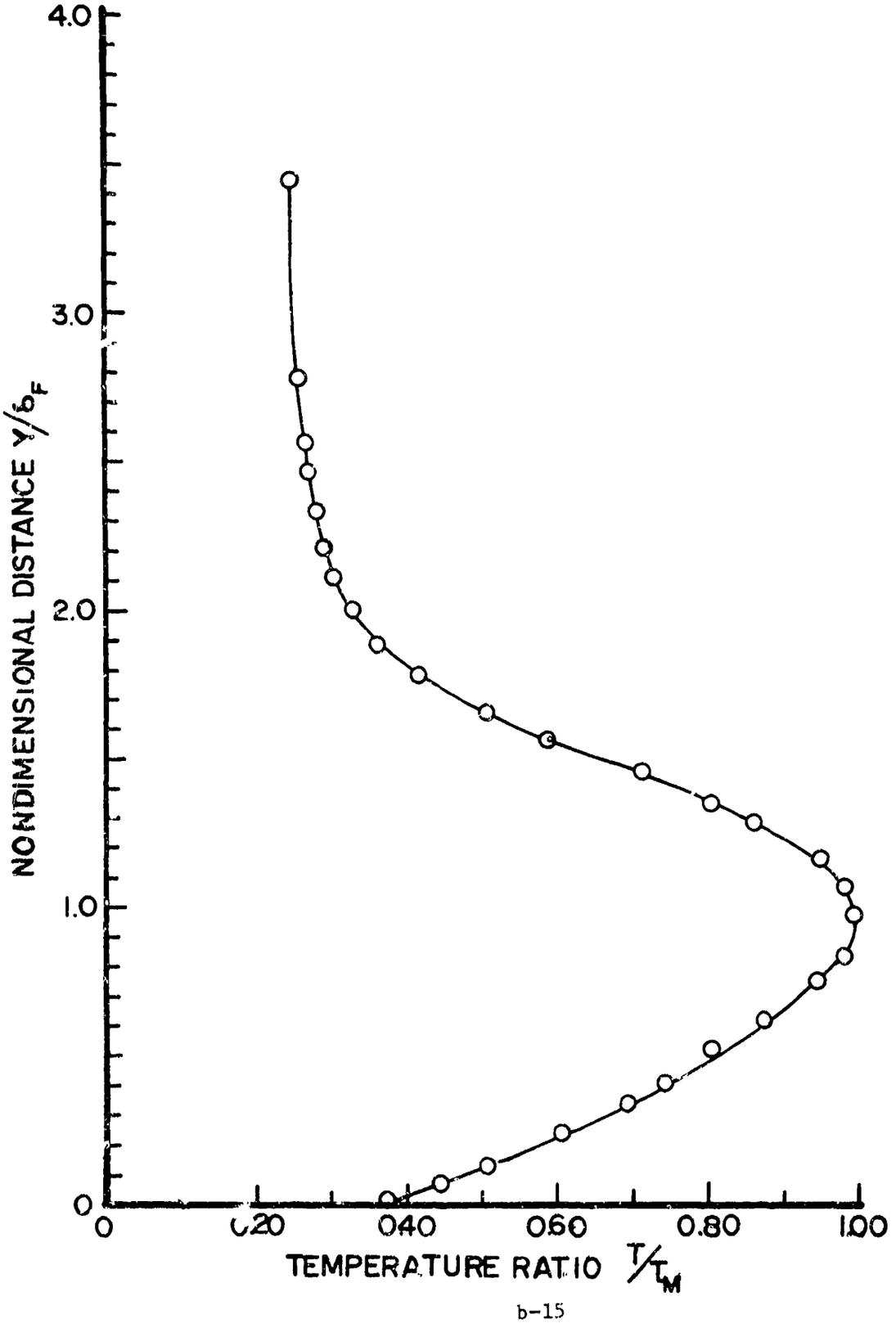

Figure 4. Temperature profile through the subsonic turbulent boundary layer with mass injection and combustion.

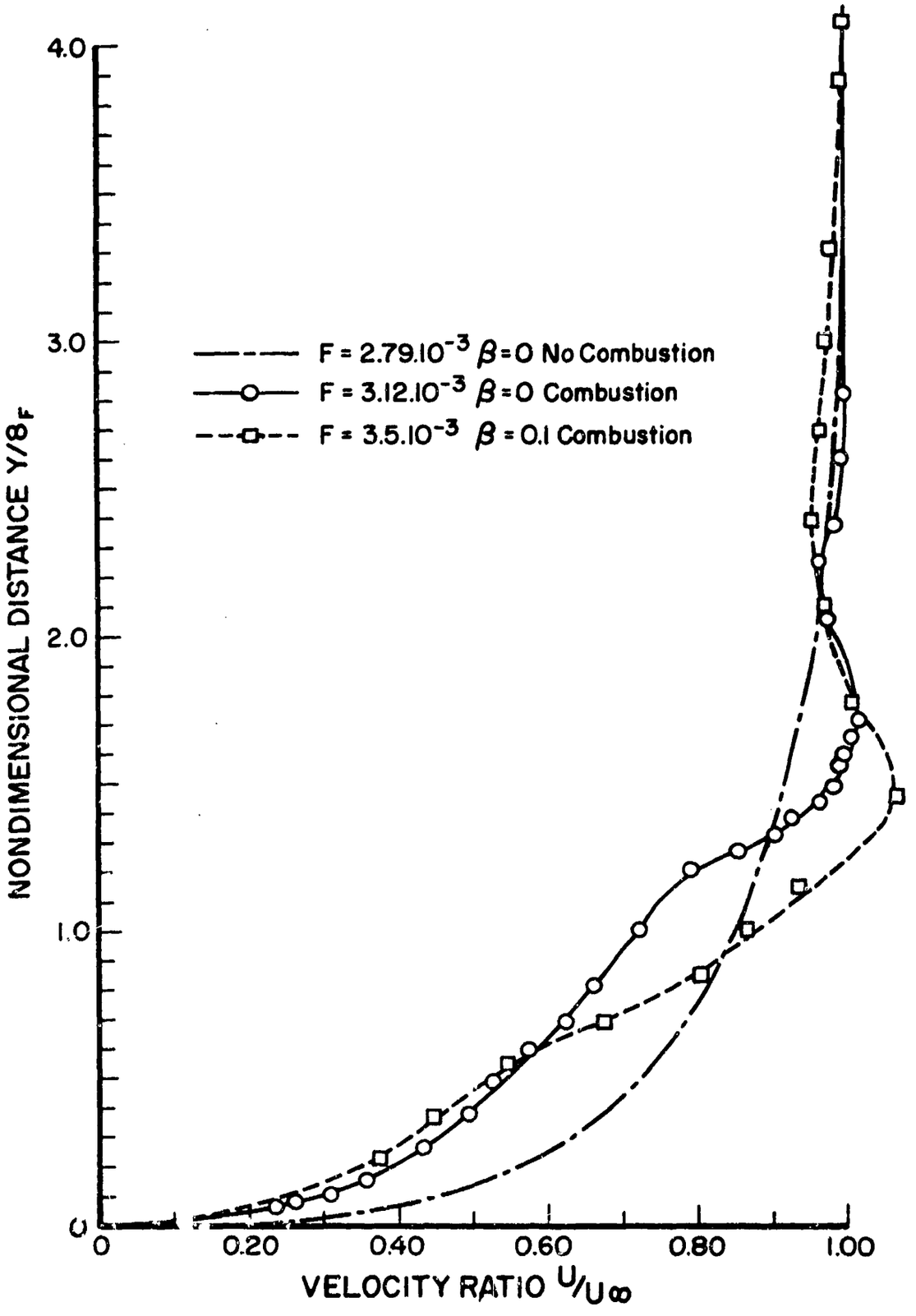

Figure 5. Velocity profiles through the subsonic turbulent boundary layer with mass injection and combustion. Non-combustion profile indicated for comparison.

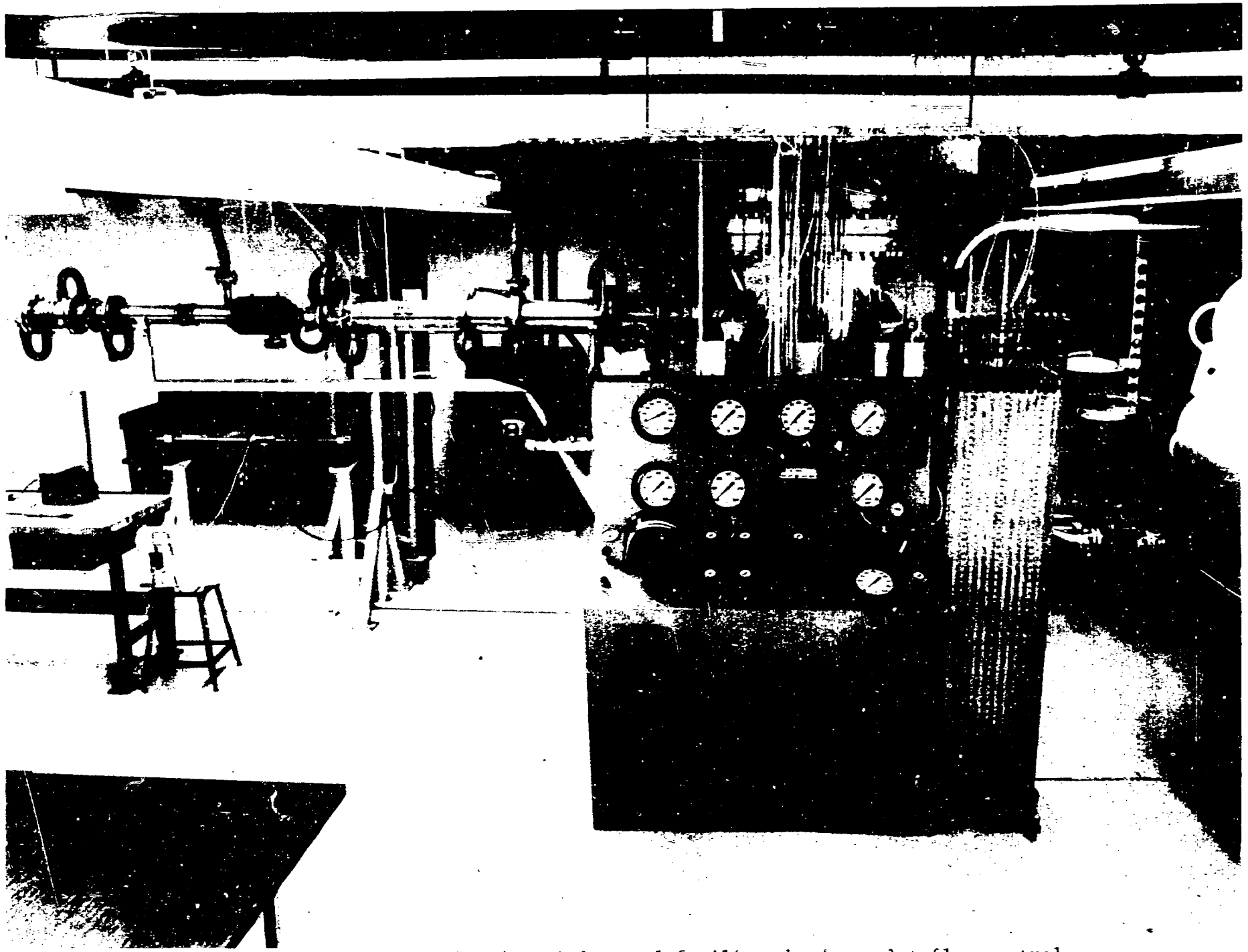

Figure 6. Mach 2.5 to 3.0 supersonic combustion wind tunnel facility showing inlet flow control valves, pebble-bed heater, tunnel, and control console.

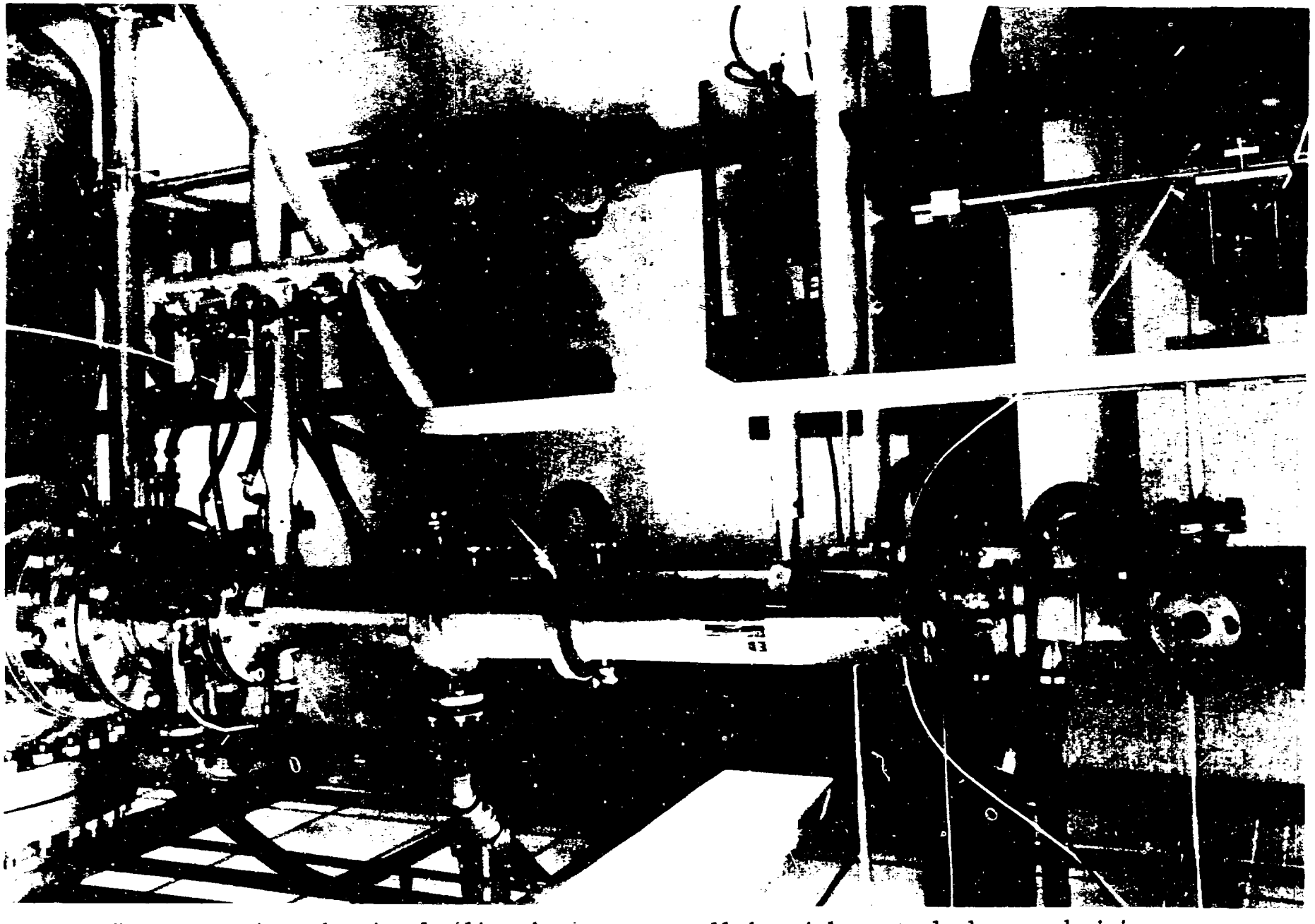

Figure 7. Supersonic combustion facility showing water-colled stainless steel plenum and mixing chamber and the water-cooled nozzle. The plenum and mixing chamber is designed for steady flow operation at a maximum pressure of 200 psia and a temperature of 2500°F.

UTEC TH 69-073c

THE CHEMISTRY AND MECHANICS OF COMBUSTION

WITH

APPLICATION TO ROCKET ENGINE SYSTEMS

Task 3 Ablation Mechanisms

J. D. Seader

September 1969

College of Engineering
UNIVERSITY OF UTAH
Salt Lake City, Utah

PREFACE

This task involves an experimental and analytical investigation of the thermal response of ablative materials to the mechanics and chemistry of combustible gas flow in certain components of a rocket motor system, as for example, nozzles. Particular attention is being focused upon the following important aspects:

Phase I: The interdependent effects of pyrolysis, surface chemical attack, and boundary layer combustion.

Phase II: The kinetics of subsurface reactions.

Phase III: The effects of surface-active agents to minimize and make more uniform the surface attack.

The general approach being taken involves an understanding of the important kinetic, transport, and surface effects at a molecular structure and interaction level. Chemical catalysis is being utilized to provide additional degrees of freedom for the development of optimal ablative structures.

During the 1968-1969 academic year, a number of high temperature polymers were obtained and effort was begun to perform thermogravimetric and effluent gas analyses. The quasilinearization technique is being applied to the data to determine pyrolysis kinetic parameters. After considerable delay, a high temperature, high pressure gas flow facility was delivered and is being installed in a specially designed tunnel for hazardous experiments. Analytical techniques for characterizing surface ablation involving melt layer flow were investigated and experiments were designed for securing the necessary property data.

It should be noted, before presenting detailed discussions covering the three phases, that this task in closely related to Task 2. In addition, the consultation with Professors R. H. Boyd, J. H. Futrell, A. D. Baer, and N. W. Ryan is acknowledged.

TABLE OF CONTENTS

TASK 3 Ablation Mechanisms

PHASE I INTERDEPENDENT EFFECTS OF PYROLYSIS, SURFACE CHEMICAL ATTACK AND BOUNDARY LAYER COMBUSTION — N. Burningham*

1.0 INTRODUCTION

The long range objective of this phase of the Task 3 program is an investigation of the thermal response of ablative materials to coupled environments, including both inert and combustive atmospheres. The contribution to this objective of the work reported here includes thermogravimetric analysis (TGA) of new high-temperature polymers, identification of pyrolysis gas species, and the use of these data to illuminate the kinetics of the decomposition mechanism. The present report summarizes progress in these fields made between September 1968 and May 1969.

The work accomplished can be outlined briefly as follows:

1. Development of TGA techniques and procedures, and calibration of all associated equipment.
2. Application of quasi-linearization to the numerical determination of kinetic parameters from TGA data.
3. Collection of thermograms, primarily in air, for phenolic, epoxy and polyimide resins.
4. Selection of chromatographic columns and sampling procedures appropriate to analysis of pyrolysis gas species.

This effort is providing the foundation for continued investigation of the interdependent effects of transpiring pyrolysis products,

---

* Mr. Norman W. Burningham received a B.S. degree in Chemical Engineering in 1960 from Princeton University with Honors in Engineering, and an M.S. degree in the same field from the University of Denver in 1965 where his thesis was entitled "Analysis of an Internally Ablating Heat Shield." He has also attended the University of Colorado and the California Institute of Technology. From 1961 to 1966 he was employed by the Martin Company, where he made significant technical contributions in the research and development of advanced high temperature composite materials. Since 1966, he has been on leave from the Martin Company to pursue a Ph.D. degree at the University of Utah. He began work on Project THEMIS in September 1967.

surface chemical attack and boundary layer combustion. For example, the determined kinetic parameters and pyrolysis gas species are input data to an existing one-dimensional ablation computer program which will be used to predict ablation performance in coupled environments.

2.0 THERMOGRAVIMETRIC ANALYSIS

The TGA equipment components, described more completely in the previous annual report, include a Cahn Model RG Automatic Recording Electrobalance, a Marshall Model 1133 base-metal furnace, an F & M Model 240M-25 Temperature Programmer, a Mosely Model 7001A X-Y Plotter and a Leeds and Northrup Speedomax W Stripchart Recorder.

The electrobalance is presently housed in a pyrex vessel suitable for flow-through operation at atmospheric or reduced pressures. The containing vessel is connected to a helium source through a precision flow valve and a two-stage, high pressure regulator. This gas delivery system is able to provide helium to sweep pyrolysis gases to collection vessels at very low flow rates, on the order of 10 cm/min in a 19 mm diameter hang-down tube. Because of the high sensitivity of the balance, it is essential that the gas flow rate be absolutely constant or resulting drag-induced noise may void an experiment.

The experimental procedure normally employed involves the suspension of a polymer sample weighing in the range of 1 mg to 20 mg on a platinum pan connected to the balance by a nichrome or tungsten wire. The samples have been mechanically ground and sized previously. Those particles which pass a 40 mesh screen are used in the experiment. Samples are heated at a programmed rate from room temperature to approximately 900°C at atmospheric pressure with helium gas sweeping the sample. A chromel-alumel thermocouple is suspended immediately above the sample pan. Both temperature and weight loss are automatically recorded as functions of time.

2.1 *Problems in Thermogravimetric Analysis*

Thermogravimetric analysis can be conducted by two basic methods. In recent years dynamic TGA has been the most common technique. Dynamic TGA provides weight loss information as a function of temperature over a relatively wide temperature range. Isothermal or static TGA yields weight data as a function of time at a fixed temperature obtained after a short period during which the sample is rapidly heated. While the dynamic technique is desirable because it generates data much more rapidly than the static method, both approaches used together are necessary for the successful analysis of complex decomposition mechanisms. Seader [1] has shown the value of the combined method in the case of the autocatalytic decomposition of polystyrene.

Another factor, which multiplies the number of experiments necessary, is the observation that significant irregularities in dynamically-produced thermograms can be completely obscured by an inopportune choice of heating rate. Such errors usually result from heating rates which are too large. However, this phenomena is completely relative and a heating rate appropriate for one transition might obscure another. Nevertheless, dynamic measurements are still attractive in surveying rapidly the complete thermal behavior, and results obtained yield, among other things, information as to regions which might be studied dynamically at lower heating rates or isothermally.

Thermogravimetric measurements are subject to errors which have been discussed at length by other authors. [2], [3], [4] Many possible errors have been avoided in the present work by the choice of equipment and experimental procedures. However, those errors remaining arise generally from convection, currents, measurement of temperature the effect of atmosphere, and changes in buoyancy.

The Cahn electrobalance nulls out buoyancy effects at the beginning of the experiment. As the environmental gas reaches increasingly higher temperatures, buoyancy effects obviously change. This error has been minimized by using small samples and selecting helium as the sweep gas. In addition, a blank thermogram is obtained

on an inert material and the resulting buoyancy changes subtracted from later data.

The problem of temperature measurement has negated the value of some published experiments. The most frequent discrepancies occur when the recorded temperature does not closely represent the sample temperature, or the sample temperature is not uniform. Temperature uniformity has been obtained by using very small, finely-divided samples. Suspension of rapidly responding thermocouples located very near the resin sample minimize temperature measurement error, which is believed to be small with respect to the magnitude of the temperature.

Readout noise in the weight measurement arising from turbulence or convection within the apparatus can seriously reduce the precision of data. Figure 1 illustrates the experimentally determined peak-to-peak noise resulting from a change in diameter of the hangdown tube in which the sample is suspended at atmospheric pressure. These data represent a non-flow situation. Figure 2 illustrates how noise in larger diameter tubes can be decreased by reducing the pressure in the apparatus. (5) It is also reported in the literature that a flow system exhibits essentially the same noise levels as those shown if low flow rates can be carefully controlled. (5)

The effects of other experimentally limiting problems such as static electricity and background building vibrations have been reduced by electrically grounding the system and by the use of vibration insulation.

The objectives of TGA experimentation are to generate thermograms from which a kinetic model can be formulated which describes thermal decomposition, and to provide pyrolysis gases evolved as a function of decomposition temperature. These data will be used in formulating and verifying postulated mechanisms of pyrolysis. Even though previous investigators have determined Arrhenius type power-law rate equations from TGA data, no attempt has been made to correlate these equations with actual decomposition processes. Such a correlation will be attempted from data obtained in this program.

Madorsky [6] has pointed out that for a complete understanding of the mechanism involved in the thermal degradation of organic polymers, it is essential to know:

1. The change in molecular weight of the polymer as a function of temperature and extent of degradation.
2. The qualitative and quantitative composition of volatile and non-volatile products of degradation.
3. The rates and activation energies of the process.

It is not always possible to obtain the aforementioned experimental data from pyrolysis work. For example, molecular weight determination usually requires solution techniques. However, residues obtained during pyrolysis, especially of aromatic heterocyclic polymers, are usually insoluble. Compositions of volatile fractions can be obtained by gas chromatography and mass spectroscopy, and TGA can provide information on activation energies and kinetic rates of the processes involved.

In the present program a number of TGA experiments have been conducted on phenolic, epoxy, and polyimide polymers. Thus far, tests have been run primarily in air but essentially all future work will be done using inert helium environments. Table 1 summarizes the TGA experiments which have been made to date. Also, Figure 3 illustrates representative TGA data which have been obtained.

The thermogram for the phenolic resin shown is typical of phenol-formaldehyde polycondensates which have been cured at low temperatures and have a relatively low degree of crosslinking. The initial weight loss is attributable to unreacted, low molecular weight fragments and included volatile materials such as water. The more drastic loss initiating at about 375°C is the result of random thermal chain scission of the aliphatic linkages and resulting loss of volatile fragments.

The polyimide thermogram reflects the higher cure temperature and greater thermal stability associated with aromatic polymers in

TABLE 1

Summary of TGA Experimentation

Material	Environment	Temperature Rise Rate °C/min
Epoxy:		
DEN-438	Air	15, 7.5
EPON-828	Air	15, 7.5
Phenolic:		
SC-1008	Air	15, 7.5, 4
	Helium	10
USP-502	Air	15, 10
Polyimide:		
Skybond 700	Air	10,5
Polyquinoxaline:		
NOL-I	Air	10

that no major weight loss is observed until about 480°C. Both the phenolic and polyimide resins yield relatively large residual char fractions.

2.2 *Analysis of Thermogravimetric Data*

Several approaches to the mathematical analysis of experimental TGA data were included in the previous report. The review of the subject by Flynn and Wall [7] is particularly comprehensive. A recently developed numerical method employing optimization procedures to determine kinetic parameters is the quasilinearization technique of Bellman and Kalaba. [8], [9]

Quasilinearization is a powerful analytical tool which offers three significant advantages over most of the presently employed techniques for analysis of TGA data:

1. It is not necessary to maintain a constant rate temperature rise during the experiment. A completely flexible temperature history, including periods of differing rates of temperature rise and even isothermal segments, can be successfully handled. The increased analytical flexibility greatly extends the types of experimentation possible.
2. Multiple experimental runs may be combined in a single analysis if desired. That is, similar experimental thermograms for a given material may be collectively analyzed to yield a single set of optimized kinetic parameters.
3. Inaccurate handling procedures such as data plotting and slope measurement errors are completely avoided.

In applying quasilinearization to TGA data, a power law rate function of the type shown in Equation (1) is usually assumed.

$$-\frac{1}{w_o}\frac{dw}{dt} = k\left[\frac{w - w_f}{w_o}\right]^n \qquad (1)$$

where w_o = initial weight of polymer,

w_f = final weight of residue after complete degradation,

w = instantaneous weight of polymer-residue material during the degradation process,

t = time

n = kinetic order of the degradation reaction.

Equation (1) assumes the degradation process is simple and irreversible and it may be written

$$-\frac{dW}{dt} = k\,W^n \tag{2}$$

where k = specific rate constant and $W = (w - w_f)/w_o$. The rate constant k is assumed to depend on the absolute temperature according to the Arrhenius law

$$k = Ae^{-\frac{E}{RT}} \tag{3}$$

where A = pre-exponential factor,

E = activation energy,

R = universal gas constant,

T = absolute temperature.

The problem of determining the kinetic parameters A, E, and n in Equation (2) is transformed into the following equivalent problem:

$$\frac{dW}{dt} = -Ae^{-\frac{E}{RT}} W^n \,,\quad W(0) = 1 - \frac{w_f}{w_o} \tag{4}$$

$$\frac{dA}{dt} = 0 \,,\quad A(0) = A_o \,; \tag{5}$$

$$\frac{dE}{dt} = 0 \,,\quad E(0) = E_o; \tag{6}$$

$$\frac{dn}{dt} = 0 \,,\quad n(0) = n_o \,; \tag{7}$$

$$\frac{dT}{dt} = \rho \,,\quad T(0) = T_o \,,$$

where ρ is a known function of time. The latter equation is equivalent to having

$$T = \phi(t) \ , \ T(0) = T_o .$$

The system of Equations (4) to (7) are linearized by converting them into sequences which, hopefully, will converge rapidly to the best values of the kinetic parameters. For example:

$$\frac{dW^{i+1}}{dt} = \frac{dW^i}{dt} + \frac{\partial(\frac{dW^i}{dt})}{\partial W^i} (W^{i+1} - W^i) + \frac{\partial(\frac{dW^i}{dt})}{\partial A^i} (A^{i+1} - A^i) +$$

$$\frac{\partial(\frac{dW^i}{dt})}{\partial E^i} (E^{i+1} - E^i) + \frac{\partial(\frac{dW^i}{dt})}{\partial n^i} (n^{i+1} - n^i) + \text{ignored higher-order terms.} \quad (9)$$

Thus, if

$$\frac{dW}{dt} = f(W,A,E,n), \quad (10)$$

then

$$\frac{dW^{i+1}}{dt} = f(W^i,A^i,E^i,n^i) + \frac{\partial f^i}{\partial W^i} (W^{i+1} - W^i) + \frac{\partial f^i}{\partial A^i} (A^{i+1} - A^i) +$$

$$\frac{\partial f^i}{\partial E^i} (E^{i+1} - E^i) + \frac{\partial f^i}{\partial n^i} (n^{i+1} - n^i) \ , \quad (11)$$

where the i superscripts indicate the particular iteration. In expanded form Equation (11) becomes

$$\frac{dW^{i+1}}{dt} = - [A^i e^{-E^i/RT} (W^i)^{n^i} + n^i A^i e^{-E^i/RT} (W^i)^{n^i-1} (W^{i+1} - W^i)$$

$$+ e^{-E^i/RT} (W^i)^{n^i} (A^{i+1} - A^i) - \frac{A^i}{RT} e^{-E^i/RT} (W^i)^{n^i} (E^{i+1} - E^i)$$

$$+ A^i e^{-E^i/RT} \ln W^i (W^i)^{n^i} (n^{i+1} - n^i)] \quad (12)$$

and

$$\frac{dA^{i+1}}{dt} = 0 \ , \tag{13}$$

$$\frac{dE^{i+1}}{dt} = 0 \ , \tag{14}$$

$$\frac{dn^{i+1}}{dt} = 0 \ . \tag{15}$$

The iterative procedure is initiated by assuming values of A^{o}, E^{o}, and n^{o} and solving Equation (4) by the Runge-Kutta numerical procedure for $W^{o}(t)$. Setting $i = 0$, the linear differential Equations (12) to (15) are solved for $W^{1}(t)$, A^{1}, E^{1}, and n^{1} by the usual procedure of forming a particular and homogeneous solution. In general,

$$W^{i+1}(t) = p^{i+1}(t) + \alpha_1^{i+1} h_1^{i+1}(t) + \alpha_2^{i+1} h_2^{i+1}(t) +$$

$$\alpha_3^{i+1} h_3^{i+1}(t). \tag{16}$$

For each interation, the method of least squares is utilized to determine the values of α_j^{i+1} such that the objective function is minimized:

$$Q = \sum \left[W^{i+1}(t_k) - W_{k_{data}} \right]^2 , \tag{17}$$

where $W^{i+1}(t_k)$ are the computed points and $W_{k_{data}}$ are the corresponding data points for the particular times. The resulting α values are related to the next set of kinetic parameters.

The iterations are continued until the kinetic parameters A,E, and n converge to reasonable tolerances. Preferably, more than one thermogram should be utilized. In this case, a set of equations of the form of Equation (12) is solved--one for each thermogram. The objective function given by Equation (17) is then expanded to include all data sets.

3.0 PYROLYSIS GAS ANALYSIS

The purpose of a detailed species analysis of the volatile products of thermal decomposition is twofold. First, a knowledge of the gases evolved as a function of pyrolysis temperature provides direct evidence as to the chemical reactions taking place in the decomposition. The temperature associated with the production of a given gas is also an indication of the energy of the bonds being broken. However, because of the complexity of the possible reactions, it is very difficult to verify a unique mechanism of reaction. Secondly, pyrolysis gas identification is input data for the ablation computer programs which will be used to predict ablation performance in velocity-coupled environments.

Other investigators have used a gas analysis approach as a key to postulate decomposition mechanisms. [10], [11] Most reported work has been concerned with the mechanism of oxidative decomposition as the researchers argued that oxygen was present in all real applications of ablative materials. However, a large body of data indicate that while oxidative attacks may be significant at the surface, there is very little, if any, oxygen penetration into the body of a char-forming ablator. For this reason most experiments conducted in this program are being made in an inert environment. It should also be noted that the mechanisms associated with oxidative and non-oxidative decomposition are not the same.

Thus far in the program only a limited amount of preliminary data have been collected on gas analysis. Gas samples, swept into collection flasks by helium carrier gas were injected into a Perkin-Elmer gas chromatograph. Columns filled with treated silicon and carbon have been used to study gases collected from SC-1008 phenolic and Skybond 700 polyimide resin.

The analysis of the phenolic produced gas conformed to expectations as CH_4, H_2, CO predominated with lesser amounts of H_2O, aliphatic and unsaturated hydrocarbons. Phenols and cresols were

not observed. This is probably due to the high-temperature cure cycle of SC-1008 resin which promotes extensive crosslinking and drives off unreacted elements.

Primary species resulting from polyimide decomposition were found to be H_2, CO, CO_2, HCN, with lesser amounts of CH_4, H_2O and NH_3. Also approximately 7% of the sample was made up of larger molecular weight compounds not successfully identified. As an example of the type of questions which arise, the origin of CO_2 was considered. Skybond 700 has a general structure as shown below.

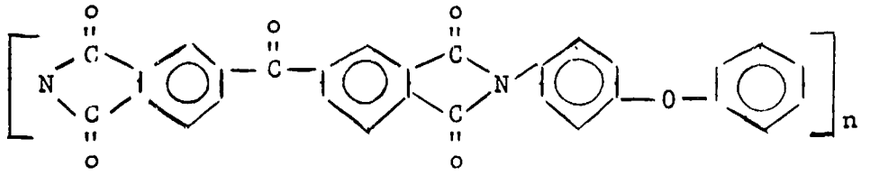

CO can easily arise from degradation of the benzophenone substructure, from the phenyl ether or from the imide, but the CO_2 source is not obvious. Bruck [12] has reported significant amounts of CO_2 in the pyrolsis of "Kapton" polyimide type H, commonly called H-film, which has a similar structure to Skybond 700. Bruck attributed the CO_2 to incomplete ring closure of the polyamic intermediate and to hydrolytic scission of the imide by adsorbed water. However, since water was not a major element of Skybond 700 pyrolysis, CO_2 is probably a primary decomposition product originating in the imide ring. Johnson and Gaulin [13] postulate two different mechanisms of CO_2 production using model compounds as a source of information. The actual mechanism has not been identified conclusively. Further, it may be impossible to select only one route. Both or many may be contributing. The complex nature of the basic polymer structure and its incomplete determination introduce additional complications.

The gas analyses just discussed are preliminary in nature and were made to ascertain the problems which would be encountered and to develop technique. Problems still to be solved exist in sampling and chromatographic analysis. For example, the very dilute

nature of the gas solutions resulting from pyrolysis of small samples raises questions concerning adsorption on sample vessels. Also accurate concentration analysis has not yet been achieved for dilute samples by gas chromatography. It may well be necessary to couple mass spectroscopy and gas chromatography to arrive at successful gas analysis. This might be necessary since mass spectroscopy is capable of providing a more sensitive analysis than is possible using the gas chromatographs presently available to the program. Also if a broad range of molecular weight gases is found in the pyrolysis gas, it may be very difficult to obtain complete identification of species in a chromatograph. In this case, a chromatographic column may be used to separate the species which are then collected and individually determined in a mass spectrograph.

4.0 PLANS FOR CONTINUED WORK

In the immediate future it is expected that TGA analyses of phenolic, polymide, polybenzimidazole, and polyphenylene polymers will be conducted. Quasilinearization analytical techniques will be applied to resultant data for the determination of kinetic parameters associated with a suitable reaction equation. Gas chromatography and mass spectroscopy will be applied to pyrolysis gas analysis and thermal decomposition kinetics will be proposed.

REFERENCES

1. Seader, J. D., "Use of Thermogravimetric Analysis in Polymer Degradation Studies," paper presented at 1969 Polymer Conference Series, Detroit, Michigan.

2. Flynn, J. H. and Wall, L. A., "Polymer Preprints," Amer. Chem. Soc., 6, 945 (1965).

3. Murphy, C. B., Anal. Chem. Rev., 36, 347R (1967).

4. Newkirk, A. E., Anal. Chem. Rev., 32, 1558 (1960).

5. Cahn, L. and Peterson, N. C., "Conditions for Optimum Thermogravimetric Analysis at Atmospheric Pressure," Anal. Chem. Rev., 39, 403-4-4, March 1967.

6. Madorsky, S. L., "Thermal Degradation of Organic Polymers," Interscience Publishers, New York, 1964.

7. Flynn, J. H. and Wall, L. A., "General Treatment of the Thermogravimetry of Polymers," J. Res. of the Nat'l. Bur. of Standards - A. Physics & Chemistry, 70A, No. 6, 487-523 (1966).

8. Bellman, R., Jacquez, J., Kalaba, R., and Schwimmer, S., "Quasilinearization and the Estimation of Chemical Rate Constants from Raw Kinetic Data," Mathematical Biosciences, 1, 71-76 (1967)

9. Bellman, R., and Kalaba, R., "Quasilinearization and Nonlinear Boundary Value Problems," American Elsivier, New York (1965).

10. Wrasidlo, W. J., "Pyrolysis of Aromatic Heterocyclic Polymers," paper presented at Polymer Conference Series, Wayne State University, May 1968.

11. Schulman, G. P., and Lochte, H. W., "Thermal Degradation of Polymers. II Mass Spectrometric Thermal Analysis of Phenol-Formaldehyde Polycondensatis," J. Applied Polymer Sci., 10, 619-635 (1966)

12. Bruck, S. D., "Thermogravimetric Studies on an Aromatic Polimide in Air and in the Vacuum Region of 10^{-2} to 10^{-3} Torr Using the Cahn RG Electrobalance," Vacuum Microbalance Techniques, Vol. 4, Plenum.

13. Johnson, T. H., and Gaulin, C. A., "Thermal Decomposition of Polimides," paper presented at Polymer Conference Series, Wayne State University, May 1968.

LIST OF FIGURES

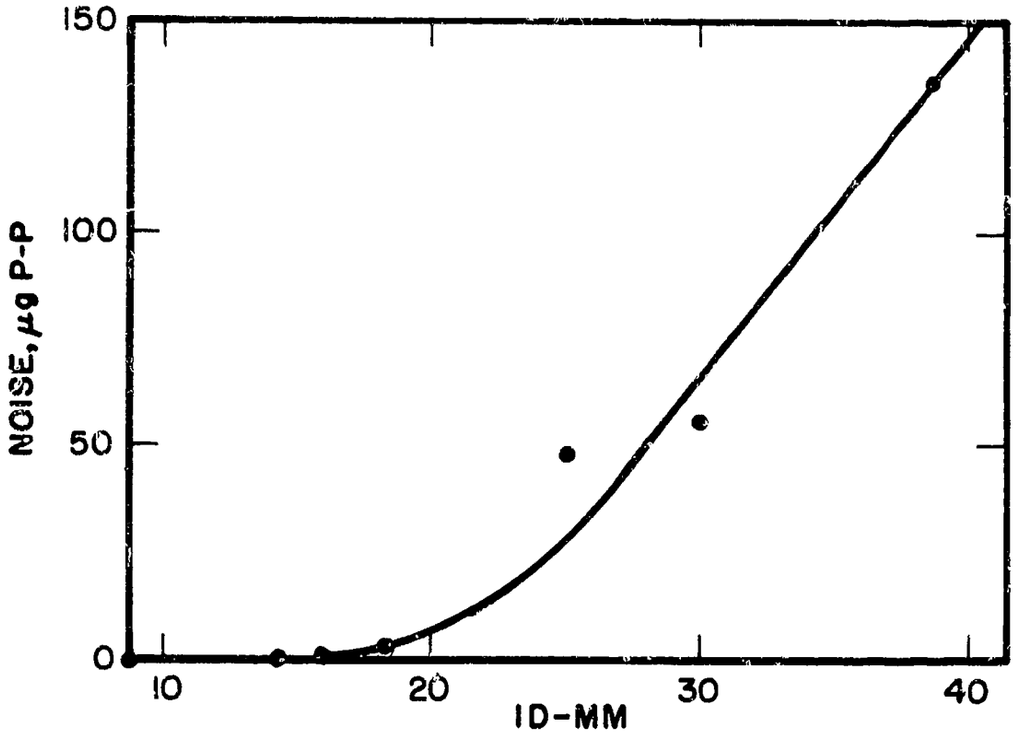

Figure 1. Peak-to-peak noise as a function of inside diameter of sample tube at atmospheric pressure.

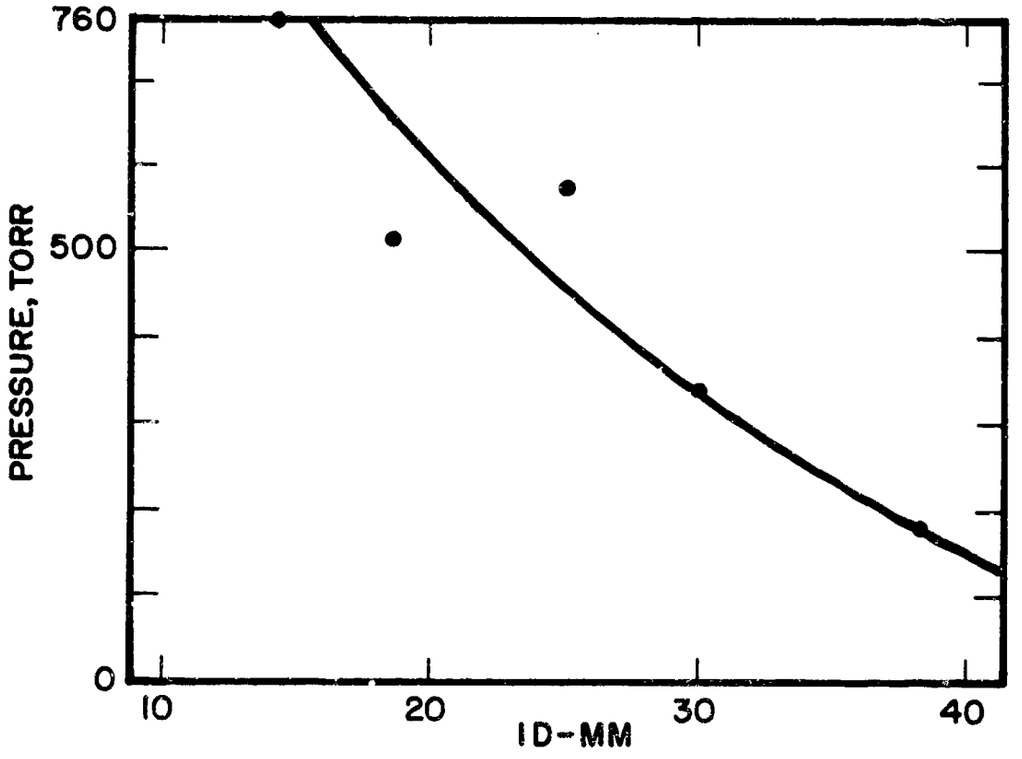

Figure 2. Pressure for 1μg peak-to-peak noise as a function of sample tube diameter.

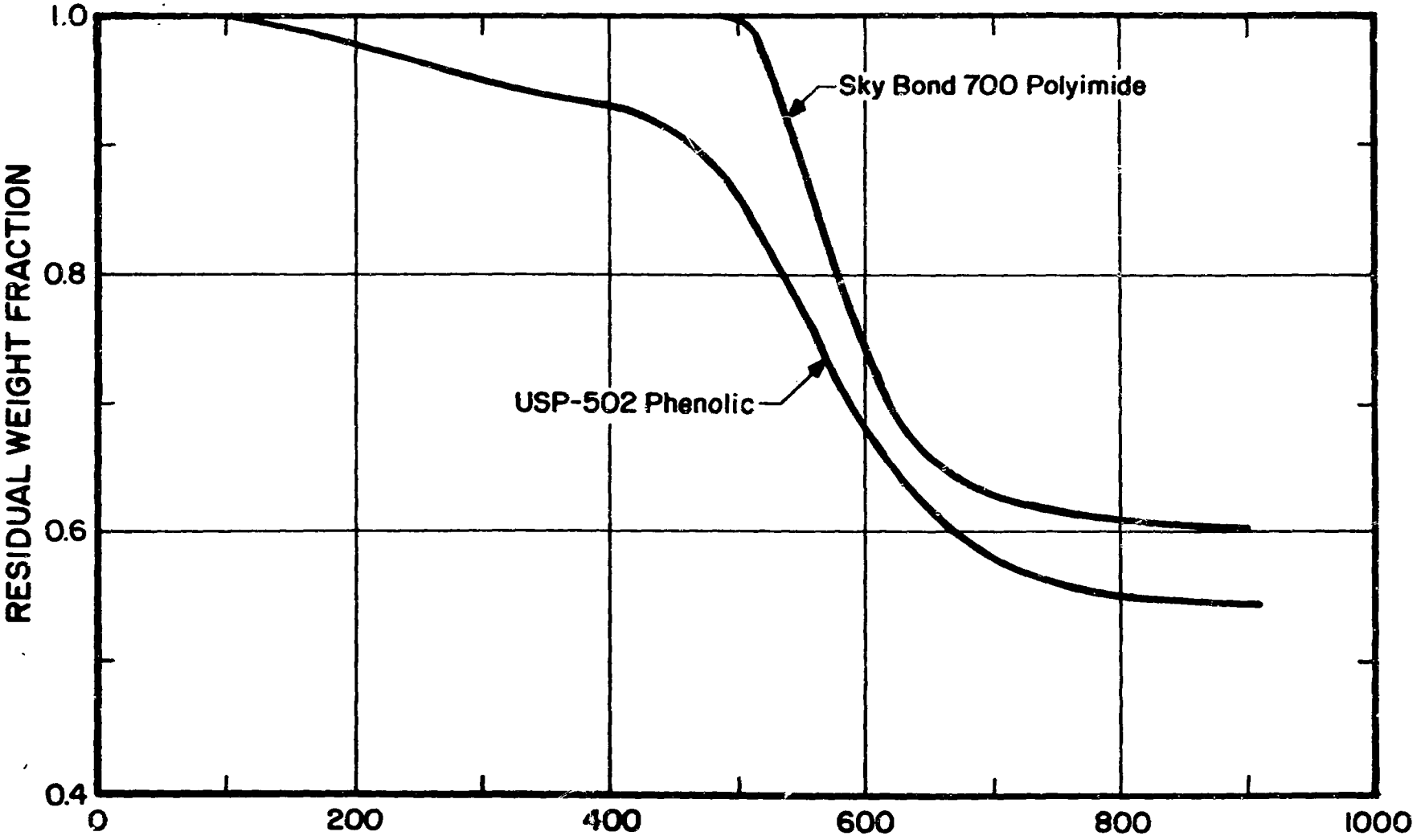

Figure 3. Sample TGA Curves

PHASE II KINETICS OF SUBSURFACE REACTIONS--J. Chidley*

1.0 INTRODUCTION

It is possible that significant increases in the amount of heat absorbed by a charring ablator could be realized by catalysis of reactions between the carbonaceous char and a siliceous reinforcement. Such reactions are known to be very endothermic, and under the proper conditions are to be expected in silica-reinforced ablators.

The role of subsurface ablation reactions has been inadequately understood with respect to the conditions under which they might occur, their rates of reaction, and their effect on the structural integrity of the charring ablator. Such reactions as:

$$SiO_{2(s)} + C_{(s)} \rightleftharpoons SiO_{(g)} + CO_{(g)} ,$$

$$SiO_{2(s)} + 2C_{(s)} \rightleftharpoons Si_{(l)} + 2CO_{(g)} ,$$

$$SiO_{2(s)} + 3C_{(s)} \rightleftharpoons SiC_{(s)} + 2CO_{(g)}$$

and subsequent reactions:

$$SiC_{(s)} + 2SiO_{2(s)} \rightleftharpoons 3SiO_{(g)} + CO_{(g)}$$

$$SiO_{2(s)} + Si_{(l)} \rightleftharpoons 2SiO_{(g)}$$

are thermodynamically possible at certain temperatures and pressures of CO in the layer. Several investigators have attempted to follow the rates of these reactions.[1-3] They have, however, carried out their experiments under near-vacuum conditions, measuring the amount of CO produced. Large discrepancies are noted in the rate expressions by the various experimenters. Since all of the reactions listed are thermo-

*Mr. John D. Chidley received a B.S. degree in Chemical Engineering from the California Institute of Technology in 1965. Since then he has attended the University of Utah where he is a Ph.D. candidate in Chemical Engineering. He began work on this phase of the program in September 1967.

dynamically feasible at low CO pressures, it is not clear whether one or all of the reactions have been observed.

The objective of this phase of Task 3 is to investigate the possibility of catalyzing the char-reinforcement reactions to increase the rates of the reactions at lower temperatures and to determine the effects of various parameters on the rates of the reactions. These parameters include the following:

1. The pressure of CO in the system.
2. The crystalline form and phase equilibria of the silica in the reinforcement.
3. The interfacial area of the reactants.

The theoretical background for this investigation has been thoroughly discussed in the previous annual report. (UTEC DO 68-065, October 1968.) Since that report, the balance of effort on this phase of Task 3 has been expended in the fabrication, acquisition, and installation of equipment to perform the experiments outlined therein. Accordingly, this report comprises a summary of the status of the various pieces of experimental apparatus acquired and the information which it is hoped will be gained therefrom.

2.0 EXPERIMENTAL APPARATUS

2.1 *Arc-Imaging Furnace*

The arc-imaging furnace provides a means of exposing an ablative sample to a high radiant energy flux in a controlled environment such as an inert or reactive gas. The Hg-Xe arc furnace available can provide a heat flux of up to 15 cal/cm^2-sec over a "hotspot" approximately 3/4" in diameter. Calibration of the flux of this furnace has recently been accomplished. It has also become possible to locate the specimens in the flux much more accurately than before.

Previous attempts to use the furnace had been troubled by delaminations of the samples, which produced inconclusive results. A series of tests shortly to be conducted will be performed on samples oriented

with the laminate grain end-on rather than perpendicularly to the direction of heat flux. It is felt that gas build-up in the laminate, leading to delamination, will be avoided in this manner.

Samples will be exposed to the flux for various time intervals. A ceramic holder-equipment shield has been fabricated for this purpose. The holder consists of a machined disk of the ceramic with a well in which the sample is held by a set-screw. The holder is secured in a drill chuck attached to a positioning mechanism. The holder is shown in Figure 1.

2.2 *Hybrid Rocket*

The plexiglas-oxygen hybrid rocket motor mentioned in the last annual report has been completely redesigned and rebuilt. The motor fires very reliably and has proven to be quite leak-free. The new system is shown in Figure 2.

The rocket is ignited by combustion of propane with the oxygen feed, which preheats the plexiglas sufficiently to allow its ignition when the propane supply is turned off. Nitrogen is used to dilute the oxygen, and also to terminate combustion and cool the apparatus after a firing. Solenoid valves are used to control the gases.

The hot combustion products are allowed to pass through a drilled hole in a piece of ablative material, usually a two-inch diameter cylinder from two to three inches long. It was found that during long runs, the ablative sample would heat up to a point where the plexiglas would soften considerably on the face in contact with the sample. Softening was aggravated when a graphite spacer was used between the plexiglas and the sample, due to the high thermal conductivity of the graphite. The spacer was used to provide an entrance orifice of constant dimensions for the hot gases. The softening was very detrimental to the reliability of the firing, as it occasionally resulted in leaks and often disrupted the test geometry. The graphite spacer also heated the entire face of the ablative samples, which was highly

undesirable. To overcome the problems due to the high conductivity of the graphite, a water-cooled entrance ring for the gases was designed and built. The major objective of the ring was to cool the end of the plexiglas fuel element enough to prevent its softening. The ring also cools the end of the ablative sample, which results in a much more desirable heating of the samples, since the heat is applied to the surface of the drilled hole only. A cross section of the ring appears as Figure 3.

The bulk of the plexiglas does not generally heat up significantly from the combustion, since its thermal conductivity is low enough that it burns away before significant heat is transferred during the duration of our firings.

The rocket has been fired several times with ablative samples in place. It is possible to use it as a screening tool for examining the response of the materials.

Investigators from the Mechanical Engineering Department have also displayed interest in using the hybrid rocket to observe burning surfaces at cracks by means of high-speed motion-picture photography. They have performed exploratory test firings and are now attempting to obtain photographs in their system.

2.3 *Hot Gas Facility*

A hot gas facility, to be used for observation of the thermal response of ablative materials to clean, high temperature products of combustion, has been on order for some time. Numerous delays were encountered, but components of this system are now being received. To date, the main combustor assembly, fuel tankage, and coolant pump have arrived. The main control console arrived as this report was written, but interconnecting lines are still to be received. Several of the components are shown in Figure 4. The facility will be installed approximately as shown schematically in Figure 5.

In addition to the facility as purchased, several necessary auxiliary items have been obtained. A 28 Volt, 15 Amp rated DC power

supply has been procured through the University surplus property agency. The power supply is necessary to provide for some of the control instrumentation of the hot gas facility. Methanol loading apparatus for transfer from drums to the pressurized fuel tank has been fabricated. A five-station high-pressure oxygen manifold has been obtained, and will be piped in and installed when the combustor assembly is finally located. High pressure piping to convey compressed air from four large (52 ft^3) tanks located just north of the engineering building has been installed.

In the interests of safety, fire protection, which had not existed at the site of the installation, was deemed necessary. A ceiling-mounted water fire extinguishing system has been installed to provide that protection. The work on the fire system was performed by the University Plumbing Shops.

When the hot gas facility is in operation, some means of cooling its effluent and absorbing unburned methanol fumes, etc., is necessary. To accomplish this task, a cooler-absorber has been designed and built in this department. The cooler-absorber system is comprised of a quenching pipe and a baffled entrainment separator. The quenching pipe is 1 foot in diameter, 1/4 inch thick and 8 feet long. It has fifteen fan spray nozzles mounted so that the plane of water flow is perpendicular to the axis of the pipe. Gases leaving the combustor will flow through the quenching tube into the entrainment separator and thence outside to the atmosphere. The entrainment separator is made of heavy culvert stock and sheet metal. The cooler-absorber is illustrated in Figure 6.

It is necessary to be able to visually monitor the facility when in operation, but personnel must not be allowed in the immediate vicinity. To be able to monitor the operations from the remote control console, the possibility of installing a closed circuit TV system has been proposed and is being pursued. Such a system would also be very useful in connection with other experiments performed in the tunnels which must be remotely operated.

2.4 *TGA Work*

A high-frequency induction heating unit is available from the Materials Science and Engineering Division. It has been proposed to use the induction heating unit, a Lepel High Frequency Laboratories product, to heat pelletized TGA samples composed mainly of graphite and silica.

The sample configuration under consideration would be a cylinder 1 cm high by 1 cm in diameter. Samples would be produced by compressing the ingredients in a high-pressure hydraulic press and machining to the correct size. A sample of the indicated size would weigh between 1 and 2 grams, thus it could be suspended from the low-sensitivity loop of the Cahn Electrobalance described under Phase 1 of this task.

Two possible methods of heating the sample inductively are under consideration. The first is to directly couple the coil of the induction heating unit to the graphite-containing sample. Direct coupling has the advantage that the heat is produced directly in the sample itself, rather than being transferred from an external source. Also, with direct coupling, the sample could probably be suspended in existing hangdown tubes made for the balance as indicated in Figure 7. The tube could be air-cooled if necessary. The possible disadvantage of direct coupling derives from the fact that if the magnetic field of the coils diverges in the region of the sample, levitating forces are induced in the sample. These forces can be fairly large. Also, it is possible that the sample might precess, which would induce excessive noise in the balance output signal. If the sample were heated directly, the temperature would have to be monitored by a radiation pyrometer.

Should it prove unfeasible to heat the samples by direct inductive coupling, a tube furnace heated by coupling the induction unit to a graphite susceptor could be built. Graham and Tripp found that levitation and precession problems were significantly reduced when they went from direct coupling to a susceptor furnace.

A sketch of the tube furnace contemplated for our work is shown in Figure 8. Such a furnace must exhibit high resistance to a CO atmosphere and to temperatures up to at least 1500°C. Also, it must be capable of being evacuated. Temperature monitoring could be achieved by a radiation pyrometer, or possibly with a Pt-Rh thermocouple if it were found that the field of the induction coils did not disturb it.

The experiments which could be performed using the electrobalance might provide more quantitative information about the effects of particle size on the kinetics of C-SiO_2 reactions. The influence of various catalyzing substances and of the crystalline state of the silica could be observed by incorporating the appropriate materials in the pelletized sample.

In addition, since it would be easy to fix the pressure of CO in the system, the role of CO in the kinetics and equilibria of C-SiO_2 reactions should become clearer.

3.0 DIRECTION OF FURTHER WORK

Experiments utilizing the hybrid rocket and arc-imaging furnace are possible now and are proceeding. The two devices can provide a comparison of the relative responses of catalyzed materials as opposed to otherwise identical uncatalyzed materials in both a moderate shear environment of combustion products and a zero shear controlled or inert atmosphere.

The hot-gas facility continues to arrive as semi-assembled components and is in the process of installation. Design of a suitable sample holder for this facility is being considered, as well as a means of visually monitoring the system.

The feasibility of heating TGA samples inductively is being vigorously pursued. The experience of other workers [4,5] in using induction heating, leads to the expectation that it may be necessary to construct a small graphite-susceptor furnace for inductively heating the samples.

REFERENCES

1. Beecher, N., and Rosensweig, R. E., "Ablation Mechanisms in Plastics with Inorganic Reinforcements," ARS Journal, Vol. 31, 1961, pp. 532-539.

2. Blumenthal, J. L., Santy, M. J., and Burns, E. A., "Kinetic Studies of High-Temperature Carbon-Silica Reactions in Charred Silica-Reinforced Phenolic Resins," AIAA Journal, Vol. 4, 1966, pp. 1053-1057.

3. Klinger, N., Strauss, E. L., and Komareck, K. L., "Reactions Between Silica and Graphite," Journal of Am. Ceramic Soc., 49 (7), 1966, pp. 369-375.

4. Carrera, N. J., etal, "Microbalance Techniques for High-Temperature Applications-Further Developments," Vacuum Microbalance Techniques, Vol. 3, 1963, pp. 153.

5. Graham, H. C. and Tripp, W. C., "Induction-Heated High-Temperature Balance System," Vacuum Microbalance Techniques, Vol. 6, 1967, pp. 63.

LIST OF FIGURES

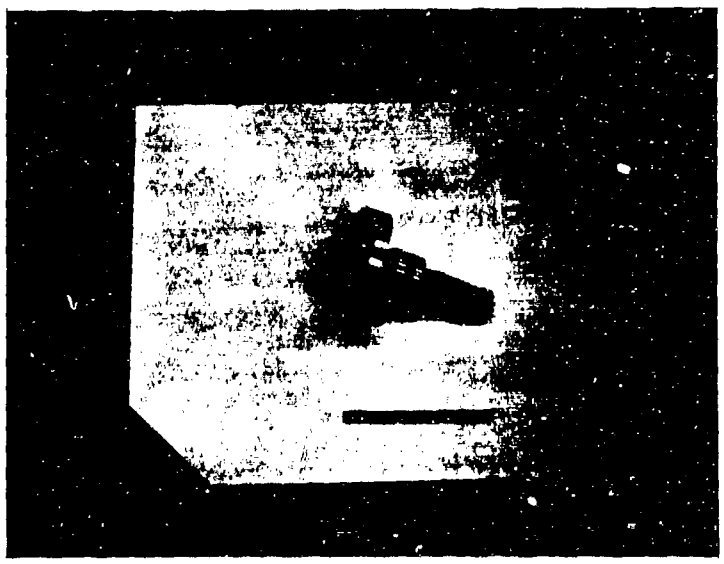

Figure 1. Ceramic sample holder.

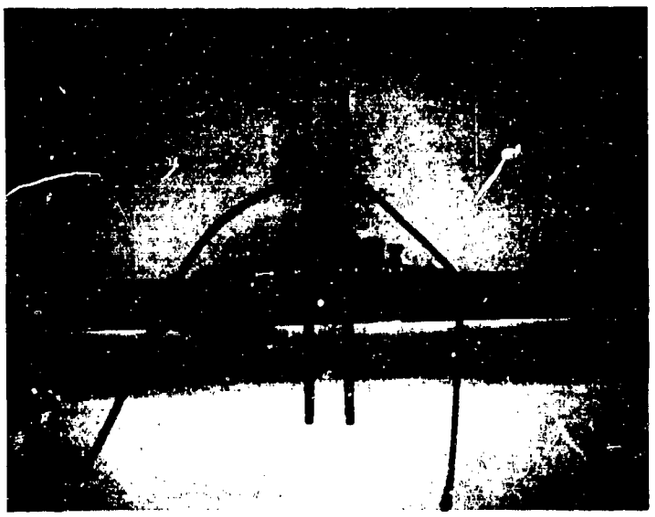

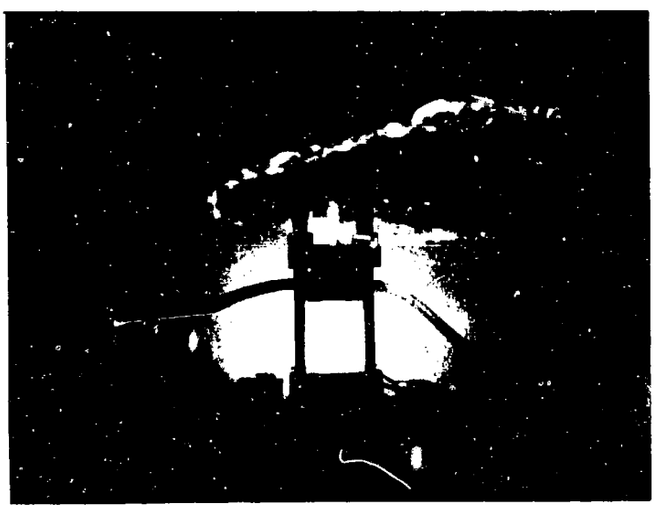

Figure 2. Hybrid rocket motor.

Scale: 1.5:1

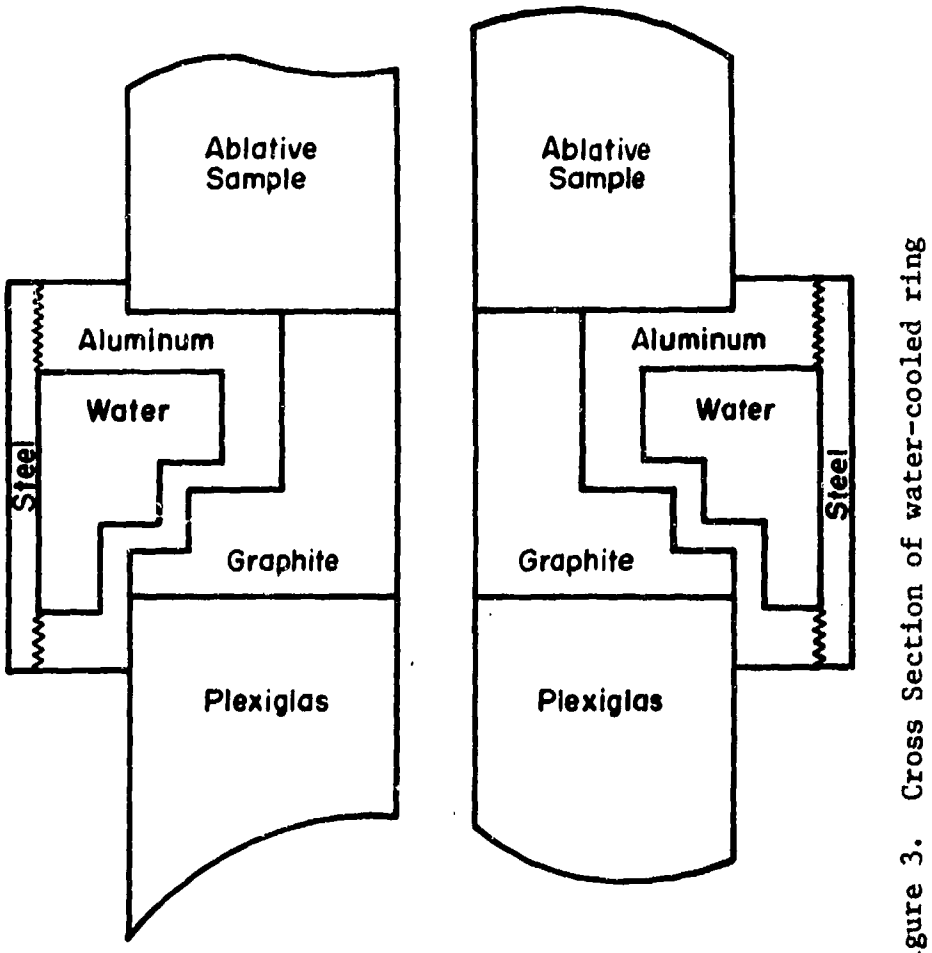

CROSS-SECTION OF COOLING RING

Figure 3. Cross Section of water-cooled ring

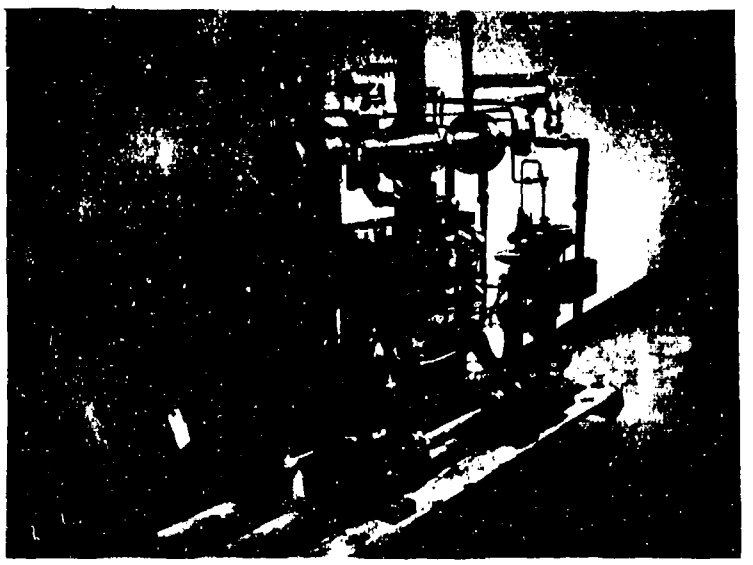

Figure 4. a. Thrust stand assembly

b. Fuel tank

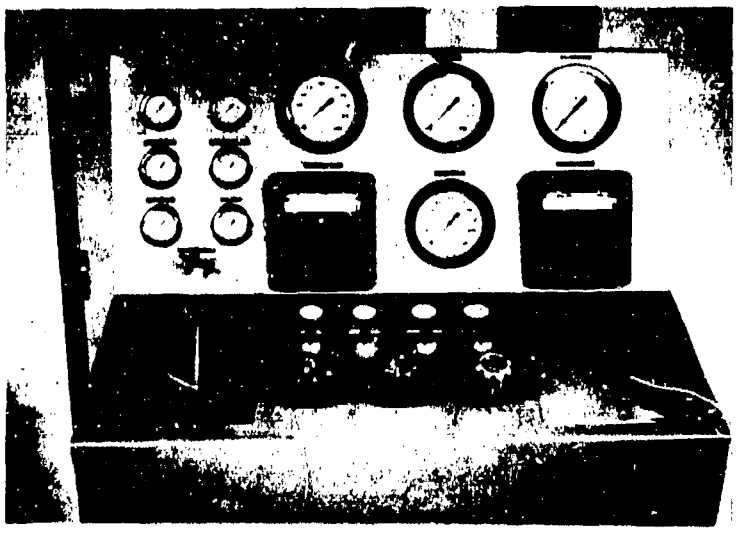

c. Control console

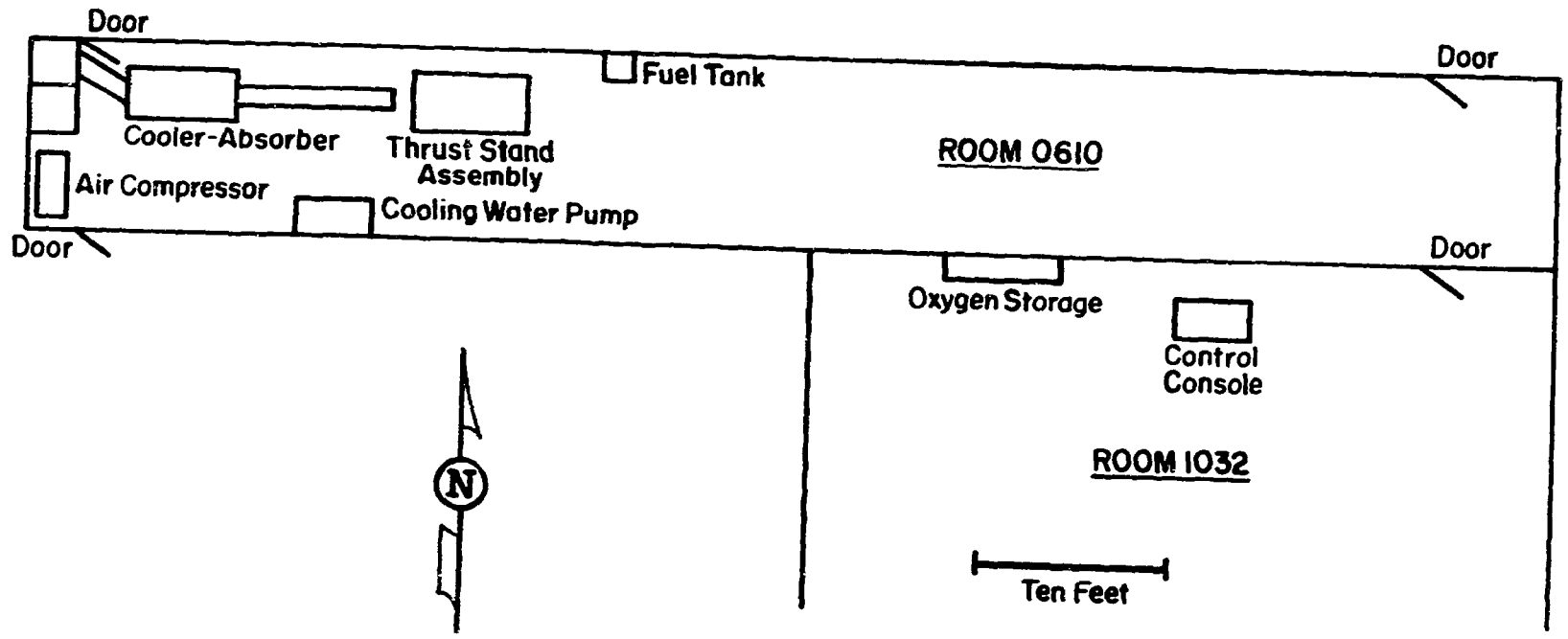

Figure 5. Schematic layout of hot-gas facility.

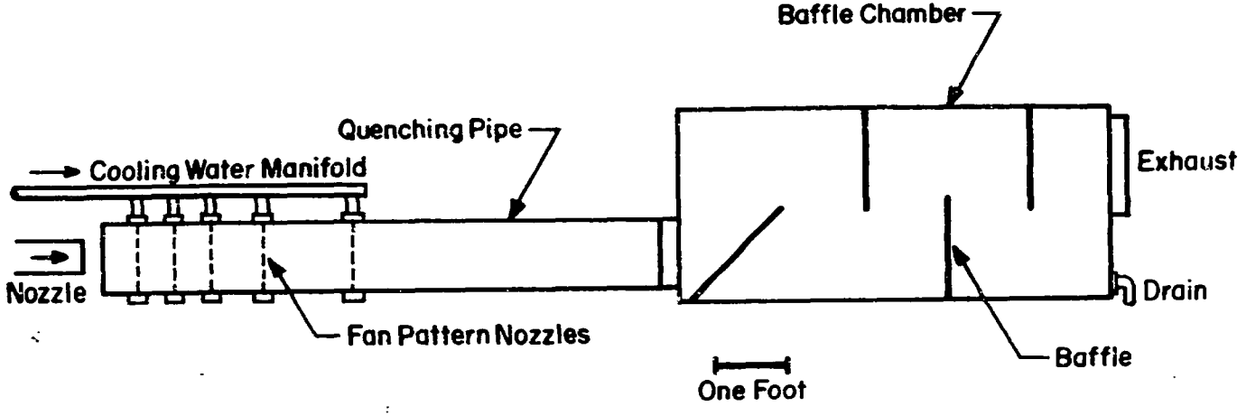

Figure 6. Cooler-absorber

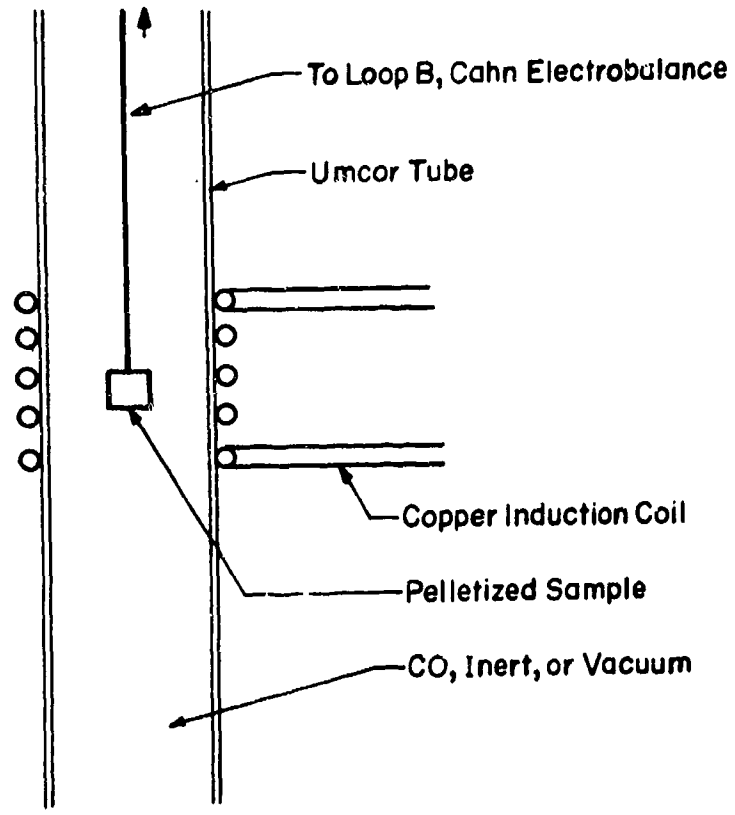

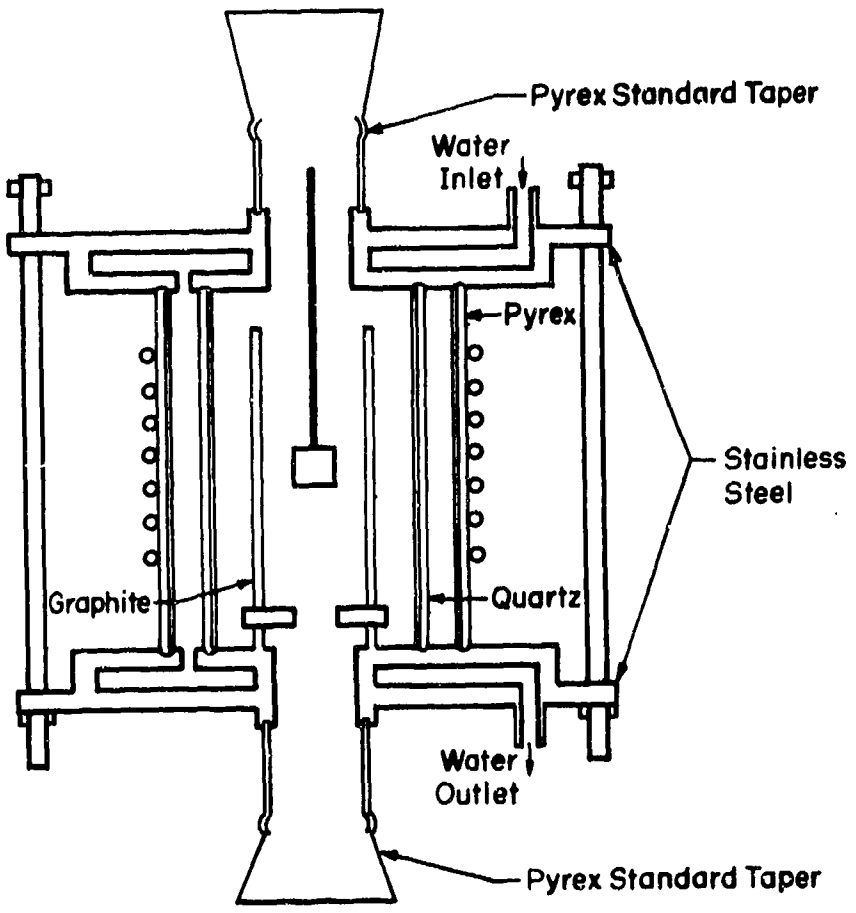

Figure 7. An induction heated graphite-susceptor furnace for heating TGA samples.

PHASE III GAS LIQUID SURFACE EFFECTS--C. Hsieh

1.0 INTRODUCTION

In the past year, a comprehensive literature survey and comparison of theoretical approaches has been accomplished. It was found that even though a number of theoretical investigations concerning the surface ablation of the molten layer have appeared during the last decade, little effort has been concerned with the system of reinforced phenolic resin.[1,2] Only a few experimental studies have been published.[3-6] All of the previous investigations neglect the effect of the pyrolysis gases which pass through the liquid layer. Except for Beecher and Rosenweig,[1] the previous investigations also neglect the chemical reactions between carbon and silica in the molten layer. Besides the energy and momentum transfer associated with the penetration of the pyrolysis gases through the molten layers, we believe that gas bubbles may have a significant effect on the viscosity, conductivity, and other physical properties. The gas bubbles might also influence the rate of chemical reactions. It is known that the viscosity of the molten-layer is the most important factor that influences surface ablation. Serious errors may arise if the effect of gas bubbles on the viscosity is neglected. Energy is transferred primarily through the liquid layer by conduction. Since the conductivity of the molten layer is almost inversely proportional to the void fraction of the gas bubbles, the assumption of constant conductivity, as in the previous studies, will give a higher heat transfer rate than the real situation. Thus, a much better insight into the ablation mechanism should be possible if the effect of gas bubbles is not neglected. It is the purpose of this study to include the effect of gas bubbles on the surface ablation. The viscosity, density, and conductivity of the molten-layer are all being considered as functions of the void fraction.

Both theoretical and experimental work has been done for increasing the performance of ablation materials, but the use of surface-active agents has attracted little attention. The neglect of the presence of gas bubbles in the molten-layer leads to the neglect of the effect of surface tension on the ablation process. If the thickness of the molten-layer is very

---

* Mr. Chia-lung Hsieh received a B.S. degree in Chemical Engineering in 1966 from Tunghai University in Taiwan. Since September 1967, he has attended the University of Utah, where he is a candidate for a Ph.D. in Chemical Engineering, and has worked on Phase III of this program.

small, and gas bubbles exist within it, the ratio of the surface to the volume of the molten-layer is so large that it is impossible to neglect the effect of surface-active agents. At the present time, no attempt at the study of the overall effect of surface-active agents is made. Individual reactions and processes which are affected by the surface-active agents are being studied theoretically and experimentally.

2.0 MECHANISM OF SURFACE ABLATION

During the past year, the mathematical details of the mechanism of surface ablation have been considered. The primary goal has been to demonstrate the possible effect of gas bubbles on ablation for the steady-state, two-dimensional, two-phase molten laminar boundary layer flow. Local similarity has been used to convert the system of partial differential equations into ordinary differential equations. Several techniques for solving the equations have been considered including small perturbation theory and asymptotic limits of unsteady-state analogs. A finite difference approach has been developed for the latter method. The details of the mathematical development are presented elsewhere.[7]

3.0 EFFECT OF SURFACE-ACTIVE AGENTS

The effect of surface-active agents on the liquid flow has drawn much attention recently. Several investigations have been reported on this subject, but little has concerned the mechanism of ablation. Steverding[8,9] has investigated the effect of surface-active agents on the vaporization and spattering of liquid. It was found that by proper choice of surfactant, it was possible to increase the vaporization rate of the liquid, and decrease the spattering loss of liquid droplets. The efficiency of ablation materials could be increased by the vaporization of liquid droplets inside the gas boundary layer. There are several more important influences of surfactants which have not been studied. The surfactants can cause a retardation effect on the bubble motion, and surface velocity. They can also influence the viscosity, stability and chemical reaction. We will study these processes separately.

3.1 *Fluid Motion*

The retardation effect of surfactants on the motions of gas bubbles in a liquid medium is caused by the gradient of surface tension. When a bubble exists in a liquid medium, surface-active agents are absorbed at

the interface. Due to the shear stress on the interface, the density of molecules of surfactants on the upstream part is lower than that corresponding to equilibrium with the bulk flow. In the rear part, it is in excess. The resulting accumulation of surfactants lowers the surface tension at the rear part of the bubble. The gradient of surface tension then creates a shear force which is exerted along the interface of the bubbles. The shear force is represented by

$$p_t = -\frac{1}{a}\frac{\partial \sigma}{\partial \theta} = -\frac{1}{a}\frac{\partial \sigma}{\partial \Gamma}\frac{d\Gamma}{d\theta} \tag{1}$$

where a is the radius of gas bubble, Γ is the surface excess of surfactants, and σ is the surface tension. The shear stress is directed toward the higher surface tension region and so tends to retard the velocity at the interface. According to Levich,[10] the terminal velocity of the creeping motion of gas bubbles in a liquid medium is expressed as

$$U = \frac{2}{3}\frac{(\rho' - \rho)ga^2}{\mu}\left(\frac{\mu + \gamma}{2\mu + 3\gamma}\right) \tag{2}$$

where γ is the retardation coefficient, μ is the viscosity and ρ' and ρ are the liquid and gas densities, respectively. The value of γ is given by

$$\gamma = \frac{2RT}{3K_2 a}\left(\frac{b^2 C_o}{1 + \frac{bC_o}{\Gamma_\infty}}\right) \tag{3}$$

if the mass transfer of surfactants is controlled by adsorption, and

$$\gamma = \frac{2RT\delta}{3Da}\, b\Gamma_o \left(1 - \frac{\Gamma_o}{\Gamma_\infty}\right) \tag{4}$$

if the mass transfer of surfactants is controlled by molecular diffusion. In the above equations, b is Langmuir's constant, D is the diffusivity, δ is the thickness of boundary layer, Γ_o is the surface excess of surfactants in equilibrium with bulk concentration C_o, and Γ_∞ is the surface excess as $C_o \to \infty$. Stoke's law for the creeping motion of a solid sphere in a liquid medium, and the Rybczynsk-Hadmard formula for gas bubbles are

$$U_g = \frac{2}{9}\frac{(\rho' - \rho)ga^2}{\mu} \tag{5}$$

$$U_R = \frac{1}{3}\frac{(\rho' - \rho)ga^2}{\mu} \qquad (6)$$

Comparing Equation (4) with (5, 6), it is obvious that as

$$\gamma \to \infty, \quad U \to U_s$$
$$\gamma \to 0, \quad U \to U_R$$

This means that the effect of the gradient of surface tension is to cause a gas bubble to behave like a solid sphere.

When gas bubbles are so large that the assumption of creeping flow is not valid, then Levich's derivation cannot be applied for predicting the bubble motion. For a bubble moving at a faster velocity, the surfactants, which are adsorbed on the bubble surface, are pushed to the rear part of the bubble and form a solid film on the cap. The interfacial velocity vanishes on the cap, while it remains unimpeded on the forward surface. The discontinuity of velocity on the bubble surface causes a separation of flow. Thus, the form drag, caused by the separation, gives a retardation effect on the bubble motion. The formation and the effect of the cap have attracted much attention recently.[11-14] However, no satisfactory solution has been obtained. If K is defined as the ratio of the terminal velocity of gas bubbles to that predicted by Stoke's law, it is found that

$$K = \frac{3}{2\ x_2} \qquad (7)$$

where x_2 is a function of cap angle and the gradient of surface tension. It is obvious that if the solid film of surfactants covers the entire surface of the gas bubble, or if the gradient of the surface tension is very large (as caused by more active surfactants) the motion of gas bubbles will be exactly the same as a solid sphere. The terminal velocity will be only two-thirds of that of a gas bubble in a pure liquid medium.

The retardation of bubble motion has several advantages for the ablation process. As discussed before, if the gas bubbles are small, the presence of surfactants will cause the bubbles to behave more like solid spheres. Thus, the apparent viscosity of the molten-layer will increase according to the formula.[15]

$$\mu_m = \mu_L(1 + 2.5\alpha)$$

where α is the void fraction of the suspended gas bubbles. The other

advantage is that, due to the increase of void fraction, the total volume of the molten-layer will increase. On the other hand, the conductivity of the molten-layer, which could be approximated by $K_e = K_L(1-\alpha)$ dec .ses. Both of the effects reduce the conductive heat flux from the liquid surface to the interior.

If the gas bubbles are large, their presence might decrease the apparent viscosity of the molten-layer. Since the retardation of bubble motion increases the void fraction, the liquid might be blown off more easily. The reduction of the bubble velocity also reduces the momentum of the gas which is ejected into the gas boundary layer. In general, it is desirable that injecting gas have a high momentum so that it can increase the thickness of gas boundary layer and reduce the velocity gradient near the gas-liquid interface.[16] Unfortunately, the surfactants have the reverse effect.

Furtherm(e, the chemical reaction of carbon and silica might be affected by the retardation of bubble motion. Several investigations[3,17-19] have shown that, at high temperature, the chemical reactions take place at the interface of the gas and liquid. The reactions are likely to be controlled by the transport of reactants. If this is true, then the transport of carbon from the bulk flow to the surface is an important step. Gas bubbles might carry carbon particles toward the reaction zone. The retardation of bubble motion might cause a slower reaction rate. This might reduce the performance of ablation materials.

By the same reason as mentioned in the bubble motion discussion, when a gradient of surface tension exists along the liquid surface, a tangential shear force also occurs on the liquid surface. At high Reynolds numbers the viscous force is small compared to the inertia force. The presence of surfactants will not influence the liquid flow. Conversely, in the viscous flow, the effect of surfactants could be very significant. As mentioned by Bethe and Adams,[20] the inertia force of the flow of the molten layer is negligible compared to the viscous force. Thus, it is expected that the surfactants might have a significant influence on the surface velocity. Several approximations of the retardation of surface velocity have been made, but they only provide initial estimates. At present, a theoretical study of the effect of surfactants on the surface velocity in ablation process is not being attempted. But from the above discussion, it is obvious that the addition of surfactant will reduce the

blow-off of the molten materials, and so increase the efficiency.

3.2 *Wave Motion and Stability*

Early developments in ablation were all concerned with the flow at the stagnation region. These theories could not give much insight into the nature and the importance of wave motion. However, the experimental result of Ostrach and McConnel[26] did show wave patterns clearly on recovered models. They also found that the molten liquid had been transported by these waves. It appears that the wave motion might be important to the flow of the liquid layer.

Little is known about the relation between the wave motion and heat transfer. Apparently, the circular motion of liquid particles might increase the heat transfer rate. The separation of the gas flow at the declivous region might prevent the heat flux from passing through it. Thus, the effective thickness of the liquid layer would increase, and the heat flux conducted through the liquid layer might be reduced. As the amplitude of waves becomes large, the waves are not stable. The unstable wave motion leads to the breaking of the liquid film. The liquid droplets thus created will be blown away by gas flow. It will also expose the bare solid surface to the hot gas stream, and produce hot spots on the surface. Both of these phenomena decrease the efficiency of ablation materials significantly. It might also cause serious damage to the materials.

The effect of surfactants on damping wave motion was known to the ancient Greeks. Sailors knew that the fury of waves could be calmed by pouring oil on the surface of the sea. There are several hypotheses to explain this phenomena.

1. The surfactants form a solid film on the liquid surface, and the film reduces the friction between the air and water. Energy transferred from air to water is then reduced.
2. Surfactants reduce the surface tension of the liquid, and so have a damping effect on the waves. Levich[10] later showed that the damping coefficient is independent of surface tension.
3. The surface viscosity of the film increases in the presence of surfactants. The deformation of the film leads to the energy dissipation within the film, thus the energy transferred to the liquid is reduced.

Levich advanced the theory by considering the effect of surfactants in terms of the change of boundary conditions. The governing equations are then solved by the small perturbation method. The solutions are

$$V_x = V_x^\circ \, e^{-\beta t} \tag{8}$$

$$V_y = V_y^\circ \, e^{-\beta t} \tag{9}$$

where V_x° and V_y° are velocity components of a potential flow, t is time, and β is the damping coefficient. These relations show that the amplitude of waves decreases with time if β is large. The damping coefficient, β, is primarily determined by the wave length, surface excess, elastic coefficient, and solubility of surfactants. For small waves (capillary waves), or large surface excess, β becomes very large, and the waves can be damped quickly. For long waves, or small surface excess (high concentration of surfactants), the damping coefficient reduces to that of a pure viscous fluid. In other words, the surfactants are effective only at a small Reynolds number and small boundary thickness. The surfactants could not have a direct effect on the sea wave, or turbulent waves, but they damp out the ripples and small waves that cover the large waves. They can reduce the interaction of gas and liquid, and so reduce the transfer of energy from gas to the liquid. The ripples caused by the bursting of gas bubbles can also be damped quickly.

In addition, the surfactants may be able to increase the wettability of surface liquid, or they may stabilize the liquid film. Both can prevent the disintegration of liquid into droplets.

3.3 *Physical Properties and Chemical Reactions*

Both theoretical and experimental investigations have shown that the viscosity of the viscous molten-layer is the most important factor influencing the performance of surface ablation. The viscosity of a glassy liquid increases as the purity increases. Any foreign molecules existing in the molten liquid will break the long chain of the silica molecule, and lower the viscosity of the liquid. The addition of surfactants, even in small amounts, may cause a significant reduction in viscosity of the liquid. On the other hand, the presence of the surfactants might also have the reverse effect. As discussed above, the surfactants might be collected on the surface of the gas bubbles such that the gas bubbles behave like a solid sphere. The suspension of solid particles in a liquid medium increases the apparent viscosity by the

factor $(1 + 2.5\alpha)$. Furthermore, the effect of collecting surfactants on the bubble surface and transporting them to the gas-liquid interface by the gas bubbles may reduce the concentration of surfactants in the bulk flow. The unfavorable decrease of viscosity of the bulk flow by the surfactants is then reduced. During ablation, all of these processes are present simultaneously. The overall effect will depend on the physical properties of the materials involved and the mechanism of ablation.

The effect of gas bubbles on the apparent viscosity depends primarily on the size of bubbles. Small bubbles will increase the apparent viscosity of the molten-layer, but large bubbles might have the reverse effect. This effect will be studied experimentally.

The overall mechanism of the carbon-silica reaction must be understood before the study of the effect of surfactants on the reactions is attempted. If the chemical reaction is rate controlled, the surfactants will not influence the chemical reactions except by possible catalysis. If the reactions are controlled by the diffusion of gaseous products, surfactants can only affect the reactions indirectly by changing the injection velocity of pyrolysis gases. At high temperature, high gas velocity, and excess of silica, it is quite reasonable to expect a reaction controlled by the transport of carbon to the reaction zone. In the previous section, it was mentioned that the retardation of gas bubbles might decrease the transportation of carbon toward the liquid surface. This is based on the assumption that the carbon particles could be collected on the bubble surface and carried through the liquid layer. If this is not true, the carbon can only be transported by the liquid flow. The retardation of bubble motion will not have an important effect. On the contrary, the addition of surfactants might have some advantages. Some kind of surfactants might be adsorbed on the carbon particles (by chemisorption or physical adsorption). The monolayer of surfactants can modify the contact angle such that a desired flotation effect is obtained. The carbon particles can then be carried upward at a much faster velocity. An experimental investigation on the controlling step, the effect of bubbles and surfactants will be prepared later.

Surfactants do not have a direct effect on the density, and conductivity of the molten layer. The retardation of bubble motion will change

the void fraction of the liquid layer. The apparent density of the liquid is

$$\rho = \rho_g \alpha + \rho_L (1 - \alpha) \tag{10}$$

Since the Reynolds number of the liquid flow is not large, the shape of the bubbles can be maintained spherical. Maxwell's model for obtaining the effective conductivity could be applied where

$$K_e = (1 - \frac{3}{2}\alpha)\, K_L \tag{11}$$

The conductivity of the gas is assumed negligible. This expression can be used for the theoretical studies.

4.0 EXPERIMENTAL STUDIES

In order to understand the mechanism of ablation, and the effect of surface-active agents, several physical properties and processes must be studied experimentally. As mentioned in ref. (7), without knowing the effect of the gas bubbles on the apparent viscosity, the numerical calculation of the ablation mechanism cannot be performed. The first experiment is the measurement of the apparent viscosity as a function of temperature and void fraction. We also have to measure the surface tension as a function of concentration of surfactants. The effect of surfactants can then be predicted by Gibbs' Law. The surfactants affect the chemical reactions only if the reactions are controlled by the transport of carbon toward the reaction zone. It is desirable to know at what conditions the reactions will be controlled by the transport of carbon. The effect of surfactants on the reactions will be studied after the controlling step is determined. Finally, the overall simulation must be verified. The overall effect of the gas bubbles and surfactants will be studied in the simulation.

4.1 *Physical Properties*

4.1.1 Apparatus

A schematic diagram of apparatus for the measurement of physical properties is shown in Fig. 1.

4.1.1.1 Viscosity

The apparent viscosity of the liquid phase is measured by a modified falling ball method.[22] A tungsten ball of about 1/4" diameter is suspended from one arm of the balance. The motion of the ball is controlled

by changing the weights on the arm.

The velocity is measured indirectly by timing the movement of the pointer of the balance. By keeping the motion of the ball at a low velocity, Stoke's law can be used to calculate the viscosity of the molten liquid. The correction for the wall effect may necessitate a more accurate measurement.

4.1.1.2 Surface tension

The surface tension of the liquid can be determined by the Wilhelmy-Silde method.[23] The balance for the viscosity measurement can be used for this method. The ball is replaced by a pure tungsten plate. The force of the detachment of the plate from the surface of liquid is obtained from the weights on the other arms. The surface tension can be calculated by

$$W_{tot} = W_{plate} + \sigma p \qquad (12)$$

where p is the perimeter of the plate.

4.1.1.3 Void fraction

The void fraction can be measured by gamma ray adsorption method.[24] When gamma-rays pass through a liquid medium, the intensity is reduced. A simple linear relation exists between the logarithmic of intensity and density. If I_m and I_L represent respectively the measured values of the radiation of an empty tube of radius D and that of the tube full of the liquid, the relation is

$$I_L = I_m e^{-\beta_L D} \qquad (13)$$

where β_L is the absorption factor of the liquid. The measured value of radiation, I_{tp}, passing through a gas-liquid mixture is related to I_m by:

$$I_{tp} = I_m e^{m\beta_L} \qquad (14)$$

where the adsorption factor of the gas is considered negligible. If the system is homogeneous, the void fraction is

$$\alpha = \frac{m}{D} \qquad (15)$$

which defines the parameter m.

A schematic diagram of the radiation-adsorption system is shown in Fig. 2. The gamma-ray is radiated from the source. It passes through the cylinder, enters the chamber and ionizes the gas contained in it. The small current caused by the ionized gas is measured by the electrometer and recorded.

4.1.1.4 Furnace

The essential part of the experimental apparatus is the furnace. It is shown in Fig. 3. The furnace will be made of tungsten. The upper part is used to melt the silica, and the lower part to preheat the gas which is injected through the porous plate and then enters the liquid. The furnace will be resistance heated. Electric current is conducted to the furnace through the copper tubes which are cooled by water. The electric power is supplied by several welding generators connected in parallel.

The thermal insulation is also shown in Fig. 3. The radiation shields are made of molybdenum or tungsten. Boron nitride or zirconium oxide insulation grains can be used to hold the shields in position.

4.1.1.5 Gas system

In order to avoid the oxidation of the apparatus, inert gas must be used. Before entering the liquid phase, the gas is preheated and passes through the porous plate such that the system is homogeneous. The hot gas is then pumped out and cooled by a heat exchanger. Another stream of cooled gas can be introduced into the chamber such that the temperature inside the chamber can be kept at the desired range.

4.1.1.6 Measurement of temperature

The wall temperature at the test section, preheat section and the porous plate will be measured by thermocouples which are spot-welded on different locations. The temperature of the radiation shields and copper buses will be measured also by thermocouples.

4.1.2 Procedure

The effect of gas bubbles and surfactants on the physical properties will be studied by experimental measurement. The effect on the apparent viscosity by gas bubbles will be studied first. The void fraction, temperature and viscosity are measured simultaneously for different temperatures and gas flow rates. The measured viscosity is then expressed as a function of temperature and void fraction. The same procedure is repeated for the system with the addition of surfactants. The effect of different kinds of surfactants on the viscosity can be determined.

The surface tension is measured at constant temperature for different concentrations of surfactants. The plot of surface tension versus concentration can be used to calculate the surface excess by Gibb's Law. The activities of different surfactants is determined by these measurements.

The retardation effect of bubble motion by surfactants can also be studied by the apparatus. A single bubble is produced by an orifice which replaces the porous plate. The velocity and the size of the bubble can be measured by gamma-rays which are radiated from two sources placed at a measured distance.

4.3 *The Chemical Reactions*

The chemical reactions can be studied by the same apparatus with minor modifications. The second gas stream must be preheated to the temperature of the liquid such that the reactions are isothermal. The output gas is connected to an analyzer which analyzes the concentration of carbon monoxide. The reaction rate is determined by the partial pressure of CO.

The main purpose of this study is to find out the controlling step of the reactions. The reactions might be controlled by the reaction rate, the diffusion of gaseous products, or the transport of the carbon. Silica is present in excess. If the reaction is kinetically controlled it will depend on temperature only. The velocity of the second gas stream and gas bubbles will not affect the reaction rate. If these conditions are not satisfied, the reaction rate must be controlled by transport. By changing the temperature, it is possible to determine a temperature range above which the reaction is controlled by transport. The diffusion of gaseous products is affected greatly by both the second gas stream and the penetrating gas, while the transport of carbon is independent of the second gas stream. By changing the relative flow rate of the two gas streams, the controlling step and its conditions can be found.

Only if the controlling step is the transport of carbon toward the reaction zone, will the effect of surfactants be studied. The surface tension has great influence on the transport of carbon particles. The higher the surface tension (pure silica), the greater the tendency to move carbon particles toward the liquid surface. The addition of surfactants decreases the surface tension, and might drive the carbon into the bulk region. On the other hand, due to the flotation effect, the gas bubbles may be able to carry the carbon upward. It is an optimization problem. At present, it can only be studied by experimental measurement. From experiment, we will search for some kinds of surfactants which have the most favorable effect on the reactions.

The vaporization of silica can also be studied here. The rate of vaporization is obtained by subtracting the mass of gaseous products from

the total mass lost. The effect of surfactants on the vaporization is determined by varying the concentration of surfactants while other conditions are kept constant.

4.4 *Overall Simulation*

No experimental work has been published concerning the effect of surfactants on ablation. No theoretical studies have considered the effect of gas bubbles within the molten-layer. From the theoretical considerations mentioned above, it is obvious that those effects play an important role in the mechanism of ablation. Many processes are affected by the gas bubbles and surfactants. Some of the processes might be able to increase the efficiency of the materials, and some might not. Most of the processes, favorable and unfavorable, exist simultaneously. The overall effect is still not clearly understood. In order to obtain an optimum ablative performance the overall effect must be studied. Unfortunately, the process is so complex that right now a theoretical study of overall mechanism is impossible. The experimental investigations should be able to give a clearer insight into the overall effect. After the individual processes have been studied, several potential surfactants will be selected. Different samples will be tested with the hot gas flow facility discussed in Phase II of this task. The data can be used to determine the accuracy of theoretical calculations and the increase in efficiency by the addition of surfactants.

REFERENCES

1. Rosenweig, R. E., Bether, R., "Theory for the Ablation of Fiberglass Reinforced Phenolic Resin," AIAA J., 1, pp. 1802-1809 (1963).

2. Steverding, B., "A Theory for the Ablation of Non-Newtonian Liquid near the Stagnation Points," AIAA J., 3, pp. 1265-1249 (1965).

3. Beecher, R., Rosenweig, R. E., "Ablation Mechanism in Plastics with Inorganic Reinforcement," ARS J., 31, pp. 532-539 (1961).

4. Lundell, J. H., Wakefield, R. M., Jones, J. W., "Experimental Investigation of a Charring Ablative Materials Exposed to Combined Convective and Radiative Heating," AIAA J., 3, pp. 2087-2095 (1965).

5. Lundell, J. H., Dickey, R. R., "Performance of Charring Ablative Materials in the Diffusion-Controlled Surface Combustion Regime," AIAA J., 6, pp. 1118-1125 (1968).

6. Sutton, G. W., "Ablation of Reinforced Plastics in Supersonic Flow," J. of Aero. Sci., 27, pp. 377-385 (1960).

7. Hsieh, C., "Mathematical Analysis of Surface Ablation," University of Utah, College of Engineering, Rpt. UTEC TH 69-071, July 1969.

8. Steverding, B., "The Increase of Ablation Effectiveness by Surface Active Compounds," The Aero. Quarterly, 16, pp. 289-300 (1965).

9. Steverding, B., "Boundary Layer Cooling by Spattered Particles," ASME Trans., J. Of Heat Trans., 89, pp. 9-10 (1967).

10. Levich, V. G., Physicochemical Hydrodynamics, Prentice-Hall, N.J. Ch. 8, Ch. 11, (1962)

11. Boud, W. N., "Bubbles, Drops, and Stoke's Law," Phil. Mag., 5 pp. 794-800 (1928).

12. Griffith, R. M., "The Effect of Surfactants on the Terminal Velocity of Drops and Bubbles," Chem. Eng. Sci., 17, pp. 1057-1070 (1962).

13. Schechter, R. S., Farley, R. W., "Interfacial Tension, Gradients and Droplet Behavior," The Canadian J. of Chem. Eng., 41, pp. 103-107 (1963).

14. Davis, R. E., Acrivos, A., "The Influence of Surfactants on the Creeping Motion of Bubbles," Chem. Eng. Sci., 21, pp. 681-685 (1966).

15. Soo, S. L., "Fluid Dynamics of Multiphase System," Blaisdell, Mass. (1967) Ch. 5.

16. Dorrance, W. H., Viscous, Hypersonic Flow, McGraw-Hill, New York (1962) pp. 56-62.

17. Blumenthal, J. L., Santy, M. J., Burns, E. A., "Kinetic Studies of High-Temperature Carbon-Silica Reactions in Charred Silica-Reinforced Phenolic Resins," AIAA J., 4, pp. 1053-1057 (1966).

18. Romie, F. E., "Carbon-Silica Reaction in Silica-Phenolic Composites," AIAA J., 5, pp. 1511-1513 (1967).

19. Ladacki, M., "Silicon Carbide in Ablative Chars," AIAA J., 4, pp. 1445-1667 (1966).

20. Bethe, H. A., Adams, M. C., "A Theory for Ablation of Glassy Materials," J. of Aero Sci., 26, pp. 321-328 (1959).

21. Ostrach, S., McConnell, D. G., "Melting Ablation About Decelerating Spehrical Bodies," AIAA J., 3, pp. 1883-1889 (1965).

22. Bockris, J. O., "Physics Chemical Measurement at High Temperature," Butterworth Scientific Publication, London, pp. 330-331 (1959).

23. Adamson, A. W., "Physical Chemistry of Surfaces," 2nd Edition Interscience Publishers, N. Y., pp. 26-28 (1967).

24. Isbin, H. S., Sher, N. C., Eddy, K. C., "Void Fractions in Two-Phase Steam-Water Flow," AICHE J., 3, pp. 136-142 (1957).

LIST OF FIGURES

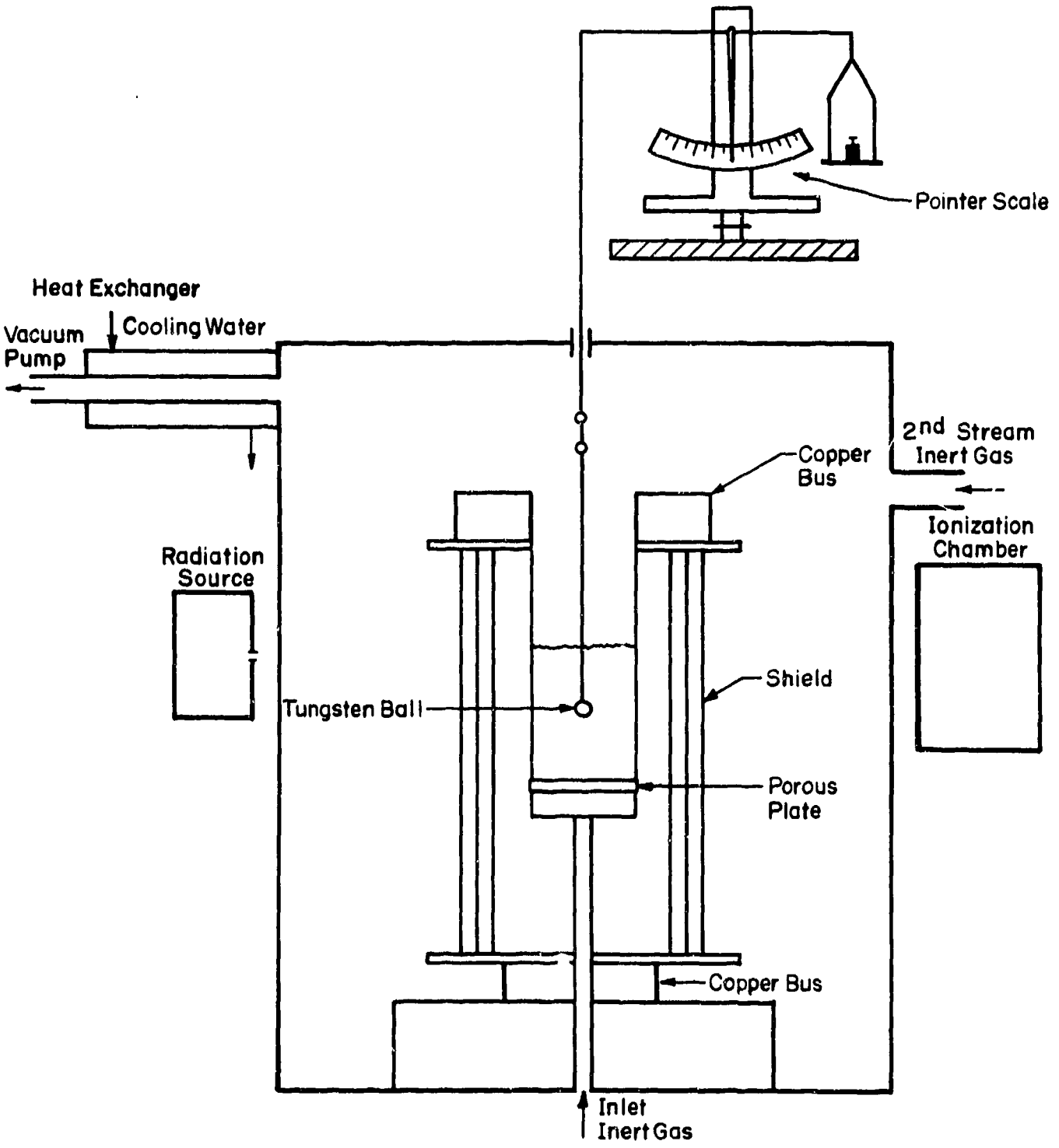

Figure 1. A schematic diagram of apparatus for the measurement of physical properties.

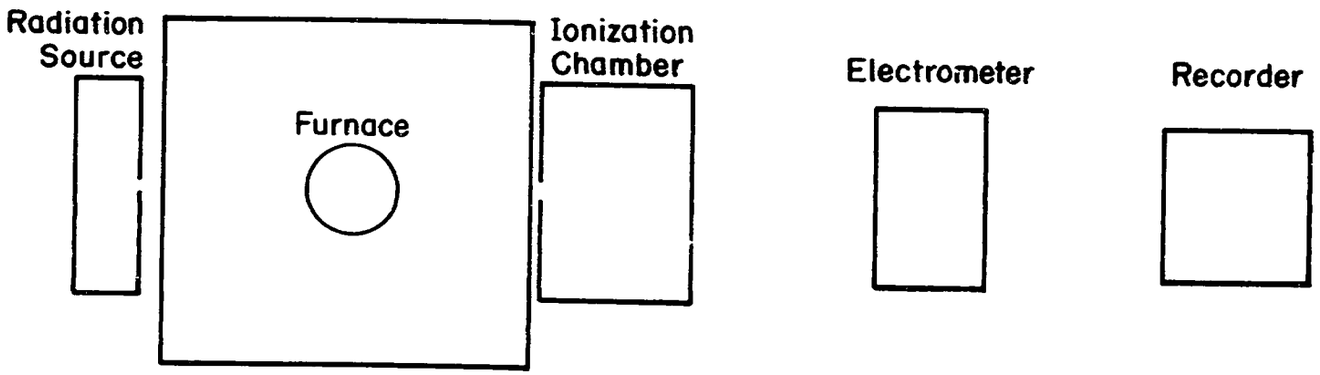

Figure 2. A schematic diagram of the radiation-adsorption system.

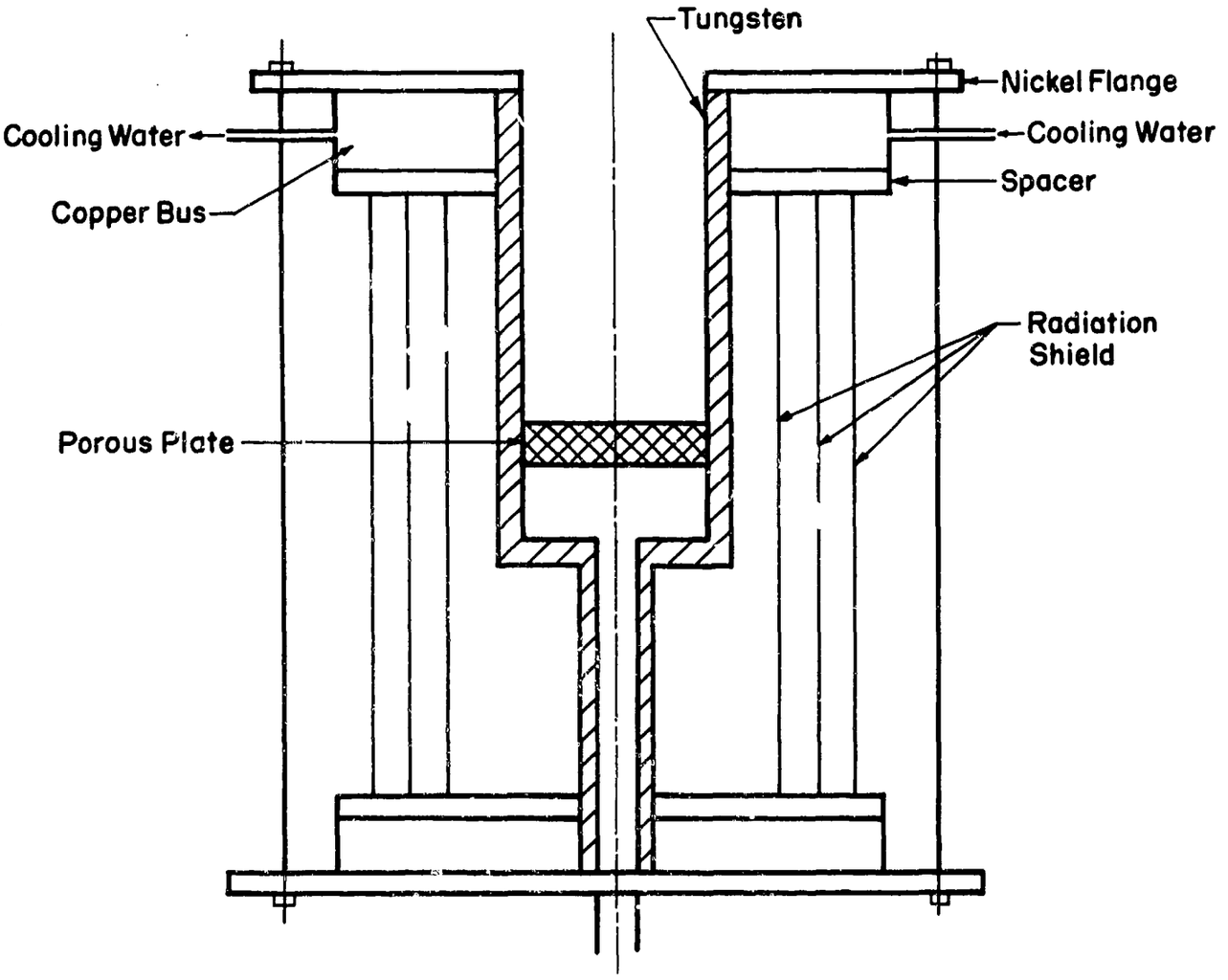

Figure 3. Experimental Apparatus -- Furnace.

UTEC TH 69-073d

THE CHEMISTRY AND MECHANICS OF COMBUSTION

WITH

APPLICATION TO ROCKET ENGINE SYSTEMS

Task 4 Radiation Attenuation and Plasma Physics

R. W. Grow

September 1969

College of Engineering
University of Utah
Salt Lake City, Utah

PREFACE

Microwave diagnostic techniques are being applied to both the problems of measuring the temperature in a combustion chamber and of detecting flaws in solid propellant fuel. For the first problem, a subscale motor has been designed and fabricated for firing fuel charges of less than one pound, for permitting 24 GHz microwave attenuation measurements through the combustion chamber. The effort is presently being made to relate the measured attenuation to the chamber temperature by using Saha's equation to determine the amount of ionization of the potassium-seeded fuel. Subsequent to the verification of the temperature with other measurements and computations, the effort will be made to extend the technique, to give temperature as a function of both time and position, so that nonuniformities in the combustion process can be observed.

In the second problem, an initial feasibility study to investigate the possibility of measuring flaws in solid propellant fuels has been carried out. It was determined that the possibility of measuring 1/1000 inch cracks up to 2 inches deep in propellant material by microwave techniques is highly promising. The effort will be made in the next year to develop a flaw detector.

TABLE OF CONTENTS

TASK 4 Radiation Attenuation and Plasma Physics

1.0 INTRODUCTION

The objective of this report is to develop a method for probing a combustion chamber by microwave techniques. Such techniques have been used for many years to measure the ionization density and collision frequency of the exhaust plasma beyond the exit plane, and elaborate probing techniques have been developed at many locations to measure attenuation through the flame for a minimum path length as well as for an oblique path length and as a function of distance from the exit plane. Ordinarily such measurements assume the plasma to consist of one thermodynamic region. This simple model has been improved in our laboratory by including the effect of thermodynamic shock waves in the plume to obtain a more exact value for the ionization density and collision frequency at the exit plane. [1-4] Reasonable agreement between theoretical predictions and experimental measurements has been obtained.

In addition, analytical techniques have also been developed to include the effect of temperature on the total ionization produced by the constituents of the flame. In general these results are difficult to apply because of the difficulty of knowing all the reactions that are taking place. Particular success was achieved, however, where there was only one source of electrons from the flame constituents. In this case Saha's equation relates the degree of ionization to the temperature. [1] This fact suggests that motors seeded with alkali metals can be used to produce a single source of electrons. Experimental verification of this technique has been achieved. [4]

The basis for relating attenuation measurements to the ionization density and hence to the temperature is given in Section 2. The application of these techniques to the measurement of the chamber conditions is the present objective of the project. Ultimately, techniques will be developed to account in the analysis for the presence of pressure waves, nonuniform combustion, and source and sink reactions. This project is continuing, and measurements on a one-pound

motor are presently being made. The effort is being made to compute temperature data from these results.

As a result of a special interest in the possible use of microwaves for nondestructive detection of voids in solid propellants, a feasibility study was undertaken to investigate this possibility. The basis of this measurement is discussed and plans to proceed with the development of a flaw detector are presented.

2.0 MICROWAVE DIAGNOSTIC STUDY

Plasma characteristics are easily determined using microwave techniques. Changes in amplitude and phase of microwave radiation are caused by the presence of the plasma, and these changes can be related to various plasma parameters such as electron density, collision frequency, and temperature. Microwave diagnostic techniques are widely used and have the important feature that no physical contact with the plasma is required. (1-4)

2.1 *Theoretical Basis for Microwave Diagnostic Measurements* *(J. L. Hou, R. W. Grow)*

A plane electromagnetic wave propagating through a conducting medium is described by Maxwell's equations:

$$\nabla \times \vec{H} = \rho\vec{v} + \frac{\partial \vec{D}}{\partial t} \tag{1}$$

$$\nabla \times \vec{E} = -\frac{\partial \vec{B}}{\partial t} \tag{2}$$

where

$\vec{v}$ = average drift velocity of the electrons through the medium

ρ = charge density of the electrons

The wave equation for the electric field intensity is given by

$$\nabla^2 E = \mu\epsilon \frac{\partial^2 E}{\partial t^2} + \rho\mu \frac{\partial \vec{v}}{\partial t} \tag{3}$$

and Langevin's force equation may be expressed as

$$\frac{\partial \vec{v}}{\partial t} + g\vec{v} = \frac{e}{m} \vec{E} \tag{4}$$

where g is the collision frequency of the electrons with neutral molecules.

If the field has a one-dimensional space dependence given by

$$E = E(\omega)\ e^{-\Gamma z} \tag{5}$$

Then the combination of Equations (4) and (5) yields the determinantal equation,

$$\Gamma^2 + k^2 - k_p^2 \frac{i\omega}{g + i\omega} = 0 \tag{6}$$

where k is the propagation constant of free space, $\frac{\omega}{c}$, and k_p is defined by

$$k_p = \frac{\omega_p}{c}$$

The quantity ω_p^2 is given by

$$\omega_p^2 = \frac{\rho e}{m\epsilon_o} \tag{7}$$

where $\rho = ne$ and n is the electron density per cubic meter. The usual identification is made that

$$\Gamma = \alpha + i\ \beta \tag{8}$$

where α is the attenuation constant in nepers per meter and β is the phase constant in radians per meter.

Equation(6)can be written as

$$\Gamma^2 + k^2 - \frac{\omega_p^2}{c^2} \frac{i}{g + i\omega} = 0 \qquad (9)$$

Substituting Equation (8) into Equation (9) and assuming $k^2 >> \alpha^2$ yields, if g is real,

$$\beta^2 = k^2 \left(1 - \frac{\omega_p^2}{g^2 + \omega^2}\right) \qquad (10)$$

$$2i\ \alpha\beta = \frac{\omega_p^2 - g\ i\omega}{c^2(g^2 + \omega^2)} \qquad (11)$$

Substituting Equation (10) into Equation (11) and solving for α, with the assumption that $\omega_p^2\ (g^2 + \omega^2) << 1$, then one obtains

$$\alpha = \frac{g}{2c} \cdot \frac{\omega_p^2}{(g^2 + \omega^2)} \qquad (12)$$

If g is complex, Equation (9) can be written

$$\alpha^2 + 2i\ \alpha\beta - \beta^2 + k^2 - \frac{\omega_p^2}{c^2} \cdot \frac{i\omega(g - i\omega)}{g^2 + \omega^2} = 0$$

and $g = g_r + j\ g_i$.

Thus a propagating electromagnetic wave will attenuate in a plasma when collisions take place. Since the collision frequency depends on the collision cross section, the density of the gas, and the velocity of the electrons, an average collision frequency for a particular velocity class can be computed on the basis of an average cross section for the neutral atoms.

$$\nu_{av} = \rho v \, Q_{av} \tag{13}$$

Langevin's equation for a velocity-dependent collision frequency is given by

$$\bar{v} = \frac{eE}{m} \frac{1}{g + i\omega} \tag{14}$$

where $\bar{v}$ is the average velocity of all the electrons in the gas in the direction of the electric field. The mean velocity of the elecrons can also be computed by integrating over the possible electron velocity

$$\bar{v} = \frac{8\pi}{3} \frac{eE}{m} \beta \left(\frac{\beta}{\pi}\right)^{3/2} \int_0^\infty \frac{v^2 \, e^{-\beta v^2} dv}{i\omega + \rho v \, Q_{av}} \tag{15}$$

where

$$\beta = \frac{m}{kT}$$

Comparing Equations (14) and (15) shows that the collision frequency is a function of

$$g = g(\omega, \rho, T) \tag{16}$$

and the attenuation constant α may be expressed in terms of

$$\alpha = \alpha(\omega, \omega_p, \rho, T) \tag{17}$$

Since the density and the temperature are given by the natural gas law in an equilibrium plasma, then

$$\rho = \frac{N_o P}{RT} \tag{18}$$

and

$$\alpha = \alpha(\omega, \omega_p, T) \tag{19}$$

It is the objective of the present diagnostic experiment to heavily seed the fuel with potassium so that only one ionizing species is present in the plasma. Under the circumstances, all the electrons will be produced by one process and Saha's equation may be used:

$$\frac{X^2N}{1 - X} = \left(\frac{\sqrt{2\pi\ km}}{h}\right)^3 T^{3/2}\ e^{-\frac{eI}{kT}} = f(T) \tag{20}$$

where X is the percent of ionization of the N potassium atoms in the plasma. Noting that XN is related to ω_p^2 allows the attenuation to be expressed as

$$\alpha = (\omega\ ,\ T)$$

and the following parameters are required to compute the equilibrium temperatures of the plasma:

1. Chamber pressure.
2. Percentage of potassium in the fuel.
3. Length of microwave path.
4. Frequency of radiation.
5. Attenuation through the chamber.

The present objective of this phase of the project is to demonstrate the feasibility of making this measurement.

2.2 *Experimental Results (J. L. Hou, H. S. Hwang, R. W. Grow)*

During the past year a one-pound solid propellant motor has been designed and constructed with quartz windows to permit microwave

attenuation measurements to be made through the combustion chamber while the motor is being fired. A sketch of the motor is shown in Figure 1. The 24 GHz microwave energy is transmitted into and out of the chamber through 1" x 2" windows placed in the side walls of a 3" outside diameter, 0.5" wall steel pipe. Special horn antennas with dielectric lenses have been developed to provide focusing of the microwave energy between the horns with an optimum separation distance between horn antennas. The quartz windows have been designed so that no transmission loss is experienced as a result of the windows. The effectiveness of the focussed antennas is indicated by the transmission measurements given in the following table.

TABLE I

Situation	Insertion Loss
Direct wave guide connection	0 dB (reference)
Propagation between antennas without the motor in place	-0.6 dB
Propagation between antennas with the motor in place	-1.6 dB
Propagation between antennas with windows on the motor blocked	-25.5 dB

These data indicate that the dynamic range of the measuring equipment is about 25.5 dB and the loss between the antennas with the motor in place is about 1.6 dB. A photograph of the experimental arrangement is shown in Figure 2. The antennas with the dielectric lens in place are shown as well as the physical placement of the antennas with respect to the one-pound rocket motor.

A number of firings have been made in the past six months in order to perfect the pressure measuring equipment and the microwave

equipment so as to get data that are consistent and reproducible. The nozzle diameter of the motor is readily variable. Typical data that are presently being analyzed are given in Table II.

A computer program for computing the chamber temperature based on the theory of Section 2.1 has been written, and the effort will be made over the next few months to compute temperature data for various pressures and seeding values. The effort will then be made to refine the technique to the point where reliable values of chamber temperature are obtained. The effort will be made to compare this value with temperature measurements obtained by other techniques and by chemical analysis of the combustion process.

TABLE II

Nozzle Size	Pressure	Attenuation
5/16"	18 psi	2.1 dB
3/16"	100 psi	2.1 dB
3/16"	74 psi	1.4 dB

3.0 FLAW DETECTION BY MICROWAVE ANALYSIS (C. H. Durney, R. W. Grow)

As a result of current interest by industrial organizations and research laboratories in nondestructive test and inspection techniques in solid fuels, for both latent defects as well as internal dewetting, the possibility of detecting small cracks or voids using microwave diagnostic techniques was investigated last year. Although the project was inactive this year, it is expected that the project will again be activated during the next year.

3.1 *Flaw Measurement Techniques*

While there are several methods for making such measurements, the method investigated was based on conventional standing wave measurements. If an electromagnetic wave passes from a first region to a second region that has a different dielectric constant than the first region, a reflection is generated. These two reflections will cancel each other if the thickness of the second region is zero, otherwise a net reflection is produced by the combination of the two reflected waves. This reflection can be used to detect the presence of a defect. The interaction of the reflection from the incident surface of the propellant and the combined reflection from the crack can be used to determine the depth of the crack below the surface. The combination of these two reflections will give a periodic variation of VSWR versus frequency, and if the period of the frequency variation is Δf, then the depth of the crack is given by

$$D = \frac{c}{2\Delta f \sqrt{\frac{\varepsilon}{\varepsilon_o}}}$$

where c is the velocity of light and $\varepsilon/\varepsilon_o$ is the relative dielectric constant of the propellant. The amplitude of the periodic variation can be used to determine thickness of the crack, since a thickness of 0, λ, $\lambda/2$, etc., will give no reflection, whereas a thickness of $\lambda/4$, $3\lambda/4$, $5\lambda/4$, etc., will give a maximum reflection.

Experimental measurements showed that the propellant at microwave frequencies is a lossy dielectric. The loss is sufficiently large, in fact, that the behavior described in the preceding paragraph is masked to some degree. Experimental measurements demonstrated the validity of the technique, but the physical loss of the propellant increases the complexity of any experimental system for applying the technique. At least two possibilities exist for overcoming the

loss. These are as follows:

1. Filling the horn antenna with dielectric material.
2. Amplifying the observed frequency-depen[illegible] variations.

The first possibility is important because the major problem with a large amount of loss is the large reflection that occurs at the front face of the propellant. If the magnitude of this reflection is reduced, the net result is an effective amplification of the ripple that will be observed. In addition, the horn antenna filled with alumina will be one-third as large as the unfilled horn, once again improving the realizability of the microwave detection.

The microwave technique has considerable promise as compared with acoustic techniques and X-ray techniques. The X-ray system has the inherent disadvantage of being noncoherent or not having a wave-like behavior, but both the acoustic and the microwave systems appear to have high promise for successful detectors. Since the wavelengths are comparable, the actual detection of cracks or voids is somewhat similar but the detection equipment frequencies, because of the higher frequency and consequently wider possible band width, have a higher potential accuracy. Computations indicate that the microwave technique should be capable of measuring crack thicknesses as small as .001" in cracks located a few inches from the propellant surface without difficulty.

3.2 *Future Plans for Developing Flaw Detection*

Because of the advantages of the microwave measurement, it is our objective to develop, as part of the diagnostic effort, the crack or void detection technique during the next year to determine the ultimate possibilities of such a measurement.

REFERENCES

1. Jones, A. S., Grow, R. W., and Johnson, C. C., "Microwave Diagnosis of Non-Ideal Plasmas," Technical Report SSD-2, September 1963.

2. Grow, R. W., Johnson, C. C. and Jones, A. S., "Multi-Frequency Attenuation Measurements Made on the Exhausts of Solid Propellant Rockets," Conference on Ions in Flames and Rocket Exhausts, Palm Springs, California, October 10-12, 1962, classified Confidential.

3. Grow, R. W., Johnson, C. C., and Jones, A. S., "Microwave Diagnostics of Plasmas," International Symposium on Plasma Phenomena and Measurement, San Diego, California, October-November 1963.
   Transactions PTGNS, January 1964.

4. Technical Documentary Report No. FFD-TDR-64-225, November 30, 1964, Vols. 1 and 2. Prepared under Contract No. AF 04 (695)-439 by the Hercules Powder Company and the University of Utah Microwave Device and Physical Electronics Laboratory, classified Confidential.

5. Grow, R. W., "The Chemistry and Mechanics of Combustion with Applications to Rocket Engine Systems, Task 4, Radar Attenuation and Plasma Physics," Technical Report UTEC DO-68-065d, College of Engineering, University of Utah, Salt Lake City, Utah, October, 1968.

List of Figures

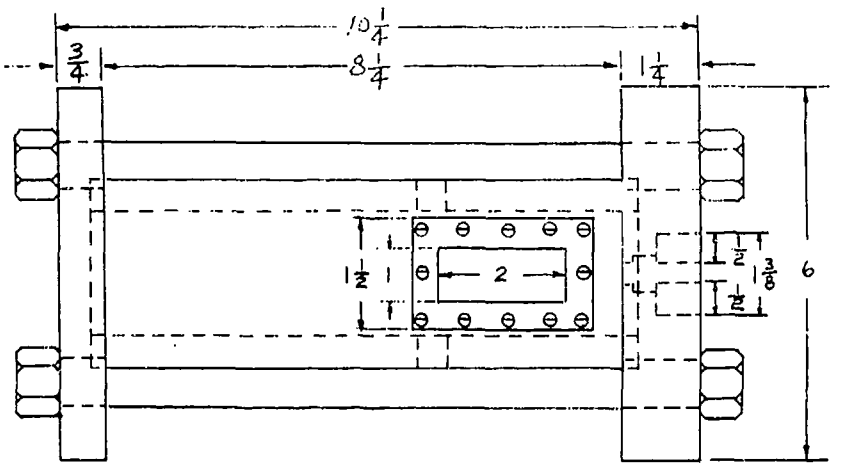

Figure 1. Drawing of one-pound rocket motor.

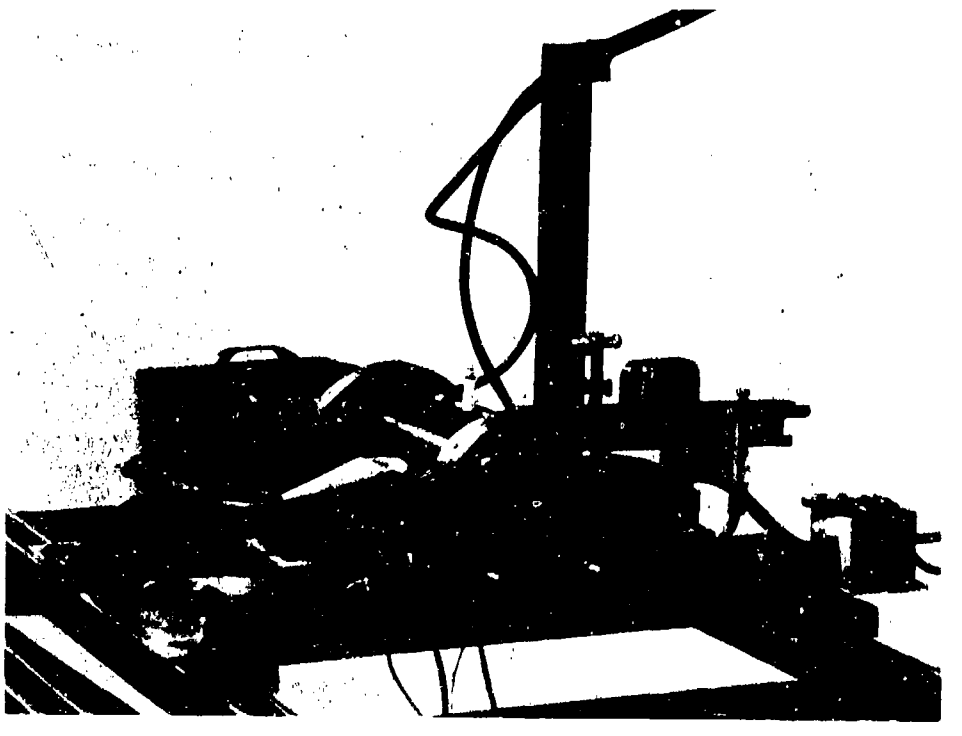

Figure 2. Photograph of experimentat arrangement used for making the microwave diagnostic equipment.

UTEC TH 69-073e

THE CHEMISTRY AND MECHANICS OF COMBUSTION

WITH

APPLICATION TO ROCKET ENGINE SYSTEMS

Task 5 High Solids Loading in Propellants

J. E. Fitzgerald

September 1969

College of Engineering
UNIVERSITY OF UTAH
Salt Lake City, Utah

PREFACE

A detailed description of one phase of Task 5 is presented. This phase concentrates on the need for developing a nonfading memory constitutive law in order to account for certain irreversible phenomena, e.g., the Mullins Effect. The general functional form of a suitable constitutive law which is also amenable to engineering analysis is presented. The results of the phase of Task 5 concentrating on thermomechanical coupling is briefly summarized.

TABLE OF CONTENTS

TASK 5 High Solids Loading in Propellants

1.0 INTRODUCTION

For nearly a decade composite solid propellant materials have for the most part been treated as linear viscoelastic materials. Today the solid propellant industry has progressed to the point where it is capable of highly sophisticated thermoviscoelastic stress analysis for linearly viscoelastic materials that are thermorheologically simple (i.e., an equivalence between time and temperature exists).

This task demonstrates that the highly loaded composite solid propellants are <u>not</u> necessarily linear viscoelastic materials, and that the criteria for linearity used by the propellant industry,[1] "doubling the strain input doubles the stress output," is a necessary but not a sufficient condition for linear viscoelastic response. Generally speaking, the industry only checks this criteria for jump strain inputs of different strain magnitudes. Because of this insufficient criteria and inadequate testing, the highly non-linear behavior of solid propellants at small strains* has for the most part escaped detection.

It is clear, however, how the problem has gone undetected for so long. The stress analysts and others who understand linear viscoelasticity usually see only the reduced data requested from their testing laboratories and usually have no idea what propellants are like on a microstructural basis, and most important of all, how they actually respond to various inputs. These analysts normally do no testing themselves and are in different departments than the testing personnel. The laboratory personnel, on the other hand, are usually very familiar with how propellants will respond but they know little or nothing about linear viscoelasticity. It is this lack of communication and perhaps a lack of true understanding of linear viscoelasticity that has led to non-linear propellants being characterized as linear viscoelastic materials.

---

* For the purpose of this discussion small strains occur with no measurable dewetting while large strains occur with dewetting. Small strains are normally less than 5% which is in the range of infinitesimal strain theory.

This task elucidates why highly loaded propellants are non-linear viscoelastic materials and why most of the existing non-linear viscoelastic theories cannot be used to accurately treat propellant data. Although the experimental data presented is minimal, the behavior discussed is characteristic of almost all composite propellants used over the past ten years.

The net result of these observations is that the propellant industry today has inaccurate constitutive laws for predicting stresses for non-equilibrium conditions. (Actually, because of the "Mullins Effect," discussed later, there also exists no accurate equilibrium constitutive law.) Effort is therefore underway to develop constitutive laws that will accurately describe propellant response for equilibrium and non-equilibrium conditions.

Previous reports (Themis Annual Report, October, 1968) discussed the thermomechanical coupling effects being investigated. This particular report will not discuss thermal effects but does refer to a copy of a recent paper[2] on that subject which indicates the use of the Fundamental Energy Inequality in determining the form of the coupled constitutive equations.

The essence of the above paper was that postulating a positive semi-definite global interval energy leads to a restriction on the constitutive equations where the deformation gradient and its first two time derivates only are permitted, i. e., all higher derivatives of the deformation gradient are suppressed.

2.0 THE NON-LINEAR BEHAVIOR OF SOLID PROPELLANTS AT SMALL STRAINS

As mentioned above, about the most complex form of analysis presented performed on highly filled propellant grains is that of treating them as thermo-rheologically simple linear viscoelastic materials. When solid propellants are tested for linear viscoelastic characterization by propellant laboratories, usually the only tests run are stress-relaxation and constant strain rate. This is normally done at a series of temperatures,

strains, and strain rates to determine if the relaxation modulus is dependent of strain and hence if linear viscoelasticity is applicable.[3] Such data also provides the time-temperature interrelations and the relaxation modulus over the entire reduced time scale.

Many propellant rheologists consider that the relaxation modulus being independent of strain is a sufficient condition for linear viscoelasticity. This however is not the case; the relaxation modulus can be independent of strain and the material can still be non-linear. A material having a relaxation modulus that is independent of strain is a necessary condition for linear viscoelasticity but not a sufficient condition. Most propellants have a relaxation modulus that, roughly speaking, does not depend upon strain when the strains are of several percent or less. Yet this relaxation modulus cannot be used to accurately predict the stress due to simple isothermal low rate strain inputs. This is perhaps best demonstrated by showing that superposition at different times is not applicable for the ramp loaded stress-relaxation test. Figure 1 illustrates typical predicted and observed stress output for a solid propellant having an interrupted ramp strain input. Linear viscoelastic theory would predict that the stress could be obtained by simply superposing the initial loading response with the continuation of the original stress-relaxation response. What actually is observed however is that the material behaves for a short time with a very high modulus until it apparently rejoins the constant rate stress-strain behavior as illustrated in Figure 2. Interestingly enough, the polymeric binders and low loaded solid propellants appear to be linear viscoelastic materials even at quite large strains.

Although it is sufficient to show that propellants fail to obey the laws of linearity in just one way in order to demonstrate they are non-linear materials, it strengthens the argument and sheds light on probable causes if other proof of non-linearity exists. Two such arguments are as follows. If a propellant is deformed uniaxially at a constant rate of strain to some strain ε_o and then allowed to recover for a sufficiently long period of time and then deformed to failure, the stress behavior in the range of strain $0 < \varepsilon < \varepsilon_o$ is far less than the original response,

while for strains $\varepsilon > \varepsilon_o$ the material appears to rejoin the constant strain rate stress-strain curve. This effect is illustrated in Figure 3 and is clearly beyond the predictability of linear viscoelasticity. Another argument proving propellants are not linearly viscoelastic is that when the above experiment is performed at strain rates low enough so that the time effects disappear, linear viscoelasticity predicts that this equilibrium output will be linearly elastic. One finds however that although there is no time effect, there is a definite strong hysteresis when the direction of straining is reversed. This hysteresis is not normally recoverable and if the material is strained again, the hysteresis path is followed until $\varepsilon > \varepsilon_o$ and then the response joins the low rate single stretch curve. This effect is illustrated in Figure 4 and it also is clearly not contained in linear viscoelastic theory.

3.0 NON-LINEAR VISCOELASTIC CHARACTERIZATIONS

About the only non-linear viscoelastic constitutive laws that have been used to date are the Frechet multiple integral expansion[5,6] and some phenomenological approaches.[7,8] The Frechet expansion is the most general mathematical representation for a non-linear representation of a non-aging material with fading memory. Mathematically this constitutive law can be written for uniaxial deformations as

$$\sigma(t) = \int_o^t E_1(t-\xi_1)\,\dot{\varepsilon}(\xi_1)d\xi_1 + \int_o^t\int_o^t E_2(t-\xi_1,t-\xi_2)\,\dot{\varepsilon}(\xi_1)\dot{\varepsilon}(\xi_2)d\xi_1 d\xi_2$$

$$+ \ldots + \int_o^t\int_o^t \ldots \int_o^t E_p(t-\xi_1,t-\xi_2,\ldots,t-\xi_p)\dot{\varepsilon}(\xi_1)\dot{\varepsilon}(\xi_2)\ldots$$

$$\dot{\varepsilon}(\xi_p)d\xi_1 d\xi_2 \ldots d\xi_p + \ldots$$

where $(\dot{\varepsilon}_i) = \dfrac{\partial \varepsilon(\xi_i)}{\partial \xi_i}$ and ξ_i = dummy time variables

Because of the difficulty in determining the kernal functions, applications of this technique almost always result in terminating the series after the third term.[6] The purpose of the following discussion is to demonstrate that such a constitutive law for propellants does not provide a much better nor more accurate representation than linear viscoelasticity (which incidentally is the first term in the Frechet expansion).

The Frechet multiple integral expansion does not in general satisfy either of our requirements for linearity. As stated above, many solid propellants appeared to satisfy the first linearity requirement while they strongly failed on superposition of the same input at different times. To determine if one can preserve the first linearity rule without forcing the second while using the Frechet expansion one can calculate the output for an arbitrary strain input $\varepsilon(\xi)$ and compare it to some multiple of it $c\varepsilon(\xi)$. The first linearity rule demands that

$$\sigma\{c\varepsilon(t)\} = c\sigma\{\varepsilon(t)\} \qquad c = \text{arbitrary scalar}$$

$$\varepsilon(t) = \text{arbitrary strain input}$$

If we force the first linearity requirement on the Frechet multiple integral expansion, we are left with just the first term which is simply linear viscoelasticity. If we force the first rule of linearity we automatically obtain the second. This argument goes both ways, if we force the second rule of linearity on the Frechet expansion we again find all terms vanish except the first term and we are left again with linear viscoelasticity.

The above discussion demonstrates that if either one of the linearity rules is forced to hold for the Frechet multiple integral expansion the other rule is forced to hold and the output reduces to linear viscoelasticity. Therefore if materials obeying one rule of linearity and not the other exist, and some solid propellants are good examples of such materials, they cannot be represented accurately by a Frechet multiple integral expansion.

All propellants tested, however, do show strong hysteresis at quasi-static equilibrium strain rates, and all propellants show non-recoverability of their properties after they have been initially deformed and then allowed

to rest for a long period of time. Neither of these conditions can be obtained using the most general Frechet expansion because

(1) at equilibrium the Frechet expansion reduces to non-linear elasticity.

(2) the Frechet expansion incorporates the concept of fading memory for viscoelastically admissible kernel functions and therefore forgets the distant past

The other types of non-linear viscoelastic constitutive laws that have been used to date are basically of the following two forms[15, 16]:

$$\sigma(t) = f(\varepsilon) \int_0^t E(t-\xi)\dot{\varepsilon}(\xi)d\xi \qquad f(\varepsilon) = \text{function of strain}$$

$$\sigma(t) = \int_0^t E(t-\xi)\dot{G}(\varepsilon)d\xi \qquad \dot{G}(\varepsilon) = \text{time derivative of some strain function}$$

Both these approaches have been used with success for describing the geometric non-linearities observed in rubbers at large deformations.[4,7,8] Although not as complex as the Frechet multiple integral expansion, these functions lend themselves to simple characterization and computation. Neither of these techniques is of great value for describing propellant behavior since propellant behavior is not reversible (e.g., Figure 4) and at equilibrium they both show a reversible non-linear elastic response and both equations allow for the complete recovery of the material response after an initial deformation.

The preceding arguments demonstrate that non-linear viscoelastic characterizations used to date are not capable of accurately describing the mechanical time dependent response of solid propellants. The main reason for the non-applicability of linear or non-linear viscoelasticity to propellant behavior is because propellants exhibit a permanent non-fading memory. Therefore non-linear viscoelasticity is no more applicable to propellant response than non-linear elasticity is to the plastic deformation of metals since neither would be of much value beyond the first stretch.

If meaningful constitutive laws are to be found, they must incorporate features such as non-fading memory and time dependence in order to explain propellant response. Such effects can usually be explained and characterized from an understanding of the microstructure of the material.

4.0 CAUSE OF PROPELLANT NON-LINEARITIES

The source of the non-linearities in the viscoelastic response of composite solid propellants is not difficult to understand from a microscopic point of view. We have provided some evidence that at low strains propellants are non-linear viscoelastic materials even though they might have a relaxation modulus that is independent of strain. At larger strains the material response is even more complicated. Generally speaking, at low strains propellants are nearly incompressible while at larger strains they become highly compressible and exhibit large amounts of volumetric dilatation during uniaxial testing.[9] The yielding behavior in the stress-strain behavior is characteristic of these materials and is always coincidental with the increase in volume. This sudden change in modulus is the only type of non-linearity that is well known and recognized by most workers in the field. At these larger strains, the relaxation modulus becomes very strained and dilatation dependent[10] and this naturally means non-linear behavior.

This large strain non-linearity is the result of microstructural failure of the composite system. Failure begins early in the stress-strain history and is first observable as a vacuole in the polymer near the surface of the filler in the direction of stretch.[11] These vacuoles increase in size and number with increasing strain which causes the volumetric increase. Vacuoles only form in the polymer where the stress and stress gradients are very high.[11] Once the vacuole forms the neighboring polymeric material is relieved of some of its strain energy which must be spent in making the vacuole grow. This growth reduces the stresses and stress gradients in the vicinity of the vacuole and therefore greatly reduces its tendency to propagate. Vacuole growth also greatly reduces the influence of the filler

particles in the neighborhood of the vacuole. It is this loss of filler support that causes the yielding in the stress-strain curve and the strain dependence of the relaxation modulus at large strains. Each filler particle is therefore a potential vacuole site and experimental evidence indicates that on a volumetric scale at large strains 70 to 100% of the filler particles have vacuoles immediately adjacent to them in the direction of stretch.[9]

Since the filler is near rigid and only gets subjected to very small stresses and the polymer is for all practical purposes incompressible, all the volumetric increase caused by strain can be attributed to this vacuole process. By attributing all the dilatation to vacuole formation, mathematical models have been developed that relate the volumetric dilatation to the frequency of vacuole formation.[10] In a similar manner the first stretch stress-strain behavior has been related to the dilatation-strain behavior and therefore to the vacuole process.[9] These models account for the non-linearities in the stress-strain behavior for the first stretch and although the models contain irreversible effects, they can not predict the observed hysteresis propellants exhibit. Others also have studied the one stretch stress-strain behavior at large strains,[12,13,14] but since nearly all these methods incorporate non-linear strain functions they contain no irreversible effects, they like the above case are of no value beyond the first stretch.

There is considerable evidence that all the hysteresis effects observed in propellants and much of the viscoelastic behavior is caused by the time dependent failure of the polymer on a molecular basis. At near equilibrium rates and small strains propellants exhibit the same type of hysteresis that many lowly filled, highly cross-linked rubbers demonstrate at large strains.[15,16,17] This phenomenon is called the "Mullins Effect" and has not attributed to microstructural failure by practically all who have investigated it. Mullins himself, who examined the behavior in great detail, postulated a breakdown of particle-particle association and possibly also particle-polymer breakdown could account for the effect.[15] Later Bueche[16,17] proposed a molecular basis for the "Mullins Effect" based on the

assumption that the centers of the filler particles are displaced in an affine manner during deformation of the composite. Such deformations would cause a highly non-uniform strain and stress gradient in the polymer between particles, especially in the direction of stretch. He assumed that polymer chains attached themselves at both ends to neighboring filler particles and that these chains ruptured when the particles were separated enough to extend the chains to near then full elongation. He derived a model from which he could calculate the difference in stress levels at a given elongation for the first and second stretching cycles. It is this type of model that is generally accepted as being representative of the molecular behavior which causes the "Mullins Effect." Figure 4 illustrates this behavior for repetitive stretching to increasing strain levels. In highly cross-linked rubbers the effect only depends upon strain and is irreversible.[15] If the pre-stressed composite is allowed to rest in the relaxed state, a portion of the original stiffness might be regained. This recovery or rehealing appears to be a complex function of the recovery temperature and time.[18]

All of the theoretical and nearly all of the experimental work done in studying this phenomenon has been on materials similar to the rubber found in automobile tires. These are highly cross-linked rubbers that are usually filled about 20 volume percent with very fine carbon black. Propellants on the other hand are lowly cross-linked and highly filled with coarse particles. The relative particle spacing is much more severe and the polymer chains are on the average hundreds of times longer in propellants than in tire rubber. The probability of finding a larger portion of the chains branching particles would be greater in propellants and the effect therefore should be much stronger and occur at smaller strains,[15] the same basic mechanism proposed by Bueche still applies. This polymeric chain failure is therefore the step which precedes the vacuole formation process which causes the stress and dilatational non-linearities at larger strains. The small strain non-linearities discussed earlier do not show any measurable volumetric increase, ($\nabla V/V_0 \leq 10^{-4}$). No dilatation however should be expected since it is not until a great

number of chains in one neighborhood have failed that an observable vacuole can exist. Multiple stretch data on propellants at large strains with and without a superimposed pressure environment[11] demonstrate that propellants can also exhibit the Mullins type hysteresis at large strains without having measurable dilatation. This data was used by Oberth[11] to demonstrate that micro-structural damage can occur without measurable dilatation.

This equilibrium "Mullins Effect" can account for the near equilibrium hysteresis observed in propellants at low strains but cannot account for the non-linear time effects. There is however considerable evidence that the "Mullins Effect" in propellants is a very strong function of time. Time dependent chain failure can be readily demonstrated by simply looking at the effect of filler on viscoelasticity and at some of the routine tests run on solid propellants.

One of the simplest ways of demonstrating a time dependent Mullins Effect is through the strain endurance test. In this test a sample is strained to some level and held there for several days or longer. The only measurement taken is the time to failure, if the sample fails. The point of interest here is that samples fail while held at conditions of constant strain when the stress is slowly relaxing or at most constant. This type of failure is clear evidence of a time dependent Mullins Effect and also demonstrates that some portion of the time dependent stress must be due to chain failure.

Another example of time dependent chain failure is that during stress-relaxation testing at strains large enough to have observable volume dilatation, the volume in many systems continues to increase during the relaxation portion of the test[10] as illustrated in Figure 5. It is difficult to imagine this volume increase being caused by any mechanism other than increasing microstructural failure since the sample is maintained at constant length and the stress is decaying. Also, some portion of the stress decay must be associated with this volume increase and therefore with chain failure.

Still another example of a time dependent Mullins Effect is that if a lowly cross-linked polymer with little or no time dependency at some temperature is filled to various degrees, we find that the composite material is generally time dependent. The more filler incorporated into the system the more marked the time effect. Many propellant polymers fall into this category and nearly all propellants show time dependency over such long times that equilibrium data can only be approximated. This time dependency in the composite material can not therefore be explained by the argument that the polymeric strain rates are higher in the composite than in the pure polymer since the time effects continue for such long times and many propellant binders show no time dependency even at very short times. This effect is illustrated by some data published by Freudenthal[12] using a sodium chloride filled polyurethane polymer.

5.0 CONTINUED RESEARCH

Our work during the past year has led primarily to a problem statement. It appears that neither linear nor non-linear viscoelastic theories can be used to accurately characterize highly filled polymers. Our present results are negative in the sense that we have not yet provided an alternate method of material characterization. The subject of accurate constitutive laws for highly filled polymers is indeed the subject of Task 5. Near term effort will determine the uniaxial constitutive equation from a statistical mechanical model which allows for time dependent microstructural failure. Once the uniaxial constitutive equation is known, the theory of continuum mechanics will be used to guide experiments and aid in developing the proper mathematical representation for the three dimensional constitutive equations. Preliminary evidence indicates that the uniaxial constitutive equation will be of the form

$$\sigma = \sum_{s=0}^{\infty} F \left(\varepsilon(t-s), \| \varepsilon \|\right).$$

Here $\underset{s=0}{\overset{\infty}{F}}$ is a functional of the strain history, $\varepsilon(t-s)$, and of the maximum strain experience in the history, $||\varepsilon||$. Such a relation is still within the framework of a simple material since $||\varepsilon||$ is contained in the history of the deformation. These relationships do not however, incorporate features such as a totally fading memory, and they therefore may contain the permanent irreversible effects, which depend on the history of the deformation, that are not contained in linear and non-linear viscoelastic theories.

6.0 SUMMARY AND CONCLUSIONS

The criteria used by the propellant industry to determine whether or not linear viscoelasticity is applicable to a material's response is shown to be a necessary but not sufficient condition. Because of this insufficient criterion and inadequate testing, many non-linearities and irreversible effects have not been detected or considered. It is shown that composite solid propellants are not linear or nonlinear viscoelastic materials and they therefore cannot be accurately treated by these methods. The preceding statements are true because propellants are not "elastic" since all the effects of the history of the deformation are not reversible. If linear or nonlinear viscoelastic theories are used to characterize these materials then errors as large as several hundred percent in the predicted stresses are to be expected even for monotonically increasing strains applied uniaxially and isothermally. These errors will occur in the range of strains where vacuole formation is not detectable as well as for strains where vacuole formation and growth greatly complicate the material's response. These irreversible effects appear to be caused by a time dependent "Mullins Effect" which is due to the time dependent failure of polymer chains which precedes vacuole formation. Polymeric viscous effects therefore do not solely control the time dependent stresses or strains since time effects can be observed in filled "elastic" polymers.

The results of this discussion indicate that elastic, linear viscoelastic, and nonlinear viscoelastic constitutive equations are not generally applicable to propellant response and therefore the propellant industry is left without meaningful stress analyses for equilibrium and non-equilibrium conditions. Even the elastic strain analysis can be questioned for repeated straining because of the hysteresis in the

equilibrium stress-strain behavior. It appears that because failure originates microscopically at apparently the onset of deformation in propellants, the constitutive laws and failure behavior are coupled equations. If meaningful constitutive laws and failure criterion are to be developed, they will have to take this into consideration.

REFERENCES

1. Williams, M. L., Blatz, P. J. and Schapery, R. A., "Fundamental Studies Relating to Systems Analysis of Solid Propellants," GALCIT SM 61-5, California Institute of Technology, Pasadena, California, February 1961. Reprinted in Interagency Chemical Rocket Propulsion Group (ICRPG) Solid Propellant Mechanical Behavior Manual, CPIA Publication No. 21 Section 2.3, Sept. 1963.

2. Fitzgerald, J. E., "Thermo-Mechanical Coupling," Presentation at the International Conference on Structure, Solid Mechanics and Engineering Design of Civil Engineering Materials, Southampton University, April 21-25, 1969.

3. Landel, R. F., "Reduced VAriable Relationships," ICRPG Solid Propellant Mechanical Behavior Manual, CPIA Publication No. 21, Section, 2.4, September 1963.

4. Tobolsky, A. V., Properties and Structure of Polymers, 104 (John Wiley and Sons, Inc., New York, 1960).

5. Volterra, V., Theory of Functionals and of Integral and Integro-Differential Equations (Dover, New York, 1959).

6. Lai, J. S. and Findley, W. N., "Prediction of Uniaxial Stress Relaxation from Creep of Nonlinear Viscoelastic Material," Trans. Soc. Rheol., 12, 2, pp. 243-257.

7. Schapery, R. A., "Nonlinear Viscoelastic Characterization and Stress Analysis of Solid Propellants," Solid Rocket Structural Integrity Abstracts, 3, 4 (October 1966).

8. Ferry, J. D., Viscoelastic Properties of Polymers, 105 (John Wiley and Sons, Inc., New York, 1956).

9. Farris, R. J., "The Influence of Vacuole Formation on the Response and Failure of Filled Elastomers," Trans. Soc. Rheol., 12, 2, pp. 315-334 (1968).

10. Majerus, J. N., "Operator Method of Materials Characterization," Technical Memorandum No. 17, SRO, Aerojet-General Corp., Sacramento, California, March 1965.

11. Oberth, A. E., "Principle of Strength Reinforcement in Filled Rubbers," Rub. Chem. & Tech., 40, 5, pp. 1347-1363 (Dec. 1967).

12. Freudenthal, A. M., "Strain-Sensitive Response of Filled Elastomers," Technical Report No. 24, Department of Civil Engineering and Engineering Mechanics, Columbia University, New York, New York, December 1968.

13. Fishman, N., and Rinde, J. A., "Development of a Dilatational Equation of State," Bull. of the Third ICRPG Working Group on Mechanical Behavior Meeting, 1 (October 1964).

14. Rinde, J. A. and Fishman, H., "Application of Finite Elasticity Theory to Propellant Behavior," Bulletin of the Third ICRPG Working Group on Mechanical Behavior Meeting, 1 (October 1964)/

15. Mullins, L. J., "Effect of Stretching on the Properties of Rubber," J. Rub. Res., 16, pp. 275-289 (1947).

16. Bueche, F., "Molecular Basis for the Mullins Effect," J. Appl. Poly. Sci., 4, 10, pp. 104-114 (1960).

17. Bueche, F., "Mullins Effect and Rubber-filler Interaction," J. Appl. Poly. Sci., 5, 15, pp. 271-281 (1961)

18. Kelley, F. N., "Properties of Highly Filled Elastomers," ICRPG Solid Propellant Mechanical Behavior Manual, CPIA Publication No. 21, Section 2.5.1, September 1963.

LIST OF FIGURES

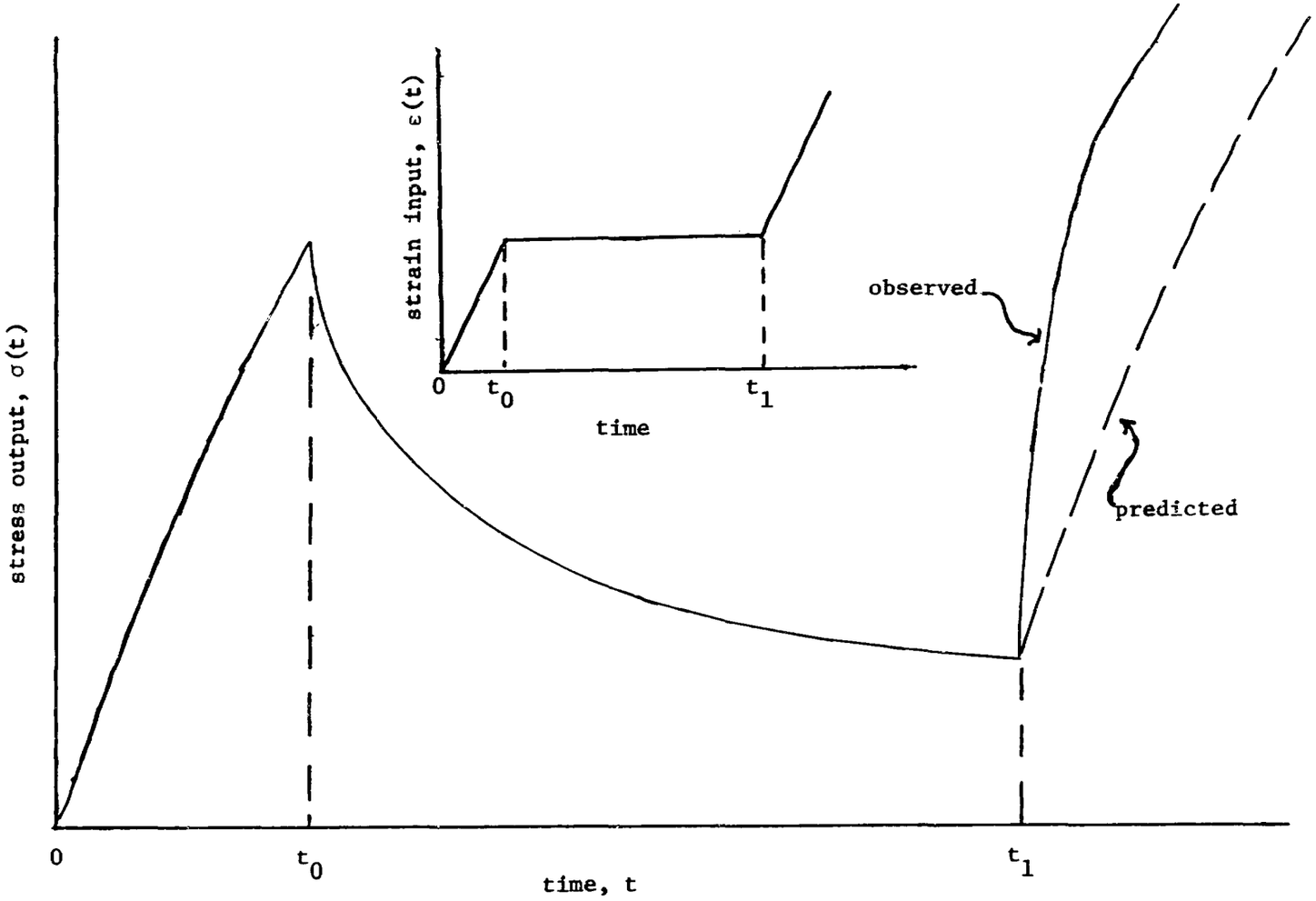

Figure 1. Linear viscoelastic stress-time predictions and experimental data for an interrupted ramp strain input on a typical composite propellant.

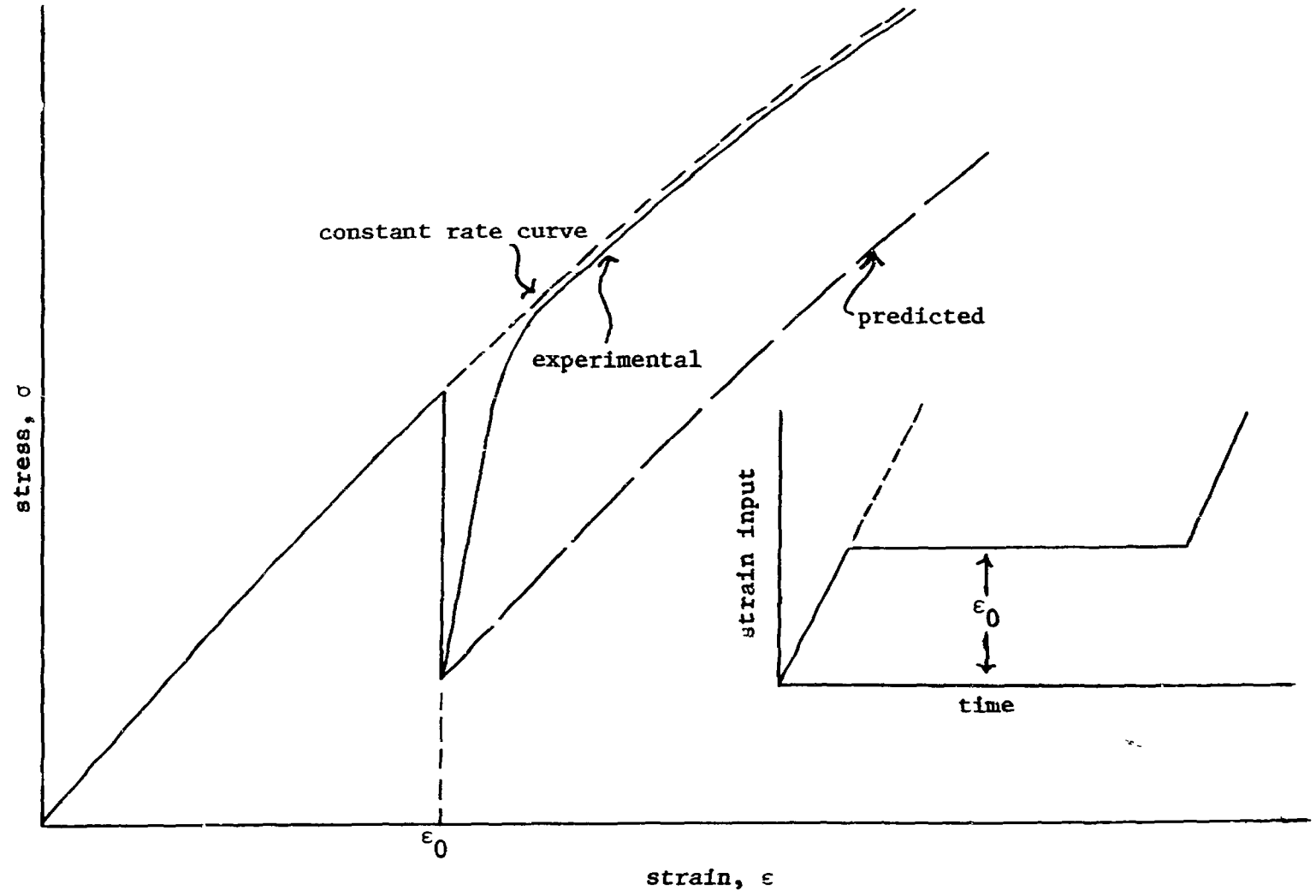

Figure 2. Linear viscoelastic stress-strain prediction and experimental data for an interrupted ramp strain input on a typical composite propellant.

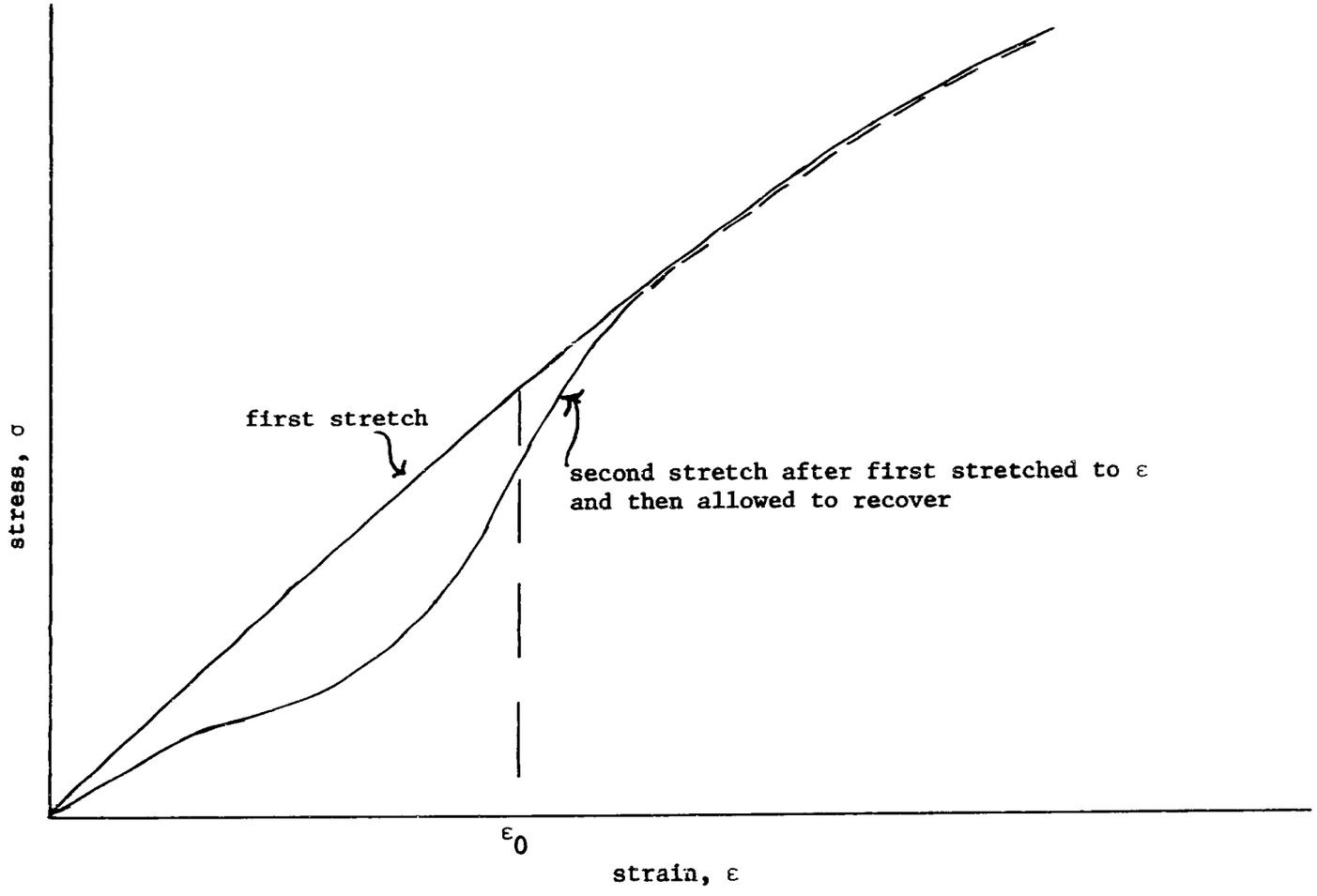

Figure 3. Typical non-equilibrium propellant stress-strain behavior after an initial deformation followed by a long recovery time.

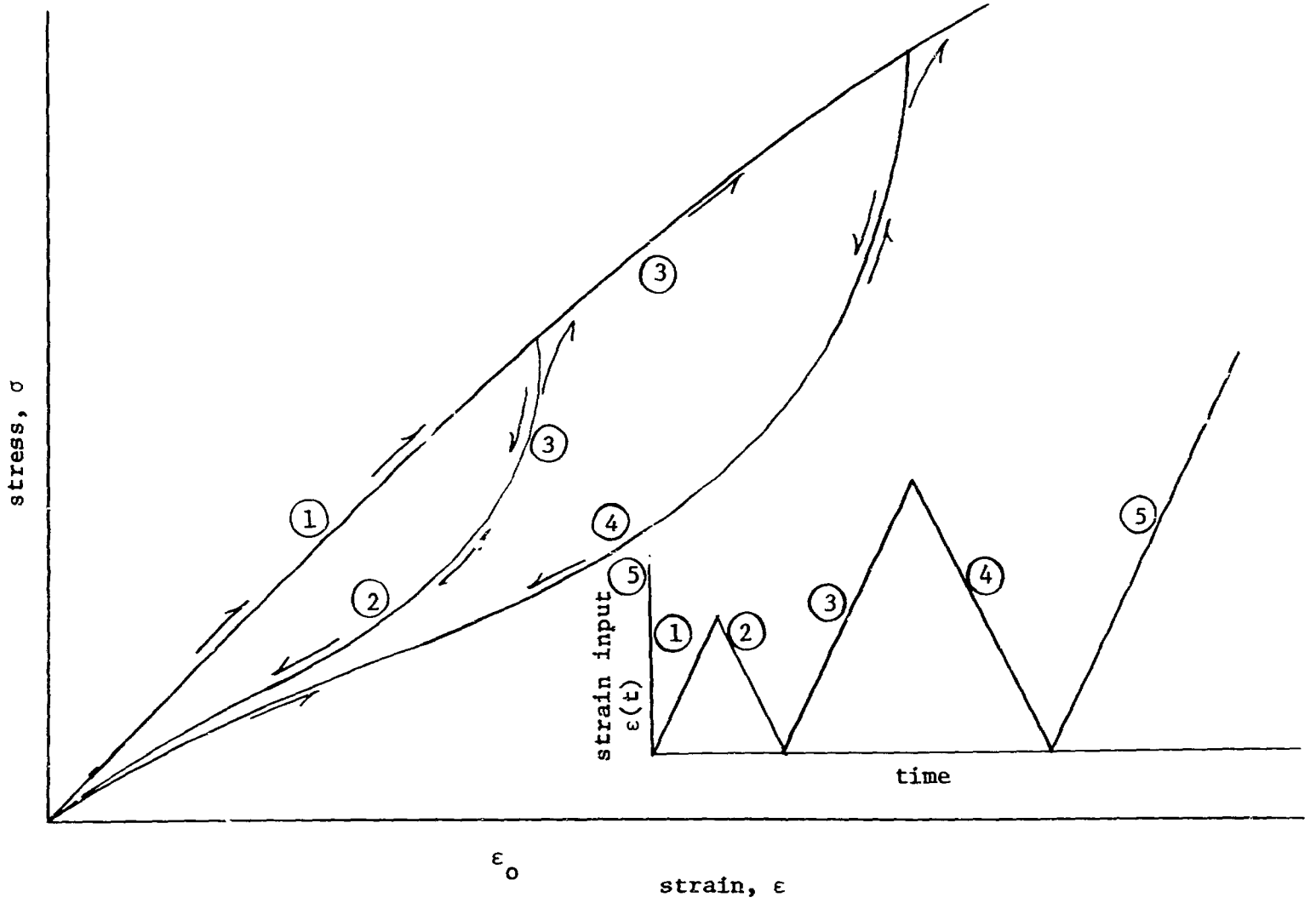

Figure 4. Typical propellant equilibrium stress strain behavior when the direction of strain is reversed.

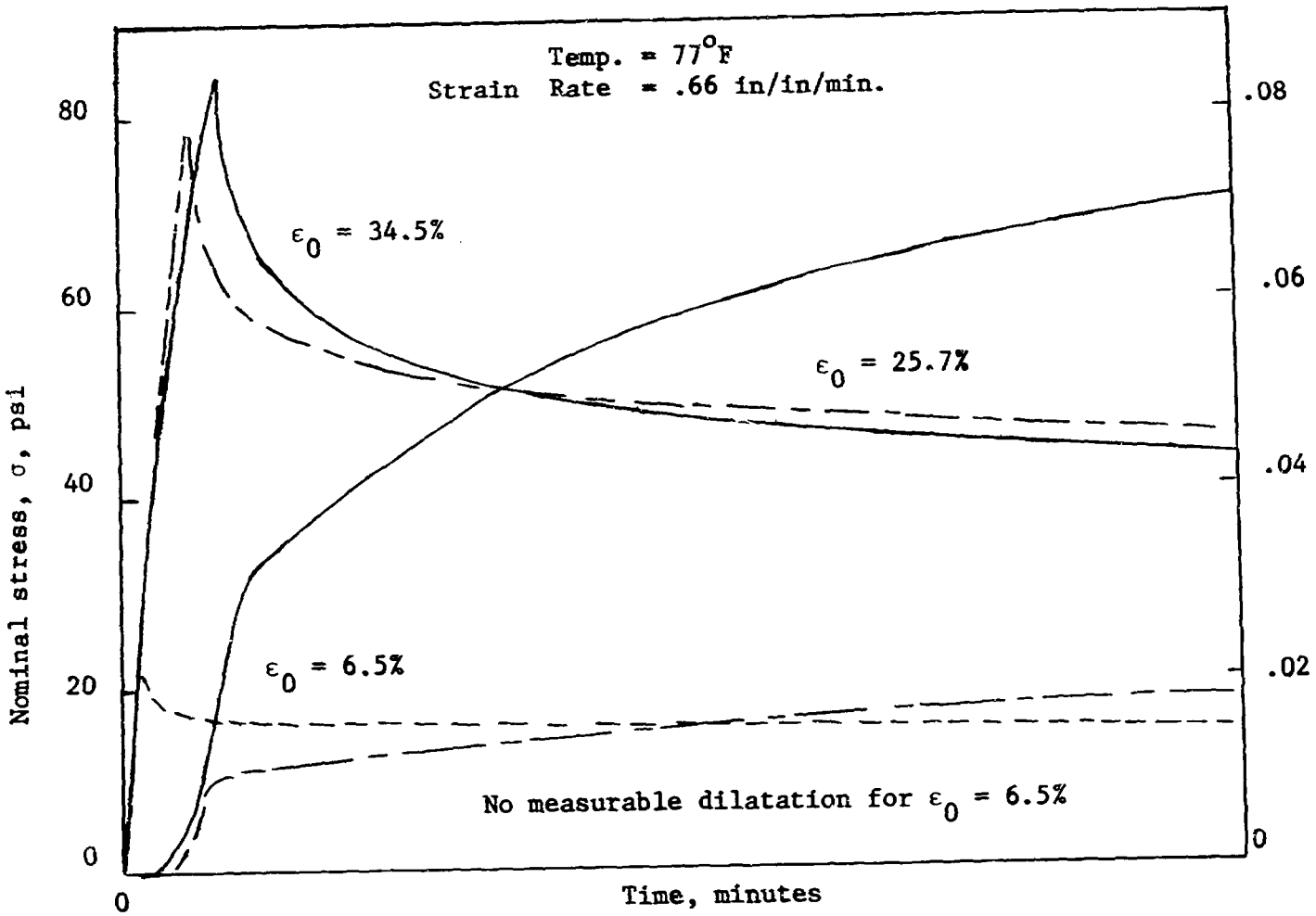

Figure 5. Experimental stress and dilatation curves for constant uniaxial strain rate followed by constant strain.

UTEC TH 69-073f

THE CHEMISTRY AND MECHANICS OF COMBUSTION

WITH

APPLICATION TO ROCKET ENGINE SYSTEMS

Task 6 Transition to Detonation Mechanisms

G. A. Secor

September 1969

College of Engineering
UNIVERSITY OF UTAH
Salt Lake City, Utah

PREFACE

Task VI, Transition to Detonation Mechanisms, has undergone a change in emphasis during the past year. Studies are now being made of the mechanics of fracture due to wave propagation, and the subsequent possibility of catastropic failure of propellants as a result of increased burning surface. With this change in emphasis, a more coherent program has been formulated and embarked upon, designed to implement the new goals.

TABLE OF CONTENTS

TASK 6 Transition to Detonation Mechanisms

1.0 INTRODUCTION

Task VI, Transition to Detonation Mechanisms, was originally designed to study the possibility of detonation resulting from dissipation in coupled thermo-viscoelastic materials. For the first year of the project, work was thus directed to the general areas of constitutive laws and possible computation techniques using those constitutive laws. The work was closely allied to that of Task V. Initial crude computations did not indicate the proposed mechanism was very promising, at least using the available information. It became apparent that the lack of reasonable, applicable, material characterization prevented any realistic study of the dissipative effects which might cause detonation.

With the above facts available, there seemed to be three roads of endeavor open at the end of the first year: 1) detailed long-range work in constitutive theory at the expense of detonation; 2) experimental studies in the general area of propellant sensitivity; or 3) some less direct approach to problems in solid rocket grain detonation. The first alternative was discarded since it was (and is) being studied under Task V. The second was discarded after discussion with experts in the field (e.g. Napadensky of IITRI) as being beyond the scope of this project. After discussions with the THEMIS industrial representatives, a new program was formulated under the third alternative, designed to utilize most effectively the capabilities existing at Utah.

Very real problems exist in which imposed or existing mechanical failure in grains may lead to subsequent unstable or uncontrolled burning. Because such problems are of practical significance and appear relatively tractable, emphasis has been transferred to this area. Since December 1968 we have been studying the effects of case rupture on the possible fragmentation of the grain, and the importance of gas-dynamics in initiating and accelerating mechanical failure in pre-cracked propellant grains. At the present time the work is primarily theoretical, although experimental effort is essential and will proceed into the year 1969-1970.

2.0 PROGRESS SINCE DECEMBER 1968

2.1 *Primary Task*

Due to the change in program emphasis less has been accomplished than would have been in a continuous program. Initial planning yielded a division of study into three general areas of emphasis: 1) failure of propellant under dynamic loading; 2) analytic techniques for study of wave propagation in realistic geometries; 3) experimental techniques to complement item 2. A subtask has also been activated studying the gas dynmaics of flow in and about cracks, as reported subsequently.

In the area of propellant failure, work was initiated by consideration of the possibility of grain failure due to release waves propagating from a case failure. Unexplained dynamic destruction of solid motors had been brought to the attention of the staff. Among several tentative explanations is one of instantaneous case failure, allowing a tensile release wave to propagate radially inward. Conceivably, such a wave may lead to sufficiently high tensile stresses to fracture the materials near the burning inner bore. The sudden increase in burning surface then leads to over-all failure of the motor. While actual detonation may not occur, the end result disables the system equally effectively. This problem is of high relevance to weapons systems. This study was presented in a THEMIS report UTEC Th 69-001.* The study served primarily to indicate numerous areas of further work required, and helped to formulate the over-all work to be done. It was, however, observed that fracture under release waves was at least feasible.

To explore the problem of propellant failure more thoroughly, an experiment was devised to study the behavior of propellants under high frequency loading. This experiment is shown schematically in Figure 1, and consists of suddenly arresting a falling body with a conical

*This report has been accepted for publication as an Engineering Note in the Journal of Spacecraft and Rockets.

apex, with magnitude increasing with decreasing distance from the apex in an inverse fashion. In principle, it is then possible to study fracture at all values of stress in a single specimen. Inclusion of viscoelastic effects of course changes the behavior of the wave, since viscous decay and geometric increase of stress intensity are competing effects. This behavior, however, is precisely the one of interest. The apparatus required has been constructed, and is now in the calibration and check-out phase. It appears, from first records made, that the experiment will bring a sample to rest in approximately 0.2 ms. This does not produce a true shock wave, but is probably the best that can be accomplished in a relatively simple fashion. At present we are studying the best method for glueing the sample to its carrier.

In the general experimental phase, we have completed the construction of a lamp system for dynamic photoelasticity. This system consists of a mercury arc lamp (PEK 112) and optical housing (PEK 911) and a power supply of our own design. We are presently working on additional optics to provide the desired beam size for various uses. Nearing completion are a discharge power supply for exploding wires, and a timing circuit for synchronization of dynamic experiments. It is anticipated that each of these will be ready for operation by summer. Much of the summer of 1969 will be spent in mastering the techniques of high-speed photography and ways of providing dynamic loadings.

While two graduate students have begun studying certain areas of wave propagation and viscoelasticity, there is no particular analytic effort to report at this time. Our work will be directed to the more mechanistic areas of wave propagation in propellant-like materials and/or propellant geometries. These studies will be of significance for at least two reasons. First, the future study of detonation in thermo-visccelastic materials requires groundwork to be laid in analytic techniques. Moreover, these techniques must be used in realistic materials of the propellant type, and in geometries

which are typical of the actual geometries of concern. Second, catastropic failure of propellant systems may well be possible for reasons connected with fracture under wave passage, even though detonation does not occur due to such wave propagation.

2.2 *Subtask on Ablation and Crack Propagation*

As a result of our close liaison with Department of Defense Agencies and the industry, the THEMIS staff became aware of the renewed interest in ablation and combustion aided crack propagation. A low effort subtask was therefore initiated in February 1969 by Dr. H. R. Jacobs.

The first item was to review the experiments on flame propagation in cracks being performed by Captain Charles E. Payne, USAF Rocket Propulsion Laboratory, as reported in Air Force document AFRPL-TR-69-66. The results of Captain Payne's work indicated that there was no minimum crack width that would impair propagation of a flame into a crack. Furthermore, he found that the time required for flame propagation into cracks decreases with decreasing crack width, and that propagation rates within a crack increase as the crack width decreases. Captain Payne did not attempt any analytical correlation and his testing was limited to a situation in which no flow existed around or over the crack.

Since the results of Captain Payne's tests at RPL did not satisfy one's initial intuitive feelings that there should be a minimum crack beyond which further decrease in crack width would not allow flame propagation, it was decided that the first item to be attacked under this subtask was an analytical investigation of the RPL tests. The second part of this subtask has been to investigate the influence of flow over a crack which is in the axial direction on the propagation of flame into said crack.

The analysis of the RPL tests was coupled with an investigation of an earlier study of flame propagation into cracks which was conducted at the Thiokol Chemical Corporation in April of 1968. Since in all of these tests no flow existed, it was decided to first

determine if thermal radiation could have any influence on the results of the above mentioned tests at Thiokol and RPL. Initial studies assuming an opaque flame and "black" surfaces indicate that radiation can cause increased burning rates in "parallel sided" slot type cracks as crack width is decreased. This fact is based upon the change in view factors for narrowing slots. Currently a computer program is being written to account for partial transparency of the combustion gases and grey surfaces for a variety of crack shapes including dog-legged cracks.

The second part of this subtask, the investigation of the effect of flow tangential to the crack and flame propagation into the crack, has been initiated with a small experimental program utilizing the small hybrid motors developed in Task III, in which axial slots of varying width and length have been machined. These plexiglas motors allow photographic observation of a typical solid propellant which is bonded to one side of the milled slot.* Photographic and visual observation of several firings to date indicate that for wide cracks (0.02-0.04 inches wide by two inches long) the flame is readily propagated into the crack by the hot gases from the main bore flowing down into the crack or slot. For the case of very narrow cracks, however, $\sim$ 0.001 inch, propagation into the crack did not occur, but rather the solid propellant burned down into the slot in the plexiglas like a typical end burning solid motor. The results of the tests to date, although not conclusive, seem to indicate that there should be a minimum crack width for flame propagation into cracks located in an axial direction with flow tangent to the crack. This conclusion is in agreement with the results of T. Godai as presented in AIAA Paper 69-561. The experimental model used by Godai was nearly the same as the above work of Captain Payne with the exception that the

*A preliminary report describing these tests are available in THEMIS report UTEC TH 69-075. This report is accompanied by films which are available on a loan basis from the project officer.

latter conducted his experiments at pressures of 49 Kg/cm^2 while Godai's experiments were primarily at ambient pressures. Godai's experiment indicated some dependence on pressure, however, for pressures less than 3 Kg/cm^2; this pressure dependence indicated a decreasing threshold crack gap for burning with increasing pressure. It should be mentioned that, although the flow and burning rates or propellants can be pressure dependent, these effects can be scaled.

3.0 PLANS FOR THE IMMEDIATE FUTURE (July - December 1969)

In the first phase of this Task we shall begin experiments relating to failure under impact loading. We shall also extend our simple analysis to the case of elastic bulk response and viscoelastic shear response.

In the experimental phase we shall begin to develop techniques applicable to dynamic studies. An additional faculty member will be supervising this phase. In the analytic phase we anticipate considerable progress during the forthcoming year. A Research Associate from France will also be associated with this part of the program.

In the subtask concerning flow in cracks, further study will be made of flame propagation into axially directed cracks using hybrid motors. This will include measurement of transient pressures within the cracks. Development of an analytical model for flow over axial slots in propellant motors will be initiated.

4.0 CONCLUSION

The first year of study resulted in a change of direction, but it is felt that the reoriented program directed toward analytic and experimental analyses of dynamic stress problems in solid fuel materials is now on a firm basis.

List of Figures

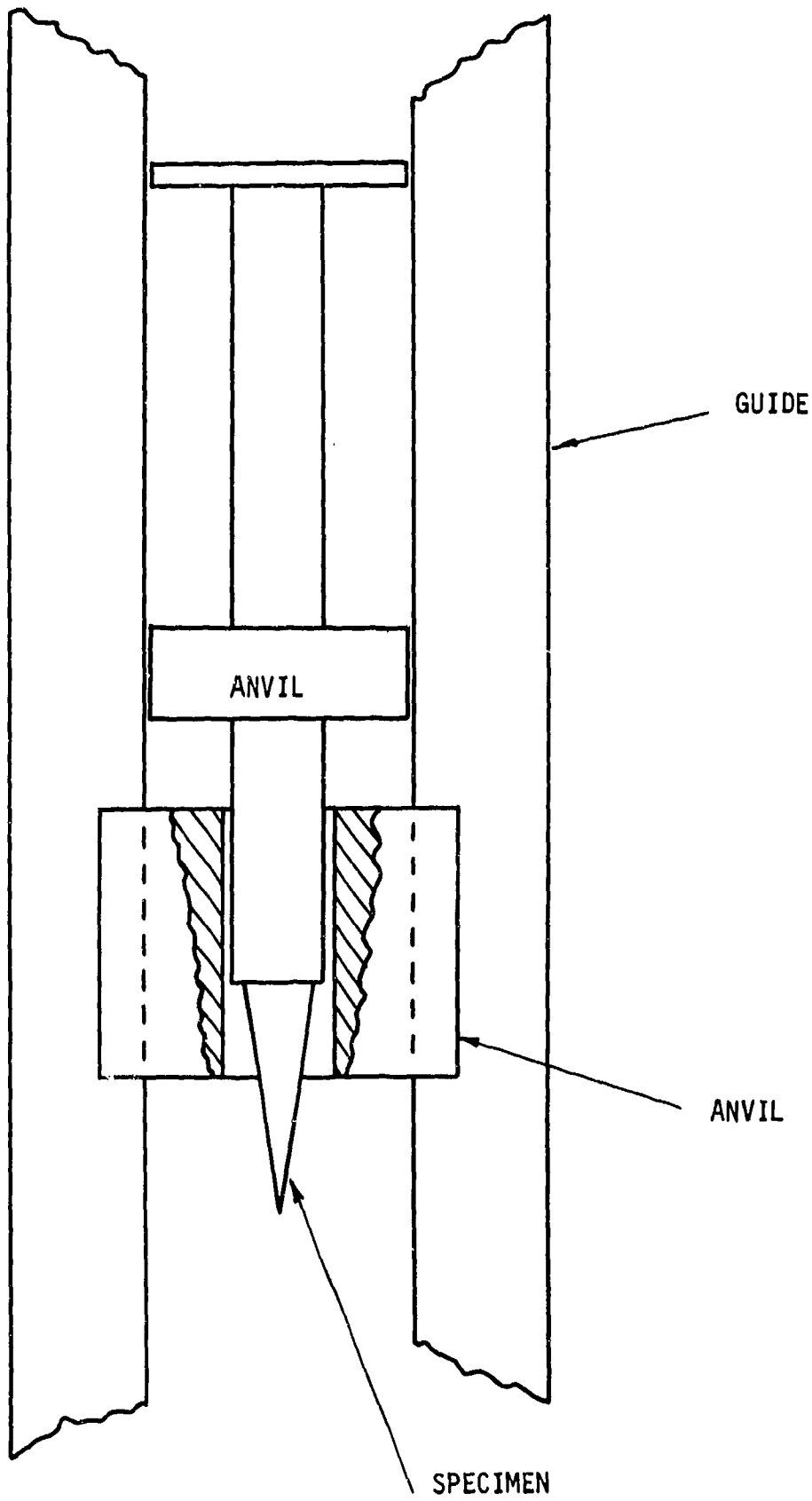

Figure 1 Schematic Diagram of Impact Experiment

UNCLASSIFIED

Security Classification

DOCUMENT CONTROL DATA - R & D

(Security classification of title, body of abstract and indexing annotation must be entered when the overall report is classified)

1. ORIGINATING ACTIVITY (Corporate author)
University of Utah
College of Engineering
Salt Lake City, Utah 84112

2a. REPORT SECURITY CLASSIFICATION
UNCLASSIFIED

2b. GROUP

3. REPORT TITLE
THE CHEMISTRY AND MECHANICS OF COMBUSTION WITH APPLICATION TO ROCKET ENGINE SYSTEMS

4. DESCRIPTIVE NOTES (Type of report and inclusive dates)
Scientific Interim

5. AUTHOR(S) (First name, middle initial, last name)
M L Williams, L K Isaacson, J E Fitzgerald, A D Baer, J D Seader, G A Secor, N W Ryan, R W Grow

6. REPORT DATE
September 1969

7a. TOTAL NO. OF PAGES
161

7b. NO. OF REFS
78

8a. CONTRACT OR GRANT NO. F44620-68-C-0022

b. PROJECT NO. 7921-02

c. 61102F

d. 681314

9a. ORIGINATOR'S REPORT NUMBER(S)
UTEC TH 69-073

9b. OTHER REPORT NO(S) (Any other numbers that may be assigned this report)
AFOSR 69-2548TR

10. DISTRIBUTION STATEMENT
1. This document has been approved for public release and sale; its distribution is unlimited.

11. SUPPLEMENTARY NOTES
TECH, OTHER

12. SPONSORING MILITARY ACTIVITY
AF Office of Scientific Research (SREP)
1400 Wilson Boulevard
Arlington, Virginia 22209

13. ABSTRACT

As part of Project THEMIS, the Department of Defense, awarded an integrated applied research program concerned with the "Chemistry and Mechanics of Combustion with application to Rocket Engine Systems" to the University. This investigation was initiated in September 1967.

The purpose of this program, which is integrated with our academic objectives, is to study the interdependence of combustion processes and the physico-mechanical behavior of solid fuel materials within the context of a rocket engine system. It is intended to capitalize upon a quantitative understanding of molecular structure, which affects both the combustion and mechanics behavior, and treat the propellant fuel and associated inert components as a materials system--from processing, to a determination of the constitutive equation as needed to assess structural integrity, and failure under various environmental and loading conditions. Concurrently, the tasks are concerned with propellant as an energy source--from ignition, through burning, gas dynamic interaction with nozzle and insulation components, and consideration of electron noise and radar attenuation in the plume.

Six task areas are presently involved in this research. The six areas, not necessarily of equal emphasis, are: (1) Combustion and Transport Mechanisms, (2) Flow and Heat Transfer, (3) Ablation Mechanisms, (4) Radiation Attenuation and Plasma Physics, (5) Mechanics of Solids, (6) Transition to Detonation Mechanisms.

DD FORM 1473

UNCLASSIFIED

Security Classification

KEY WORDS	LINK A		LINK B		LINK C	
	ROLE	WT	ROLE	WT	ROLE	WT
Solid Propellant Rocket Systems						
Solid Propellant Ignition						
Solid Rocket Plume radar Attenuation and Plasma Physics						
Solid Rocket Plumes						
Solid Rocket Combustion and Transport Mechanisms						
Mechanics of Solid Rockets						
Transition to Detonation Mechanisms in Solid Rockets						